Supplementary information for "High-entropy alloy screening for halide perovskites"

Christopher P. Muzzillo,[1]* Cristian V. Ciobanu,[2] and David T. Moore[1]

1. National Renewable Energy Laboratory, Golden, CO, USA
2. Colorado School of Mines, Golden, CO, USA
*Corresponding author email: christopher.muzzillo@nrel.gov

Table S1. Experimental III-V[1-3] and II-VI[4-10] room temperature single-phase alloy and multiple phase data, along with the ES term at 300 K, S/R, and UCV values calculated in this work, confirming how sorting by ES term and UCV creates a phase boundary that correctly separates 42 out of 45 alloys by their miscibility at 300 K (incorrect alloys are in red). UCV also correlates well with mixing enthalpy at 300 K (Fig. S1). The III-V line is in Fig. 1; the II-VI line is at UCV = 0.114.

Alloy composition	ES term (kJ/mol)	S/R	UCV	Exp. mixing enthalpy (kJ/mol)	Single phase?
Al0.5Ga0.5As0.5P0.5	-1.73	0.69	0.019	-	Yes
Al0.5In0.5As0.5P0.5	-1.73	0.69	0.038	-	No
Ga0.5In0.5As0.5P0.5	-1.73	0.69	0.038	-	No
Al0.5Ga0.5As0.5Sb0.5	-1.73	0.69	0.040	-	No
Al0.5In0.5As0.5Sb0.5	-1.73	0.69	0.048	-	No
Ga0.5In0.5As0.5Sb0.5	-1.73	0.69	0.049	-	No
Al0.5Ga0.5P0.5Sb0.5	-1.73	0.69	0.058	-	No
Ga0.5In0.5P0.5Sb0.5	-1.73	0.69	0.063	-	No
Al0.5In0.5P0.5Sb0.5	-1.73	0.69	0.063	-	No
Al0.5Ga0.5P	-0.86	0.35	0	0	Yes
Al0.5Ga0.5As	-0.86	0.35	0.001	0	Yes
Al0.5Ga0.5Sb	-0.86	0.35	0.001	0	Yes
InAs0.5P0.5	-0.86	0.35	0.014	0.42	Yes
GaAs0.5P0.5	-0.86	0.35	0.018	0.42	Yes
AlAs0.5P0.5	-0.86	0.35	0.019	0.42	Yes
Al0.5In0.5Sb	-0.86	0.35	0.028	0.63	Yes
Ga0.5In0.5Sb	-0.86	0.35	0.030	1.99	Yes
Al0.5In0.5As	-0.86	0.35	0.032	2.62	No
Ga0.5In0.5As	-0.86	0.35	0.033	3.14	No
InAs0.5Sb0.5	-0.86	0.35	0.036	2.35	No
Al0.5In0.5P	-0.86	0.35	0.037	3.66	No
Ga0.5In0.5P	-0.86	0.35	0.037	3.66	No
GaAs0.5Sb0.5	-0.86	0.35	0.040	4.71	No
AlAs0.5Sb0.5	-0.86	0.35	0.040	-	No
InP0.5Sb0.5	-0.86	0.35	0.050	-	No
GaP0.5Sb0.5	-0.86	0.35	0.058	-	No
AlP0.5Sb0.5	-0.86	0.35	0.059	-	No
Cd0.5Hg0.5Se	-0.86	0.35	0.003	-	Yes
Cd0.5Hg0.5Te	-0.86	0.35	0.005	-	Yes
Cd0.5Hg0.5S	-0.86	0.35	0.008	-	Yes
HgS0.5Se0.5	-0.86	0.35	0.059	-	No
CdS0.5Se0.5	-0.86	0.35	0.063	-	Yes
ZnS0.5Se0.5	-0.86	0.35	0.070	-	Yes
Hg0.5Zn0.5Te	-0.86	0.35	0.085	-	No
Cd0.5Zn0.5Te	-0.86	0.35	0.090	-	Yes
HgSe0.5Te0.5	-0.86	0.35	0.090	-	Yes
CdSe0.5Te0.5	-0.86	0.35	0.098	-	Yes
Cd0.5Zn0.5Se	-0.86	0.35	0.102	-	Yes
Hg0.5Zn0.5Se	-0.86	0.35	0.106	-	No
Cd0.5Zn0.5S	-0.86	0.35	0.109	-	Yes
ZnSe0.5Te0.5	-0.86	0.35	0.110	-	Yes
Hg0.5Zn0.5S	-0.86	0.35	0.117	-	No
HgS0.5Te0.5	-0.86	0.35	0.148	-	No
CdS0.5Te0.5	-0.86	0.35	0.160	5.14	No
ZnS0.5Te0.5	-0.86	0.35	0.179	5.72	No

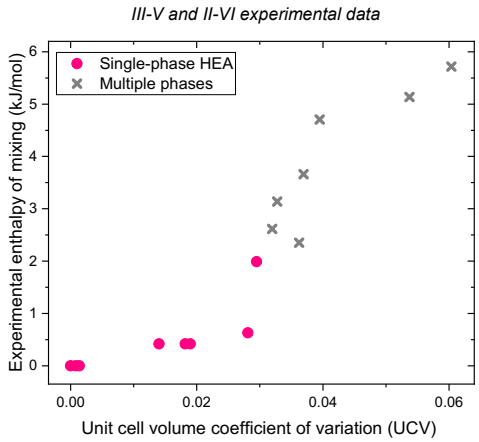

Fig. S1. Experimental III-V[3] and II-VI[8] enthalpy of mixing at 300 K as a function of UCV for single-phase alloy (pink circles) and multiple phase (gray Xs) data, showing that UCV predicts mixing enthalpy.

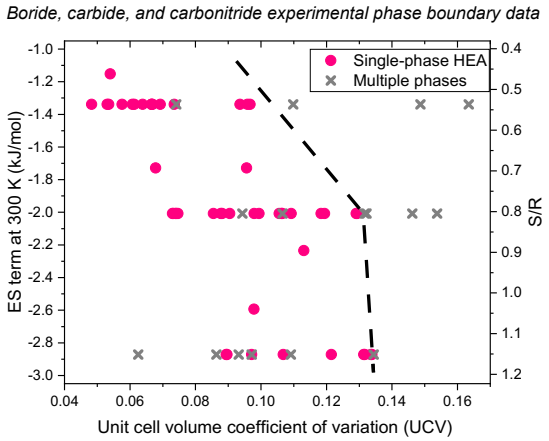

Fig. S2. Experimental boride, carbide, and carbonitride single-phase alloy (pink circles) and multiple phase (gray Xs) data,[12] confirming that plotting the ES term at 300 K (or S/R) as a function of UCV leads to a phase boundary (black dashed line) which correctly groups 56 of the 64 data.

Table S2. Ceramic unit cell volume (V): we use the median values of all Materials Project crystal structure entries.[11] Hermann-Mauguin space group, crystal system, and space group number are listed. Borides use the standard P6/mmm symmetry (3 atoms/unit cell; 1 formula unit/unit cell), while carbides and carbonitrides use the standard Fm-3m symmetry (8 atoms/unit cell; 4 formula units/unit cell).

Ceramic crystal	V (Å^3)	Structure
CrB2	23.50	P6/mmm, hexagonal, 191
VB2	23.78	P6/mmm, hexagonal, 191
MnB2	23.80	P6/mmm, hexagonal, 191
TiB2	25.67	P6/mmm, hexagonal, 191
WB2	26.74	P63/mmc, hexagonal, 194
TaB2	26.79	P6/mmm, hexagonal, 191

MoB2	27.41	P6/mmm, hexagonal, 191
NbB2	27.42	P6/mmm, hexagonal, 191
HfB2	29.72	P6/mmm, hexagonal, 191
ZrB2	30.70	P6/mmm, hexagonal, 191
YB2	36.00	P6/mmm, hexagonal, 191
CrC	65.21	Fm-3m, cubic, 225
VC	72.28	Fm-3m, cubic, 225
TiC	80.95	Fm-3m, cubic, 225
MoC	82.34	Fm-3m, cubic, 225
WC	83.00	P-6m2, hexagonal, 187
TaC	88.36	Fm-3m, cubic, 225
NbC	89.31	Fm-3m, cubic, 225
ScC	93.31	Fm-3m, cubic, 225
HfC	99.51	Fm-3m, cubic, 225
ZrC	103.36	Fm-3m, cubic, 225
CrC0.5N0.5	70.14	Fm-3m, cubic, 225
VC0.5N0.5	70.70	Fm-3m, cubic, 225
TiC0.5N0.5	78.37	Fm-3m, cubic, 225
MoC0.5N0.5	81.36	P-6m2, hexagonal, 187
WC0.5N0.5	81.99	P-6m2, hexagonal, 187
TaC0.5N0.5	85.71	Fm-3m, cubic, 225
NbC0.5N0.5	87.17	Fm-3m, cubic, 225
HfC0.5N0.5	95.54	Fm-3m, cubic, 225
ZrC0.5N0.5	99.67	Fm-3m, cubic, 225

Table S3. Experimental boride, carbide, and carbonitride room temperature single-phase alloy and multiple phase data,[12] along with the ES term at 300 K, S/R, and UCV values calculated in this work, confirming how sorting by ES term and UCV creates a phase boundary that correctly separates 56 of the 64 alloys by their miscibility at 300 K (incorrect alloys are in red). The line is in Fig. S2.

Alloy composition	ES term (kJ/mol)	S/R	UCV	Single phase?
Hf0.2Mo0.2Nb0.2Ta0.2W0.2C0.5N0.5	-2.87	1.15	0.062	No
Cr0.2Mo0.2Ta0.2V0.2W0.2C0.5N0.5	-2.87	1.15	0.086	No
Hf0.2Nb0.2Ta0.2Ti0.2Zr0.2C0.5N0.5	-2.87	1.15	0.089	Yes
Mo0.2Nb0.2Ta0.2Ti0.2Zr0.2C0.5N0.5	-2.87	1.15	0.090	Yes
Mo0.2Nb0.2Ti0.2W0.2Zr0.2C0.5N0.5	-2.87	1.15	0.093	No
Cr0.2Nb0.2Ta0.2Ti0.2V0.2C0.5N0.5	-2.87	1.15	0.097	Yes
Hf0.2Ta0.2Ti0.2W0.2Zr0.2C0.5N0.5	-2.87	1.15	0.097	No
Hf0.2Nb0.2Ta0.2Ti0.2V0.2C0.5N0.5	-2.87	1.15	0.107	Yes
Cr0.2Hf0.2Nb0.2Ta0.2Ti0.2C0.5N0.5	-2.87	1.15	0.109	No
Nb0.2Ta0.2Ti0.2V0.2Zr0.2C0.5N0.5	-2.87	1.15	0.122	Yes
Hf0.2Nb0.2Ti0.2V0.2Zr0.2C0.5N0.5	-2.87	1.15	0.131	Yes
Hf0.2Ta0.2Ti0.2V0.2Zr0.2C0.5N0.5	-2.87	1.15	0.132	Yes
Cr0.2Hf0.2Nb0.2Ti0.2Zr0.2C0.5N0.5	-2.87	1.15	0.134	Yes
Cr0.2Hf0.2Ta0.2Ti0.2Zr0.2C0.5N0.5	-2.87	1.15	0.134	Yes
Hf0.2Ti0.2V0.2W0.2Zr0.2C0.5N0.5	-2.87	1.15	0.134	No
Hf0.25Nb0.25Ti0.25Zr0.25C0.5N0.5	-2.59	1.04	0.098	Yes
Hf0.33Ti0.33Zr0.33C0.5N0.5	-2.23	0.90	0.113	Yes
Mo0.2Nb0.2Ta0.2V0.2W0.2C	-2.01	0.80	0.073	Yes
Hf0.2Nb0.2Ta0.2Ti0.2W0.2C	-2.01	0.80	0.073	Yes
Nb0.2Ta0.2Ti0.2V0.2W0.2C	-2.01	0.80	0.074	Yes
Mo0.2Nb0.2Ta0.2Ti0.2V0.2C	-2.01	0.80	0.074	Yes
Hf0.2Mo0.2Nb0.2Ta0.2Ti0.2C	-2.01	0.80	0.075	Yes
Hf0.2Sc0.2Ta0.2Ti0.2Zr0.2C	-2.01	0.80	0.085	Yes
Hf0.2Nb0.2Ta0.2Ti0.2Zr0.2C	-2.01	0.80	0.088	Yes
Nb0.2Ta0.2Ti0.2W0.2Zr0.2C	-2.01	0.80	0.088	Yes
Cr0.2Mo0.2Ti0.2V0.2W0.2C	-2.01	0.80	0.090	Yes
Hf0.2Mo0.2Ta0.2W0.2Zr0.2C	-2.01	0.80	0.094	No
Hf0.2Ta0.2Ti0.2W0.2Zr0.2C	-2.01	0.80	0.098	Yes
Hf0.2Mo0.2Ta0.2Ti0.2Zr0.2C	-2.01	0.80	0.099	Yes
Hf0.2Nb0.2Ta0.2Ti0.2V0.2C	-2.01	0.80	0.106	Yes
Cr0.2Mo0.2Nb0.2Ta0.2W0.2C	-2.01	0.80	0.106	Yes
Cr0.2Mo0.2Ta0.2V0.2W0.2C	-2.01	0.80	0.107	Yes
Hf0.2Mo0.2Ti0.2W0.2Zr0.2C	-2.01	0.80	0.107	No
Cr0.2Mo0.2Nb0.2V0.2W0.2C	-2.01	0.80	0.109	Yes

Nb0.2Ta0.2Ti0.2V0.2Zr0.2C	-2.01	0.80	0.118	Yes
Hf0.2Nb0.2Ta0.2V0.2Zr0.2C	-2.01	0.80	0.119	Yes
Hf0.2Nb0.2Ti0.2V0.2Zr0.2C	-2.01	0.80	0.129	Yes
Hf0.2Ta0.2Ti0.2V0.2Zr0.2C	-2.01	0.80	0.129	Yes
Hf0.2Mo0.2V0.2W0.2Zr0.2C	-2.01	0.80	0.132	No
Cr0.2Hf0.2Mo0.2Ti0.2W0.2C	-2.01	0.80	0.132	No
Cr0.2Mo0.2Ti0.2W0.2Zr0.2C	-2.01	0.80	0.146	No
Cr0.2Hf0.2Ta0.2W0.2Zr0.2C	-2.01	0.80	0.154	No
Hf0.25Nb0.25Ta0.25Zr0.25C	-1.73	0.69	0.068	Yes
Hf0.25Ta0.25Ti0.25Zr0.25C	-1.73	0.69	0.096	Yes
Hf0.2Mo0.2Nb0.2Ta0.2Ti0.2B2	-1.34	0.54	0.048	Yes
Cr0.2Mo0.2Ta0.2Ti0.2W0.2B2	-1.34	0.54	0.053	Both (Yes)
Hf0.2Mo0.2Nb0.2Ta0.2Zr0.2B2	-1.34	0.54	0.054	Yes
Hf0.2Nb0.2Ta0.2W0.2Zr0.2B2	-1.34	0.54	0.058	Both (Yes)
Mo0.2Nb0.2Ta0.2Ti0.2Zr0.2B2	-1.34	0.54	0.061	Yes
Cr0.2Mo0.2Ti0.2V0.2W0.2B2	-1.34	0.54	0.061	Yes
Hf0.2Mo0.2Nb0.2Ti0.2Zr0.2B2	-1.34	0.54	0.064	Both (Yes)
Hf0.2Nb0.2Ta0.2Ti0.2Zr0.2B2	-1.34	0.54	0.067	Yes
Hf0.2Mo0.2Ta0.2Ti0.2Zr0.2B2	-1.34	0.54	0.067	Yes
Hf0.2Mo0.2Ti0.2W0.2Zr0.2B2	-1.34	0.54	0.067	Both (Yes)
Hf0.2Ta0.2Ti0.2W0.2Zr0.2B2	-1.34	0.54	0.069	Yes
Hf0.2Nb0.2Ta0.2Ti0.2V0.2B2	-1.34	0.54	0.074	Yes
Cr0.2Hf0.2Mo0.2Ta0.2W0.2B2	-1.34	0.54	0.074	No
Hf0.2Ta0.2Ti0.2V0.2Zr0.2B2	-1.34	0.54	0.094	Yes
Cr0.2Hf0.2Nb0.2Ti0.2Zr0.2B2	-1.34	0.54	0.096	Yes
Cr0.2Hf0.2Ta0.2Ti0.2Zr0.2B2	-1.34	0.54	0.097	Yes
Hf0.2Mn0.2Ti0.2V0.2Zr0.2B2	-1.34	0.54	0.110	No
Cr0.2Hf0.2Ti0.2Y0.2Zr0.2B2	-1.34	0.54	0.149	No
Cr0.2Hf0.2Nb0.2V0.2Y0.2B2	-1.34	0.54	0.163	No
Hf0.25Nb0.25Ta0.25Ti0.25B2	-1.15	0.46	0.054	Yes

Table S4. Experimentally observed inorganic HP single-phase alloys, along with the ES term at 300 K, S/R, and UCV values calculated in this work.

Alloy composition	ES term (kJ/mol)	S/R	UCV	Ref.
CsPbBrClI	-1.64	0.66	0.225	[13]
CsPb0.33Sn0.33Sr0.33Br1.5I1.5	-1.59	0.64	0.092	[14]
CsGe0.33Pb0.33Sn0.33Br1.5I1.5	-1.59	0.64	0.103	[14]
CsMn0.33Pb0.33Sn0.33Br1.5I1.5	-1.59	0.64	0.114	[14]
CsPb0.33Sn0.33Zn0.33Br1.5I1.5	-1.59	0.64	-	[14]
Cs0.5Rb0.5PbBr1.5Cl1.5	-1.38	0.55	0.028	[15-16]
CsCa0.5Eu0.5Br1.5I1.5	-1.38	0.55	0.079	[17]
CsCd0.5Mn0.5Br1.5Cl1.5	-1.38	0.55	0.081	[18]
CsEu0.5Sr0.5Br1.5I1.5	-1.38	0.55	0.089	[17]
Cs0.5Rb0.5PbBr1.5I1.5	-1.38	0.55	0.090	[19-20]
CsPb0.5Sn0.5Br1.5I1.5	-1.38	0.55	0.094	[21-26]
CsGe0.5Pb0.5Br1.5I1.5	-1.38	0.55	0.100	[27]
CsFe0.5Pb0.5Br1.5Cl1.5	-1.38	0.55	0.140	[28-29]
CsEu0.5Sr0.5Br1.5Cl1.5	-1.38	0.55	0.183	[17]
CsPb0.5Zn0.5Br1.5Cl1.5	-1.38	0.55	-	[30]
CsPb0.5Zn0.5Br1.5I1.5	-1.38	0.55	-	[31]
K0.5Na0.5Co0.2Fe0.2Mg0.2Mn0.2Ni0.2F3	-1.15	0.46	0.084	[32]
CsPbBr1.5Cl1.5	-1.04	0.42	0.033	[33-35]
CsSnBr1.5Cl1.5	-1.04	0.42	0.044	[36-39]
CsGeBr1.5Cl1.5	-1.04	0.42	0.052	[40-41]
CsCdBr1.5Cl1.5	-1.04	0.42	0.064	[42]
CsCaBr1.5Cl1.5	-1.04	0.42	0.081	[43]
K0.5Na0.5Co0.25Mn0.25Ni0.25Zn0.25F3	-1.04	0.42	0.083	[44]
CsPbBr1.5I1.5	-1.04	0.42	0.088	[33-35, 39, 45-46]
CsCaBr1.5I1.5	-1.04	0.42	0.096	[43]
CsSnBr1.5I1.5	-1.04	0.42	0.098	[36-37, 39]
CsPbCl1.5I1.5	-1.04	0.42	0.120	[33]
CsHgBr1.5Cl1.5	-1.04	0.42	0.158	[47]
CsSnCl1.5I1.5	-1.04	0.42	0.165	[39]
RbFeBr1.5Cl1.5	-1.04	0.42	-	[48-49]
TlPbBr1.5Cl1.5	-1.04	0.42	-	[50]
KCo0.17Fe0.17Mg0.17Mn0.17Ni0.17Zn0.17F3	-0.89	0.36	0.049	[51]

K0.5Na0.5Co0.33Mn0.33Ni0.33F3	-0.89	0.36	0.088	52
KCo0.2Cu0.2Mg0.2Ni0.2Zn0.2F3	-0.80	0.32	0.021	32
NaCo0.2Fe0.2Mn0.2Ni0.2Zn0.2F3	-0.80	0.32	0.042	32
KCo0.2Fe0.2Mn0.2Ni0.2Zn0.2F3	-0.80	0.32	0.046	32
NaCo0.2Mg0.2Mn0.2Ni0.2Zn0.2F3	-0.80	0.32	0.047	32
NaCo0.2Fe0.2Mg0.2Mn0.2Ni0.2F3	-0.80	0.32	0.049	32
KCo0.2Mg0.2Mn0.2Ni0.2Zn0.2F3	-0.80	0.32	0.053	32, 51
KCo0.2Fe0.2Mg0.2Mn0.2Ni0.2F3	-0.80	0.32	0.054	32, 53-54
KCo0.25Mg0.25Ni0.25Zn0.25F3	-0.69	0.28	0.022	51
KCo0.25Fe0.25Ni0.25Zn0.25F3	-0.69	0.28	0.026	51
KCo0.25Fe0.25Mg0.25Zn0.25F3	-0.69	0.28	0.030	51
KCo0.25Fe0.25Mg0.25Ni0.25F3	-0.69	0.28	0.032	51, 54
KFe0.25Mg0.25Ni0.25Zn0.25F3	-0.69	0.28	0.033	51
KCo0.25Fe0.25Mn0.25Zn0.25F3	-0.69	0.28	0.041	51
KFe0.25Mn0.25Ni0.25Zn0.25F3	-0.69	0.28	0.048	51
KCo0.25Fe0.25Mn0.25Ni0.25F3	-0.69	0.28	0.051	51, 54
KCo0.25Mn0.25Ni0.25Zn0.25F3	-0.69	0.28	0.051	51
KFe0.25Mg0.25Mn0.25Zn0.25F3	-0.69	0.28	0.052	51
KCo0.25Mg0.25Mn0.25Zn0.25F3	-0.69	0.28	0.054	51
KCo0.25Fe0.25Mg0.25Mn0.25F3	-0.69	0.28	0.054	51, 54
KMg0.25Mn0.25Ni0.25Zn0.25F3	-0.69	0.28	0.058	51
KCo0.25Mg0.25Mn0.25Ni0.25F3	-0.69	0.28	0.059	51, 54
KFe0.25Mg0.25Mn0.25Ni0.25F3	-0.69	0.28	0.059	51, 54
KCo0.33Ni0.33Zn0.33F3	-0.55	0.22	0.019	55
KMn0.33Ni0.33Zn0.33F3	-0.55	0.22	0.056	56-57
KCo0.33Mn0.33Ni0.33F3	-0.55	0.22	0.059	58-64
CsMn0.33Ni0.33Pb0.33Br3	-0.55	0.22	0.089	65
Cs0.5Rb0.5GeBr3	-0.35	0.14	0.001	41
Cs0.5Rb0.5PbCl3	-0.35	0.14	0.003	15, 66-67
CsCd0.5Mn0.5Br3	-0.35	0.14	0.004	68
RbCa0.5Cd0.5F3	-0.35	0.14	0.005	69-70
KCu0.5Mg0.5F3	-0.35	0.14	0.006	71-72
KMg0.5Ni0.5F3	-0.35	0.14	0.006	32, 73
CsPb0.5Sn0.5Br3	-0.35	0.14	0.006	74-75
KCo0.5Zn0.5F3	-0.35	0.14	0.010	32, 55
K0.5Tl0.5CuCl3	-0.35	0.14	0.011	76-78
K0.5Rb0.5SrCl3	-0.35	0.14	0.011	79
Cs0.5Rb0.5CaCl3	-0.35	0.14	0.012	80-82
KFe0.5Zn0.5F3	-0.35	0.14	0.012	32
Cs0.5K0.5PbBr3	-0.35	0.14	0.013	83-84
KCo0.5Ni0.5F3	-0.35	0.14	0.013	32, 55
CsPb0.5Sr0.5Cl3	-0.35	0.14	0.014	85
CsCo0.5Mn0.5F3	-0.35	0.14	0.015	86
CsMn0.5Ni0.5F3	-0.35	0.14	0.016	86
CsPb0.5Sn0.5I3	-0.35	0.14	0.017	39, 87-89
KCo0.5Mg0.5F3	-0.35	0.14	0.019	32
K0.5Rb0.5MnF3	-0.35	0.14	0.020	90-92
Cs0.5Rb0.5PbBr3	-0.35	0.14	0.021	15, 66-67, 93-94
Cs0.5Rb0.5CaF3	-0.35	0.14	0.021	69, 95
KNi0.5Zn0.5F3	-0.35	0.14	0.023	32, 55
CsCa0.5Pb0.5Br3	-0.35	0.14	0.023	96
CsPb0.5Sr0.5Br3	-0.35	0.14	0.024	85, 96-97
K0.5Rb0.5NiCl3	-0.35	0.14	0.024	98
KMg0.5Zn0.5F3	-0.35	0.14	0.029	32
Cs0.5Rb0.5SnBr3	-0.35	0.14	0.031	99
K0.5Rb0.5CaF3	-0.35	0.14	0.031	100-101
Cs0.5Rb0.5CaBr3	-0.35	0.14	0.031	102-103
KFe0.5Mn0.5F3	-0.35	0.14	0.032	32
K0.5Rb0.5CdF3	-0.35	0.14	0.032	104
CsCd0.5Mn0.5Cl3	-0.35	0.14	0.033	105-107
CsGe0.5Mn0.5I3	-0.35	0.14	0.033	108
K0.5Rb0.5MnF3	-0.35	0.14	0.038	90, 109
RbCo0.5Mg0.5F3	-0.35	0.14	0.044	110
CsGe0.5Sn0.5I3	-0.35	0.14	0.046	89, 111
CsGe0.5Sn0.5Br3	-0.35	0.14	0.047	112
CsGe0.5Mn0.5Br3	-0.35	0.14	0.048	108
Cs0.5Rb0.5MnF3	-0.35	0.14	0.052	91
CsMg0.5Pb0.5I3	-0.35	0.14	0.052	113
Cs0.5K0.5CaCl3	-0.35	0.14	0.053	80
KCo0.5Mn0.5F3	-0.35	0.14	0.053	114-116

K0.5Na0.5MgF3	-0.35	0.14	0.058	117-120
Cs0.5Rb0.5CoF3	-0.35	0.14	0.059	121
CsMn0.5Pb0.5I3	-0.35	0.14	0.062	122
CsCd0.5Pb0.5Br3	-0.35	0.14	0.062	123-124
CsHg0.5Tl0.5Cl3	-0.35	0.14	0.066	125
CsMn0.5Pb0.5Br3	-0.35	0.14	0.066	126-127
KMn0.5Ni0.5F3	-0.35	0.14	0.067	128-130
Cs0.5Rb0.5FeCl3	-0.35	0.14	0.070	131
K0.5Na0.5MnF3	-0.35	0.14	0.072	132-134
Cs0.5K0.5MnF3	-0.35	0.14	0.072	91
KMg0.5Mn0.5F3	-0.35	0.14	0.072	135
CsMg0.5Mn0.5F3	-0.35	0.14	0.073	86
CsAg0.5Au0.5Cl3	-0.35	0.14	0.081	136
KCa0.5Mg0.5Cl3	-0.35	0.14	0.082	137
K0.5Rb0.5CaF3	-0.35	0.14	0.084	138-141
CsPb0.5Ti0.5Br3	-0.35	0.14	0.085	142
K0.5Rb0.5CaCl3	-0.35	0.14	0.089	137
Cs0.5K0.5CaCl3	-0.35	0.14	0.089	137
CsMn0.5Sn0.5Cl3	-0.35	0.14	0.097	143
KCa0.5Mg0.5F3	-0.35	0.14	0.101	118
CsCo0.5Mg0.5Cl3	-0.35	0.14	0.117	144-145
CsBa0.5Pb0.5Br3	-0.35	0.14	0.117	96, 146
Cs0.5Rb0.5CaCl3	-0.35	0.14	0.125	137
CsMn0.5Pb0.5Cl3	-0.35	0.14	0.126	147
Rb0.5Tl0.5PbCl3	-0.35	0.14	0.131	50
CsEu0.5Ni0.5Cl3	-0.35	0.14	0.133	148
CsFe0.5Pb0.5Cl3	-0.35	0.14	0.139	149
CsCa0.5Sr0.5Cl3	-0.35	0.14	0.156	79
RbCo0.5Ni0.5F3	-0.35	0.14	0.180	150
CsPb0.5Zn0.5Cl3	-0.35	0.14	0.235	30, 151
CsCo0.5Mg0.5Br3	-0.35	0.14	-	152-154
CsPb0.5Ce0.5Br3	-0.35	0.14	-	155
CsPb0.5Zn0.5Br3	-0.35	0.14	-	156-158
CsPb0.5Zn0.5I3	-0.35	0.14	-	159
KCa0.5Sr0.5I3	-0.35	0.14	-	160-161

Table S5. Experimentally observed hybrid organic-inorganic HP single-phase alloys, along with the ES term at 300 K, S/R, and UCV values calculated in this work.

Alloy composition	ES term (kJ/mol)	S/R	UCV	Ref.
MAPbBrClI	-1.64	0.66	0.134	162
Cs0.33FA0.33Rb0.33PbBr1.5Cl1.5	-1.59	0.64	0.049	163
Cs0.33FA0.33MA0.33PbBr1.5Cl1.5	-1.59	0.64	0.056	164
Cs0.33FA0.33MA0.33PbBr1.5I1.5	-1.59	0.64	0.096	164-166
ACA0.33Cs0.33FA0.33PbBr1.5I1.5	-1.59	0.64	-	167
Cs0.33DMA0.33FA0.33PbBr1.5I1.5	-1.59	0.64	-	167
Cs0.33GA0.33FA0.33PbBr1.5I1.5	-1.59	0.64	-	167
Cs0.5FA0.5PbBr1.5Cl1.5	-1.38	0.55	0.051	168
FA0.5MA0.5SnBr1.5I1.5	-1.38	0.55	0.079	169
Cs0.5FA0.5SnBr1.5I1.5	-1.38	0.55	0.085	169
FA0.5MA0.5PbBr1.5I1.5	-1.38	0.55	0.093	170
Cs0.5FA0.5PbBr1.5I1.5	-1.38	0.55	0.095	171
Cs0.5NH40.5PbBr1.5Cl1.5	-1.38	0.55	-	172
Cs0.5NH40.5PbBr1.5I1.5	-1.38	0.55	-	173
EA0.5MA0.5PbBr1.5I1.5	-1.38	0.55	-	174
GA0.5MA0.5PbBr1.5I1.5	-1.38	0.55	-	175
IM0.5MA0.5PbCl1.5I1.5	-1.38	0.55	-	176
MACd0.5Pb0.5Br1.5I1.5	-1.38	0.55	-	177
MACo0.5Pb0.5Br1.5Cl1.5	-1.38	0.55	-	178
MAMn0.5Pb0.5Br1.5Cl1.5	-1.38	0.55	-	179
MAPbBr1.5Cl1.5	-1.04	0.42	0.064	180-182
MASnBr1.5I1.5	-1.04	0.42	0.084	183
FAPbBr1.5I1.5	-1.04	0.42	0.088	184
MAPbBr1.5I1.5	-1.04	0.42	0.097	183, 185
Cs0.33FA0.33MA0.33Pb0.5Sn0.5I3	-0.89	0.36	0.024	183, 186
Cs0.33FA0.33Rb0.33Pb0.5Sn0.5I3	-0.89	0.36	0.050	187
Cs0.33FA0.33GA0.33Pb0.5Sn0.5I3	-0.89	0.36	-	183

Cs0.5MA0.5Pb0.5Sn0.5I3	-0.69	0.28	0.021	183
FA0.5MA0.5Pb0.5Sn0.5I3	-0.69	0.28	0.021	183, 188
Cs0.5FA0.5Pb0.5Sn0.5I3	-0.69	0.28	0.025	183, 189-190
Cs0.5GA0.5Ge0.5Pb0.5I3	-0.69	0.28	-	191
FA0.5MA0.5Ba0.5Pb0.5I3	-0.69	0.28	-	192
GA0.5MA0.5Pb0.5Sn0.5I3	-0.69	0.28	-	183
Cs0.33FA0.33MA0.33PbCl3	-0.55	0.22	0.025	164
Cs0.33FA0.33MA0.33PbBr3	-0.55	0.22	0.029	164
Cs0.33FA0.33MA0.33PbI3	-0.55	0.22	0.030	164-165
Cs0.33FA0.33Rb0.33PbBr3	-0.55	0.22	0.047	163
FA0.33MA0.33Rb0.33PbI3	-0.55	0.22	0.050	193
Cs0.33DMA0.33MA0.33PbI3	-0.55	0.22	0.050	194
FA0.33K0.33MA0.33PbI3	-0.55	0.22	0.068	195
EA0.33GA0.33MA0.33PbI3	-0.55	0.22	-	196
FA0.33GA0.33MA0.33PbI3	-0.55	0.22	-	197-199
GA0.33MA0.33Rb0.33PbI3	-0.55	0.22	-	196
MAPb0.33Sn0.33Zn0.33I3	-0.55	0.22	-	200
Cs0.5FA0.5SnI3	-0.35	0.14	0.007	189
FA0.5MA0.5PbI3	-0.35	0.14	0.008	201-203
MAPb0.5Sn0.5Br3	-0.35	0.14	0.008	183, 204
FAPb0.5Sn0.5I3	-0.35	0.14	0.011	183, 205
Cs0.5MA0.5GeI3	-0.35	0.14	0.012	206
Cs0.5MA0.5PbCl3	-0.35	0.14	0.013	207
FA0.5MA0.5PbBr3	-0.35	0.14	0.017	164
Cs0.5MA0.5PbBr3	-0.35	0.14	0.018	207
FAGe0.5Sn0.5I3	-0.35	0.14	0.019	208
MAPb0.5Sn0.5I3	-0.35	0.14	0.021	183, 209-210
Cs0.5MA0.5PbI3	-0.35	0.14	0.027	203
K0.5MA0.5PbBr3	-0.35	0.14	0.031	211
DMA0.5MA0.5PbI3	-0.35	0.14	0.034	212
Cs0.5FA0.5PbI3	-0.35	0.14	0.035	203, 213
Cs0.5FA0.5PbBr3	-0.35	0.14	0.035	214
FA0.5MA0.5SnBr3	-0.35	0.14	0.039	215
MAGe0.5Sn0.5I3	-0.35	0.14	0.047	216
FA0.5Rb0.5PbI3	-0.35	0.14	0.057	193
DMA0.5MA0.5SnBr3	-0.35	0.14	-	215
FA0.5MA0.5GeBr3	-0.35	0.14	-	217
FACd0.5Pb0.5Br3	-0.35	0.14	-	218
FAGe0.5Sn0.5Br3	-0.35	0.14	-	217
FAMn0.5Pb0.5Br3	-0.35	0.14	-	179
GA0.5MA0.5PbI3	-0.35	0.14	-	219
MA0.5NH40.5PbBr3	-0.35	0.14	-	220
MACd0.5Pb0.5Br3	-0.35	0.14	-	221
MACo0.5Pb0.5I3	-0.35	0.14	-	222
MAFe0.5Pb0.5I3	-0.35	0.14	-	222
MAMg0.5Pb0.5I3	-0.35	0.14	-	222
MAMn0.5Pb0.5Br3	-0.35	0.14	-	179
MAMn0.5Pb0.5I3	-0.35	0.14	-	222
MANi0.5Pb0.5I3	-0.35	0.14	-	222
MAPb0.5Sr0.5I3	-0.35	0.14	-	222
MAPb0.5Zn0.5Br3	-0.35	0.14	-	223-224
MAPb0.5Zn0.5I3	-0.35	0.14	-	225
NH4Mn0.5Zn0.5F3	-0.35	0.14	-	226

Table S6. DFT HEAHP composition, along with the ES term at 300 K, S/R, UCV from Table S10, UCV from DFT, mean unit cell volume from Table S10, mean unit cell volume from DFT, and DFT mixing enthalpy, confirming that UCV correlates with DFT mixing enthalpy for HEAHP.

Alloy composition	ES term (kJ/mol)	S/R	UCV (Table S10)	UCV (DFT)	$\bar{V}$ (Table S10) (Å)	$\bar{V}$ (DFT) (Å)	DFT mixing enthalpy (kJ/mol)
Cs0.5Rb0.5Ca0.25Ge0.25Pb0.25Sn0.25Br1.5Cl1.5	-2.07	0.83	0.068	0.108	729.5	729.6	3.70
Cs0.5Rb0.5Ca0.25Ge0.25Pb0.25Sn0.25Br1.5I1.5	-2.07	0.83	0.102	0.125	838.7	874.0	-2.23
Cs0.5Rb0.5Ca0.25Ge0.25Pb0.25Sn0.25Cl1.5I1.5	-2.07	0.83	0.146	0.191	804.3	819.8	15.2
Cs0.5Rb0.5Ca0.25Ge0.25Pb0.25Sn0.25I3	-1.04	0.42	0.053	0.068	913.5	964.2	-5.65

Cs0.5Rb0.5Ca0.25Ge0.25Pb0.25Sn0.25Br3	-1.04	0.42	0.040	0.075	763.9	783.8	-2.78
Cs0.5Rb0.5Ca0.25Ge0.25Pb0.25Sn0.25Cl3	-1.04	0.42	0.057	0.081	695.2	675.4	-3.33

Table S7. All 1,340,752 equimolar inorganic HEAHP with experimentally-observed end-members and 5 or more components: alloy composition, ES term at 300 K (kJ/mol), UCV, mean unit cell volume (Å^3), and mean band gap (eV). NA means not available. The table is included as a supplementary tab-separated value text file: "TableS7.txt".

Table S8. All 14,270 equimolar hybrid organic-inorganic HEAHP with experimentally-observed end-members and 5 or more components: alloy composition, ES term at 300 K (kJ/mol), UCV, mean unit cell volume (Å^3), and mean band gap (eV). NA means not available. The table is included as a supplementary tab-separated value text file: "TableS8.txt".

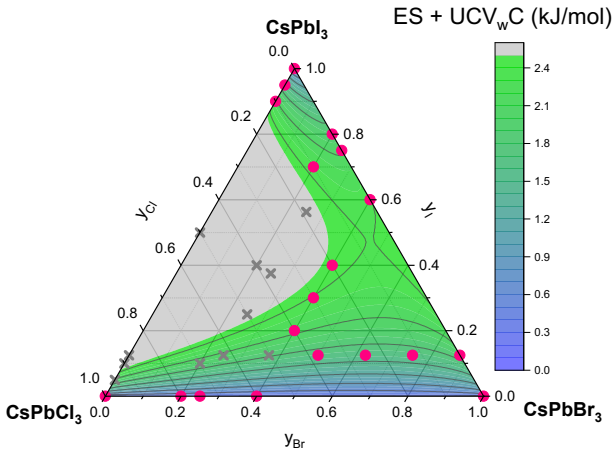

Fig. S3. ES + UCV$_w$C contours for CsPb(Br,Cl,I)$_3$. Experimental HP single-phase alloy (pink circles) and multiple phase (gray Xs) data are overlaid,[13] confirming that C = 40 kJ/mol leads to a phase boundary at G_{ES} = 2.5 kJ/mol that correctly groups 23 of the 27 data (85%).

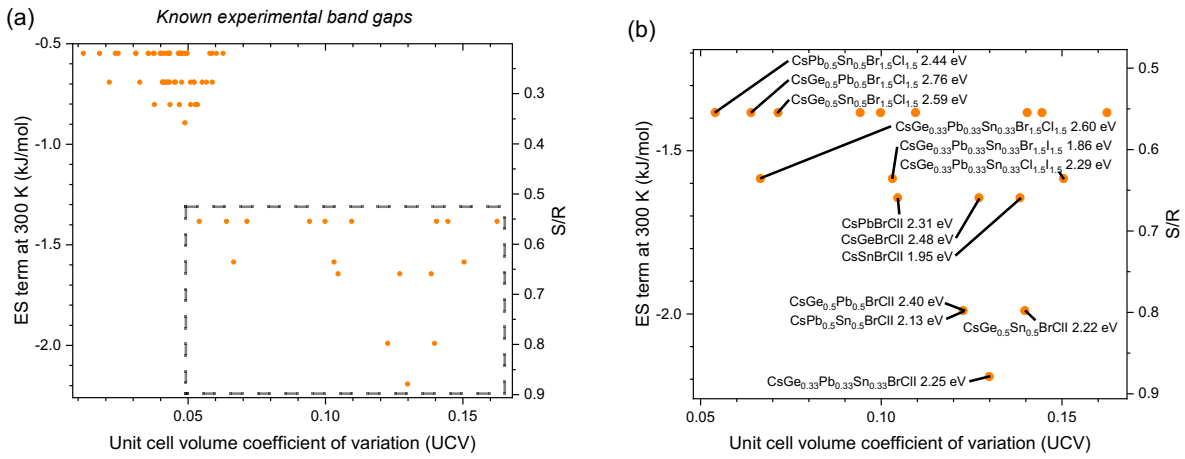

Fig. S4. Entropy stabilization (ES term at 300 K) as a function of enthalpic penalty (unit cell volume coefficient of variation (UCV)), for equimolar inorganic HP compositions with experimentally observed constitutive end-members and known experimental band gaps: (a) all data and (b) zoomed in, with promising alloys labeled.

Table S9. Inorganic HP compositions whose band gaps are known and end-members are all experimentally observed, with the maximum experimental band gap bowing (the difference between the linearly-interpolated-band gap and the actual band gap) and references.

Alloy composition	ES term (kJ/mol)	S/R	UCV	Band gap (eV)	Exp. bowing (eV)
					$Cs(Pb,Sn)Br_3 \leq 0.14$[74]
					$Cs(Ge,Sn)Br_3 \leq 0.16$[112]
					$Cs(Pb,Sn)I_3 \leq 0.07$[183]
CsGe0.33Pb0.33Sn0.33BrClI	-2.19	0.88	0.130	2.25	$CsGe(Br,Cl)_3 \leq 0.49$[40]
CsGe0.5Pb0.5BrClI	-1.99	0.80	0.123	2.40	$CsGe(Br,Cl)_3 \leq 0.49$[40]
					$Cs(Pb,Sn)Br_3 \leq 0.14$[74]
CsPb0.5Sn0.5BrClI	-1.99	0.80	0.123	2.13	$Cs(Pb,Sn)I_3 \leq 0.07$[183]
					$Cs(Ge,Sn)Br_3 \leq 0.16$[112]
CsGe0.5Sn0.5BrClI	-1.99	0.80	0.140	2.22	$CsGe(Br,Cl)_3 \leq 0.49$[40]
CsPbBrClI	-1.64	0.66	0.105	2.31	-
CsGeBrClI	-1.64	0.66	0.127	2.48	$CsGe(Br,Cl)_3 \leq 0.49$[40]
CsSnBrClI	-1.64	0.66	0.138	1.95	-
					$Cs(Pb,Sn)Br_3 \leq 0.14$[74]
					$Cs(Ge,Sn)Br_3 \leq 0.16$[112]
CsGe0.33Pb0.33Sn0.33Br1.5Cl1.5	-1.59	0.64	0.067	2.60	$CsGe(Br,Cl)_3 \leq 0.49$[40]
					$Cs(Pb,Sn)Br_3 \leq 0.14$[74]
					$Cs(Ge,Sn)Br_3 \leq 0.16$[112]
CsGe0.33Pb0.33Sn0.33Br1.5I1.5	-1.59	0.64	0.103	1.86	$Cs(Pb,Sn)I_3 \leq 0.07$[183]
					$Cs(Ge,Sn)Br_3 \leq 0.16$[112]
CsGe0.33Pb0.33Sn0.33Cl1.5I1.5	-1.59	0.64	0.150	2.29	$Cs(Pb,Sn)I_3 \leq 0.07$[183]
					$Cs(Pb,Sn)Br_3 \leq 0.14$[74]
CsPb0.5Sn0.5Br1.5Cl1.5	-1.38	0.55	0.054	2.44	$Cs(Pb,Sn)I_3 \leq 0.07$[183]
CsGe0.5Pb0.5Br1.5Cl1.5	-1.38	0.55	0.064	2.76	$CsGe(Br,Cl)_3 \leq 0.49$[40]
					$Cs(Ge,Sn)Br_3 \leq 0.16$[112]
CsGe0.5Sn0.5Br1.5Cl1.5	-1.38	0.55	0.071	2.59	$CsGe(Br,Cl)_3 \leq 0.49$[40]
					$Cs(Pb,Sn)Br_3 \leq 0.14$[74]
CsPb0.5Sn0.5Br1.5I1.5	-1.38	0.55	0.094	1.79	$Cs(Pb,Sn)I_3 \leq 0.07$[183]
CsGe0.5Pb0.5Br1.5I1.5	-1.38	0.55	0.100	2.03	-
CsGe0.5Sn0.5Br1.5I1.5	-1.38	0.55	0.110	1.77	$Cs(Ge,Sn)Br_3 \leq 0.16$[112]
CsGe0.5Pb0.5Cl1.5I1.5	-1.38	0.55	0.140	2.41	-
CsPb0.5Sn0.5Cl1.5I1.5	-1.38	0.55	0.144	2.17	$Cs(Pb,Sn)I_3 \leq 0.07$[183]
CsGe0.5Sn0.5Cl1.5I1.5	-1.38	0.55	0.162	2.29	-
CsCa0.17Eu0.17Ge0.17Pb0.17Sn0.17Sr0.17Cl3	-0.89	0.36	0.049	4.66	-
CsEu0.2Ge0.2Pb0.2Sn0.2Sr0.2Cl3	-0.80	0.32	0.038	3.97	-
CsCa0.2Eu0.2Ge0.2Sn0.2Sr0.2Cl3	-0.80	0.32	0.043	5.02	-
CsCa0.2Eu0.2Pb0.2Sn0.2Sr0.2Cl3	-0.80	0.32	0.047	4.91	-
CsCa0.2Eu0.2Ge0.2Pb0.2Sn0.2Cl3	-0.80	0.32	0.051	4.05	-
CsCa0.2Ge0.2Pb0.2Sn0.2Sr0.2Cl3	-0.80	0.32	0.053	4.98	-
CsCa0.2Eu0.2Ge0.2Pb0.2Sr0.2Cl3	-0.80	0.32	0.053	5.03	-
CsEu0.25Pb0.25Sn0.25Sr0.25Cl3	-0.69	0.28	0.021	4.11	-
CsEu0.25Ge0.25Sn0.25Sr0.25Cl3	-0.69	0.28	0.032	4.26	-
CsCa0.25Eu0.25Ge0.25Sn0.25Cl3	-0.69	0.28	0.041	4.35	-
Cs0.5Rb0.5Pb0.5Sn0.5I3	-0.69	0.28	0.041	1.67	$Cs(Pb,Sn)I_3 \leq 0.07$[183]
CsEu0.25Ge0.25Pb0.25Sn0.25Cl3	-0.69	0.28	0.041	3.04	-
CsEu0.25Ge0.25Pb0.25Sr0.25Cl3	-0.69	0.28	0.042	4.27	-
CsGe0.25Pb0.25Sn0.25Sr0.25Cl3	-0.69	0.28	0.042	4.20	-
CsAu0.25Ge0.25Pb0.25Sn0.25I3	-0.69	0.28	0.043	1.50	-
CsCa0.25Eu0.25Sn0.25Sr0.25Cl3	-0.69	0.28	0.043	5.42	-
CsCa0.25Ge0.25Sn0.25Sr0.25Cl3	-0.69	0.28	0.045	5.51	-
					$Cs(Pb,Sn)Br_3 \leq 0.14$[74]
CsGe0.25Hg0.25Pb0.25Sn0.25Br3	-0.69	0.28	0.046	2.37	$Cs(Ge,Sn)Br_3 \leq 0.16$[112]
CsCa0.25Eu0.25Ge0.25Sr0.25Cl3	-0.69	0.28	0.048	5.58	-
CsCa0.25Eu0.25Pb0.25Sn0.25Cl3	-0.69	0.28	0.051	4.21	-
CsCa0.25Pb0.25Sn0.25Sr0.25Cl3	-0.69	0.28	0.052	5.36	-

CsCa0.25Eu0.25Pb0.25Sr0.25Cl3	-0.69	0.28	0.052	5.44	-
CsCa0.25Ge0.25Pb0.25Sn0.25Cl3	-0.69	0.28	0.055	4.30	-
CsCa0.25Eu0.25Ge0.25Pb0.25Cl3	-0.69	0.28	0.057	4.37	-
CsCa0.25Ge0.25Pb0.25Sr0.25Cl3	-0.69	0.28	0.059	5.52	-
CsEu0.33Sn0.33Sr0.33Cl3	-0.55	0.22	0.012	4.53	-
CsEu0.33Pb0.33Sr0.33Cl3	-0.55	0.22	0.018	4.55	-
CsPb0.33Sn0.33Sr0.33Cl3	-0.55	0.22	0.024	4.45	-
CsEu0.33Pb0.33Sn0.33Cl3	-0.55	0.22	0.025	2.91	-
CsEu0.33Ge0.33Sn0.33Cl3	-0.55	0.22	0.031	3.11	-
CsAu0.33Ge0.33Pb0.33I3	-0.55	0.22	0.031	1.56	-
CsCa0.33Ge0.33Sn0.33Cl3	-0.55	0.22	0.035	4.78	-
CsGe0.33Sn0.33Sr0.33Cl3	-0.55	0.22	0.036	4.64	-
CsEu0.33Ge0.33Sr0.33Cl3	-0.55	0.22	0.037	4.74	-
CsGe0.33Pb0.33Sn0.33I3	-0.55	0.22	0.038	1.56	-
Cs0.33Rb0.33Tl0.33PbI3	-0.55	0.22	0.040	1.99	-
CsGe0.33Hg0.33Pb0.33Br3	-0.55	0.22	0.040	2.58	-
					$Cs(Pb,Sn)Br_3 \leq 0.14$[74]
CsGe0.33Pb0.33Sn0.33Br3	-0.55	0.22	0.041	2.16	$Cs(Ge,Sn)Br_3 \leq 0.16$[112]
CsCa0.33Eu0.33Ge0.33Cl3	-0.55	0.22	0.042	4.87	-
CsAu0.33Pb0.33Sn0.33I3	-0.55	0.22	0.043	1.45	$Cs(Pb,Sn)I_3 \leq 0.07$[183]
CsCa0.33Eu0.33Sn0.33Cl3	-0.55	0.22	0.043	4.66	-
CsHg0.33Pb0.33Sn0.33Br3	-0.55	0.22	0.043	2.37	$Cs(Pb,Sn)Br_3 \leq 0.14$[74]
CsGe0.33Hg0.33Sn0.33Br3	-0.55	0.22	0.046	2.38	$Cs(Ge,Sn)Br_3 \leq 0.16$[112]
CsGe0.33Pb0.33Sn0.33Cl3	-0.55	0.22	0.047	3.03	-
CsEu0.33Ge0.33Pb0.33Cl3	-0.55	0.22	0.047	3.12	-
CsAu0.33Ge0.33Sn0.33I3	-0.55	0.22	0.047	1.42	-
CsCa0.33Sn0.33Sr0.33Cl3	-0.55	0.22	0.048	6.20	-
CsGe0.33Pb0.33Sr0.33Cl3	-0.55	0.22	0.048	4.66	-
CsCa0.33Ge0.33Sr0.33Cl3	-0.55	0.22	0.049	6.41	-
CsCa0.33Eu0.33Sr0.33Cl3	-0.55	0.22	0.050	6.30	-
CsCa0.33Pb0.33Sn0.33Cl3	-0.55	0.22	0.058	4.58	-
CsCa0.33Eu0.33Pb0.33Cl3	-0.55	0.22	0.059	4.68	-
CsCa0.33Pb0.33Sr0.33Cl3	-0.55	0.22	0.060	6.22	-
CsCa0.33Ge0.33Pb0.33Cl3	-0.55	0.22	0.063	4.79	-

Table S10. A-site constituent, B-site constituent, X-site constituent, Pnma unit cell volume (or 20 atom equivalent for different symmetries; from the Materials Project[11] unless noted), structure (Hermann-Mauguin space group, crystal system, and space group number), experimental band gap, and reference(s) for all of the experimentally-observed inorganic ABX_3 HP.

A-site	B-site	X-site	V ($Å^3$)	Structure	Band gap (eV)	Ref.
Li	Mg	F	220.48	Pm-3m, cubic, 221	-	227-228
Rb	Be	F	231.25	Pm-3m, cubic, 221	-	227, 229-231
Na	Mg	F	234.87	Pnma, orthorhombic, 62	-	232-233
Na	Ni	F	235.03	Pnma, orthorhombic, 62	-	232, 234
Li	Mn	F	241.51	Pccn, orthorhombic, 56	-	227, 235
Na	Co	F	245.30	Pnma, orthorhombic, 62	-	232, 236
Na	Cu	F	245.83	P-1, triclinic, 2	-	232, 237
Na	Zn	F	246.26	Pnma, orthorhombic, 62	-	232, 238
Ag	Mg	F	253.76	Pm-3m, cubic, 221	-	232, 239
Na	Fe	F	254.63	Pnma, orthorhombic, 62	-	232, 240
Na	Cr	F	255.92	P-1, triclinic, 2	-	232, 241
Ag	Ni	F	256.76	Pm-3m, cubic, 221	-	232, 239
Ag	Cu	F	257.64	Pm-3m, cubic, 221	-	232, 242
Na	V	F	257.70	Pnma, orthorhombic, 62	-	232, 243
Ag	Co	F	264.72	Pm-3m, cubic, 221	-	232, 239
Li	Ba	F	266.24	Pm-3m, cubic, 221	-	227, 244
K	Mg	F	266.40	Pm-3m, cubic, 221	-	232, 244
Na	Mn	F	266.54	Pnma, orthorhombic, 62	-	232, 245
K	Cu	F	269.40	Pm-3m, cubic, 221	-	232, 246
K	Ni	F	269.52	Pm-3m, cubic, 221	-	232, 247
Ag	Zn	F	270.28	Pm-3m, cubic, 221	-	232, 248
K	Co	F	276.76	Pm-3m, cubic, 221	-	232, 249
Rb	Mg	F	281.40	Pm-3m, cubic, 221	-	227, 250
K	Zn	F	282.12	Pm-3m, cubic, 221	-	232, 251
Rb	Cu	F	284.08	Pm-3m, cubic, 221	-	232, 252
Tl	Ni	F	284.44	Pm-3m, cubic, 221	-	253-254

Tl	Mg	F	285.24	Pm-3m, cubic, 221	-	227, 255-256
Tl	Cu	F	288.96	Pm-3m, cubic, 221	-	232, 252
K	Fe	F	289.08	Pm-3m, cubic, 221	-	232, 246, 257
Tl	Zn	F	296.36	Pm-3m, cubic, 221	-	227, 258
Tl	Co	F	296.44	Pm-3m, cubic, 221	-	232, 252
Rb	Fe	F	300.76	Pm-3m, cubic, 221	-	232, 259
K	V	F	301.76	Pm-3m, cubic, 221	-	232, 260
Rb	Co	F	307.33	P63/mmc, hexagonal, 194	-	232, 261
Rb	Zn	F	307.51	P63/mmc, hexagonal, 194	-	232, 262
Cs	Mg	F	307.56	Pm-3m, cubic, 221	-	232, 263
K	Mn	F	308.00	Pnma, orthorhombic, 62	-	232, 264
Tl	Fe	F	308.04	Pm-3m, cubic, 221	-	232, 240
K	Cr	F	308.40	P4/mmm, tetragonal, 123	-	232, 265
Rb	V	F	312.48	Pm-3m, cubic, 221	-	232, 243
Rb	Cr	F	319.48	P4/mmm, tetragonal, 123	-	232, 266
K	Pd	F	320.08	Pm-3m, cubic, 221	-	227, 267
Rb	Mn	F	320.76	Pm-3m, cubic, 221	-	232, 268
Tl	Mn	F	321.64	Pm-3m, cubic, 221	-	232, 269
Rb	Pd	F	328.28	Pm-3m, cubic, 221	-	227, 270
Tl	Pd	F	329.52	Pm-3m, cubic, 221	-	253, 270
K	Ag	F	340.09	Pnma, orthorhombic, 62	-	227, 271
Cs	Fe	F	340.33	P63/mmc, hexagonal, 194	-	121, 227
K	Cd	F	342.48	Pnma, orthorhombic, 62	-	232, 272
Ag	Mn	F	343.04	Pm-3m, cubic, 221	-	232, 239
Cs	Pd	F	344.08	Pm-3m, cubic, 221	-	227, 270
Cs	Co	F	345.67	R-3m, trigonal, 166	-	227, 273
K	Ca	F	346.66	Pnma, orthorhombic, 62	-	232, 274
Rb	Ag	F	349.55	I4/mcm, tetragonal, 140	-	227, 271
Rb	Yb	F	352.16	Pm-3m, cubic, 221	-	227, 275
K	Ge	F	352.72	Pm-3m, cubic, 221	-	227, 276-277
Cs	Mn	F	355.93	P63/mmc, hexagonal, 194	-	227, 254
Tl	Cd	F	357.50	Pbam, orthorhombic, 55	-	232, 278
Rb	Cd	F	365.20	Pm-3m, cubic, 221	-	232, 278
Cs	Yb	F	366.64	Pm-3m, cubic, 221	-	227, 275
Cs	Ni	F	367.84	P63/mmc, hexagonal, 194	-	227, 279
Rb	Ca	F	368.68	Pm-3m, cubic, 221	-	232, 280
Cs	Ag	F	376.36	I4/mcm, tetragonal, 140	-	227, 281
Tl	Hg	F	379.45	Pbam, orthorhombic, 55	-	227, 282-283
Cs	Cd	F	380.00	Pm-3m, cubic, 221	-	232, 284
Cs	Ca	F	384.76	Pm-3m, cubic, 221	-	232, 244
Cs	Be	F	388.93	Pnma, orthorhombic, 62	-	232, 285
K	Hg	F	389.64	Pm-3m, cubic, 221	-	232, 286
Rb	Hg	F	395.80	Pm-3m, cubic, 221	-	232, 286
Li	Mg	Cl	397.14	P1, triclinic, 1	-	227, 287-289
K	Sn	F	402.49	P-1, triclinic, 2	-	227, 290
Tl	Sn	F	408.26	Cc, monoclinic, 9	-	253, 290
Cs	Hg	F	408.76	Pm-3m, cubic, 221	-	232, 286
K	Ba	F	433.85	P1, triclinic, 1	-	227, 287, 291
Rb	Ni	F	442.23	P63/mmc, hexagonal, 194	-	227, 292
Rb	Sn	F	444.06	P21/c, monoclinic, 14	-	253, 290
Cs	Sr	F	451.60	Pm-3m, cubic, 221	-	232, 244
Cs	Eu	F	453.36	Pm-3m, cubic, 221	-	227, 293
Rb	Pb	F	459.64	Pm-3m, cubic, 221	-	232, 294
Cs	Tl	F	464.78	Fm-3m, cubic, 225	-	227, 295
Li	Mg	Br	469.30	P1, triclinic, 1	-	227, 287, 296
Li	Ga	Cl	471.30	Pnma, orthorhombic, 62	-	227, 297
Cs	Pb	F	471.32	Pm-3m, cubic, 221	-	232, 298
Rb	Sr	F	477.84	Pm-3m, cubic, 221	-	227, 299-301
Na	Mn	Cl	480.69	R-3, trigonal, 148	-	227, 302
Cs	Sn	F	483.02	P21/c, monoclinic, 14	-	253, 303
K	Ni	Cl	488.61	P63cm, hexagonal, 185	-	227, 304
Cs	Zn	Cl	488.69	Pm-3m, cubic, 221	-	227, 305-306
K	Cr	Cl	489.51	R3c, trigonal, 161	-	253, 307
K	Fe	Cl	492.97	Pnma, orthorhombic, 62	-	232, 308
Rb	Fe	Cl	495.54	P63/mmc, hexagonal, 194	-	227, 309-310
Tl	Co	Cl	496.56	P63/mmc, hexagonal, 194	-	227, 311
K	Mg	Cl	498.96	Pnma, orthorhombic, 62	-	227, 312
K	Mn	Cl	509.05	Pnma, orthorhombic, 62	-	232, 313
Tl	Mg	Cl	511.70	Pnma, orthorhombic, 62	-	227, 314
Rb	Ni	Cl	512.56	P63/mmc, hexagonal, 194	-	227, 315

K	Ti	Cl	518.93	P63, hexagonal, 173	-	227, 316
Rb	Co	Cl	523.30	P63/mmc, hexagonal, 194	-	227, 317
In	Fe	Br	523.77	Pnma, orthorhombic, 62	-	227, 318
K	Cu	Cl	523.89	P121/c1, monoclinic, 14	-	227, 319-320
Tl	Mn	Cl	525.89	Pnma, orthorhombic, 62	-	232, 321
K	V	Cl	527.86	P63/mmc, hexagonal, 194	-	227, 322
Rb	Ti	Cl	533.96	P63cm, hexagonal, 185	-	227, 323
Tl	Cu	Cl	535.32	P21/c, monoclinic, 14	-	253, 324
Tl	V	Cl	537.10	P63/mmc, hexagonal, 194	-	227, 325
Rb	Mg	Cl	539.81	P63/mmc, hexagonal, 194	-	227, 326
Rb	Mn	Cl	543.00	P63/mmc, hexagonal, 194	-	232, 327
K	Cd	Cl	546.83	Pnma, orthorhombic, 62	-	232, 328
Rb	Cu	Cl	548.07	Pbcn, orthorhombic, 60	-	227, 329
K	Tc	Cl	549.35	C1c1, monoclinic, 9	-	227, 330
Rb	V	Cl	552.42	P63/mmc, hexagonal, 194	-	227, 331
Cs	Ni	Cl	552.86	P63/mmc, hexagonal, 194	-	332-333
Cs	Co	Cl	555.38	P63/mmc, hexagonal, 194	-	227, 334
Rb	Cu	Br	558.08	Pm-3m, cubic, 221	-	253, 335
Ag	Pb	Br	560.55	Cmcm, orthorhombic, 63	-	227, 336-337
Tl	Fe	Br	562.13	P63cm, hexagonal, 185	-	227, 338
Tl	Cd	Cl	563.38	Pnma, orthorhombic, 62	-	232, 339
Cs	Fe	Cl	569.82	P63/mmc, hexagonal, 194	-	227, 340
Rb	Cr	Cl	573.17	C2/c, monoclinic, 15	-	232, 307
Na	Hg	Cl	573.54	Pnma, orthorhombic, 62	-	227, 341
Cs	Ti	Cl	575.92	P63/mmc, hexagonal, 194	-	227, 342
Tl	Pb	Cl	576.63	Fmm2, orthorhombic, 42	-	50, 227
Tl	Mn	Br	578.70	Pnma, orthorhombic, 62	-	227, 343
Li	Ga	Br	578.93	P121/m1, monoclinic, 11	-	227, 344
Rb	Cd	Cl	581.10	Pnma, orthorhombic, 62	-	232, 345
Cs	Cu	Cl	581.37	P612-2, hexagonal, 178	-	227, 346
K	Fe	Br	584.01	Pnma, orthorhombic, 62	-	227, 347
Cs	Cr	Cl	584.74	P63/mmc, hexagonal, 194	-	227, 348
Cs	Mn	Cl	585.48	R-3m, rhombohedral, 166	-	232, 349
K	Ca	Cl	587.95	Pnma, orthorhombic, 62	-	232, 328
Cs	V	Cl	590.08	P63/mmc, hexagonal, 194	-	227, 350
Tl	Ca	Cl	592.61	Cmcm, orthorhombic, 63	-	253, 351
K	Cd	Br	595.05	Pnma, orthorhombic, 62	-	227, 352
Cs	Mg	Cl	596.78	P63/mmc, hexagonal, 194	-	227, 334
In	Mn	Br	596.85	Pnma, orthorhombic, 62	-	227, 353
K	Mn	Br	599.18	Pnma, orthorhombic, 62	-	227, 354
Cs	Tm	Cl	599.64	Pm-3m, cubic, 221	-	227, 355
Rb	Ni	Br	602.52	P63/mmc, hexagonal, 194	-	227, 315
Cs	Ag	Cl	603.61	I4/mmm, tetragonal, 139	-	227, 356
Tl	Hg	Cl	604.96	Pnma, orthorhombic, 62	-	227, 357
In	Mg	Br	605.54	Pnma, orthorhombic, 62	-	227, 358
Cs	Sc	Cl	607.48	P63/mmc, hexagonal, 194	-	227, 359
Cs	Pd	Br	607.52	Pm-3m, cubic, 221	-	253, 360-361
K	Ge	Cl	612.00	Cm, monoclinic, 8	-	362-363
K	Ti	Br	614.63	P63, hexagonal, 173	-	227, 316
In	Cr	Br	617.05	P21/c, monoclinic, 14	-	227, 318
Cs	Fe	Br	618.20	P63/mmc, hexagonal, 194	-	227, 364
Rb	Tm	Cl	619.03	Pnma, orthorhombic, 62	-	227, 365
Na	Ca	Br	624.56	R-3, trigonal, 148	-	227, 366
Cs	Cd	Cl	625.27	P63/mmc, hexagonal, 194	-	232, 367
Rb	Ti	Br	629.60	P63cm, hexagonal, 185	-	227, 316
Cs	Hg	Cl	630.84	Pm-3m, cubic, 221	-	232, 368
In	Cd	Br	632.19	Pnma, orthorhombic, 62	-	227, 369
Li	Ca	Cl	634.24	Pm-3m, cubic, 221	-	227, 287, 370
Tl	Hg	Br	635.20	Pnma, orthorhombic, 62	2.44	227, 371-372
Tl	Fe	I	635.31	Pnma, orthorhombic, 62	-	227, 373
Rb	Ca	Cl	638.78	Cm, monoclinic, 8	-	232, 374
Cs	Yb	Cl	638.92	Pm-3m, cubic, 221	-	227, 355
Tl	Cd	Br	641.98	Pnma, orthorhombic, 62	-	227, 339
Rb	V	Br	646.99	P63cm, hexagonal, 185	-	227, 375
Cs	Ni	Br	650.02	P63/mmc, hexagonal, 194	-	332, 376
Li	Sc	I	650.72	P-6c2, hexagonal, 188	-	227, 377
Cs	Ca	Cl	654.16	Pm-3m, cubic, 221	8.10	232, 378-379
Cs	Au	Cl	654.19	I4/mmm, tetragonal, 139	-	227, 380
Rb	Mn	Br	663.28	P63/mmc, hexagonal, 194	-	227, 381
Cs	Cu	Br	665.27	C2221, orthorhombic, 20	-	227, 382

Cs	Sm	Cl	665.44	Pm-3m, cubic, 221	-	227, 355
Cs	Ge	Cl	672.15	R3m, rhombohedral, 160	3.43	383
K	Ca	Br	674.88	Cmcm, orthorhombic, 63	-	227, 366
Rb	Cd	Br	675.15	Pnma, orthorhombic, 62	-	232, 345
Cs	Cr	Br	677.16	P63/mc, hexagonal, 186	-	227, 384
Rb	Ge	Cl	678.48	P121/m1, monoclinic, 11	-	227, 385
In	Ca	Br	678.51	Cmcm, orthorhombic, 63	-	227, 386
Cs	Ti	Br	678.80	P63/mmc, hexagonal, 194	-	227, 387
Cs	V	Br	680.72	P63/mmc, hexagonal, 194	-	227, 375
K	Dy	Br	682.28	Pnma, orthorhombic, 62	-	227, 388
K	Sr	Cl	682.71	Pm-3m, cubic, 221	-	227, 287, 389
Tl	Ca	Br	685.09	Cmcm, orthorhombic, 63	-	227, 386
Cs	Pd	Cl	689.47	Ibam, orthorhombic, 72	-	227, 390
Cs	In	Cl	696.73	Fm-3m, cubic, 225	-	332, 391
Rb	Sr	Cl	697.65	P21/m, monoclinic, 11	-	227, 392
Cs	Sc	Br	700.82	P63/mmc, hexagonal, 194	-	253, 359
K	Sn	Cl	700.96	Pm-3m, cubic, 221	-	362, 393-394
Cs	Mg	Br	701.44	P63/mmc, hexagonal, 194	-	227, 395
Rb	Sn	Cl	702.05	R3c, trigonal, 161	-	253, 396
Cs	Tm	Br	704.68	P4/mbm, tetragonal, 127	-	227, 397
Cs	Mn	Br	705.64	P63/mmc, hexagonal, 194	-	332, 398
K	Sn	Br	710.10	Pnma, orthorhombic, 62	-	362, 393, 399
Cs	Cd	Br	711.24	Pm-3m, cubic, 221	-	232, 400
Cs	Sn	Cl	711.88	Pm-3m, cubic, 221	2.80	37-38, 232
Rb	Yb	Br	713.90	Pnma, orthorhombic, 62	-	227, 397
Cs	Eu	Cl	722.69	Pnma, orthorhombic, 62	3.09	232, 355, 401
Rb	Ca	Br	723.13	Pnma, orthorhombic, 62	-	227, 366
Rb	Eu	Cl	723.68	Pm-3m, cubic, 221	-	227, 392
Li	Ga	I	726.11	P121/m1, monoclinic, 11	-	227, 297
Tl	Mn	I	727.35	Pnma, orthorhombic, 62	-	232, 402
Rb	Au	Br	729.83	C12/m1, monoclinic, 12	-	227, 403
Cs	Tl	Cl	730.22	Fm-3m, cubic, 225	-	227, 295
Cs	Sr	Cl	732.88	Pnma, orthorhombic, 62	7.70	232, 379, 404
Li	Ca	Br	734.94	Pm-3m, cubic, 221	-	227, 287, 405
Cs	Dy	Br	736.62	P4/mbm, tetragonal, 127	-	227, 388
Cs	Au	Br	737.38	I4/mmm, tetragonal, 139	-	227, 406
In	Sn	Cl	738.56	R-3, trigonal, 148	-	253, 407
Cs	Hg	Br	738.84	Pm-3m, cubic, 221	3.00	232, 408
K	In	Br	739.45	P-3, trigonal, 147	-	227, 409
Rb	Sn	Br	740.72	Pnma, orthorhombic, 62	-	253, 410
Cs	Ge	Br	741.96	R3m, rhombohedral, 160	2.38	383, 411
Rb	Ge	Br	742.79	Pna21, orthorhombic, 33	2.74	41, 362, 412
Cs	Ni	I	744.78	P63/mmc, hexagonal, 194	-	227, 413
Rb	Pb	Cl	749.80	Pm-3m, cubic, 221	-	227, 414
Cs	Pb	Cl	754.08	Pm-3m, cubic, 221	2.85	232, 415-416
Cs	Yb	Br	755.40	Pm-3m, cubic, 221	-	227, 397
Tl	Ge	I	768.29	Pnma, orthorhombic, 62	-	227, 417
Cs	Ca	Br	769.44	Pm-3m, cubic, 221	-	227, 366
Rb	Pb	Br	771.86	Cmcm, orthorhombic, 63	-	227, 418
K	Tm	I	773.85	Cmcm, orthorhombic, 63	-	227, 397
Cs	Eu	I	777.26	Orthorhombic	-	227, 419
Tl	Cd	I	777.88	Pnma, orthorhombic, 62	-	227, 402
K	Pb	Br	784.49	Pm-3m, cubic, 221	-	362, 420-421
In	Sn	Br	785.07	R3c, trigonal, 161	-	253, 407
Rb	Cr	I	793.27	C12/m1, monoclinic, 12	-	227, 422
K	Ti	I	794.75	P63, hexagonal, 173	-	227, 316
Rb	Tm	I	795.51	Pnma, orthorhombic, 62	-	397, 423
Cs	In	Br	795.52	Fm-3m, cubic, 225	-	332, 391
K	Dy	I	798.22	Cmcm, orthorhombic, 63	-	227, 386
Rb	V	I	798.93	P63cm, hexagonal, 185	-	227, 422
Cs	Pb	Br	805.45	Pnma, orthorhombic, 62	2.36	232, 424-425
Rb	Sr	Br	805.75	Pnma, orthorhombic, 62	-	227, 426
Rb	Ti	I	808.79	P63cm, hexagonal, 185	-	227, 422
Cs	Sn	Br	815.68	Pm-3m, cubic, 221	1.75	37-38, 232
Rb	Ge	I	823.34	P21-21-21, orthorhombic, 19	-	227, 427
Cs	V	I	828.90	P63/mmc, hexagonal, 194	-	332, 413
Cs	Eu	Br	832.70	Pnma, orthorhombic, 62	-	227, 428
K	Yb	I	834.62	Cmcm, orthorhombic, 63	-	227, 397
Cs	Ba	Cl	838.34	Pm-3m, cubic, 221	-	227, 287, 429
K	Ca	I	842.54	Cmcm, orthorhombic, 63	-	227, 386

Cs	Ti	I	843.44	P63/mmc, hexagonal, 194	-	227, 430
K	Au	I	843.44	P121/c1, monoclinic, 14	-	227, 403
Cs	Sr	Br	844.87	Pnma, orthorhombic, 62	-	227, 386
Cs	Mn	I	848.66	P63/mmc, hexagonal, 194	-	332, 431
Rb	Dy	I	860.52	Pnma, orthorhombic, 62	-	388, 423
K	Sn	I	862.75	Pnma, orthorhombic, 62	-	362, 432-433
Cs	Mg	I	865.54	P63/mmc, hexagonal, 194	-	332, 413
Rb	Yb	I	869.74	Pnma, orthorhombic, 62	-	227, 434
Tl	Pb	I	871.24	Cmcm, orthorhombic, 63	2.25	232, 435-436
Rb	Au	I	875.14	C12/m1, monoclinic, 12	-	227, 403
Rb	Ca	I	878.95	Pnma, orthorhombic, 62	-	227, 386
Cs	Tm	I	880.11	Pnma, orthorhombic, 62	-	397, 423
K	Pb	I	882.24	Pnma, orthorhombic, 62	-	227, 402
Cs	Dy	I	891.96	Pnma, orthorhombic, 62	-	423, 437
Rb	Sn	I	893.32	Pnma, orthorhombic, 62	1.62	232, 438-439
Cs	Au	I	895.13	I4/mmm, tetragonal, 139	1.31	440-441
Cs	Ge	I	906.57	R3m, rhombohedral, 160	1.63	442
Rb	Pb	I	919.08	Pnma, orthorhombic, 62	2.00	227, 443-444
Cs	Ca	I	932.40	Pnma, orthorhombic, 62	-	386, 423
Cs	Yb	I	933.60	Pnma, orthorhombic, 62	-	423, 445
Rb	Hg	I	959.40	Ama2, orthorhombic, 40	-	362, 446
Cs	Pb	I	960.71	Pnma, orthorhombic, 62	1.73	423, 447-448
Cs	Sn	I	993.64	Pm-3m, cubic, 221	1.31	37-38, 232
Cs	Sr	I	999.33	Cmcm, orthorhombic, 63	-	227, 386
Cs	Ba	Br	1019.36	Pm-3m, cubic, 221	-	227, 449-450
Cs	Cd	I	-	-	-	332, 451
Cs	Ga	Cl	-	-	-	332
Cu	Cd	Cl	-	Tetragonal	-	227, 452
K	Cd	I	-	-	-	227, 453
K	Co	Br	-	-	-	227, 283, 454
K	Pb	F	-	-	-	227, 455
K	Sr	F	-	-	-	227, 301
Li	Co	Br	-	Pm-3m, cubic, 221	-	227, 456-457
Li	V	Cl	-	Fd-3m, cubic, 227	-	227, 458
Li	Zn	F	-	-	-	227, 459
Na	Ca	Cl	-	-	-	227, 460
Na	Cd	Cl	-	-	-	227, 461
Na	Cr	Cl	-	-	-	227, 462
Na	Ni	Cl	-	-	-	227, 463
Na	Sr	F	-	-	-	227, 301
Na	Ti	Cl	-	-	-	227, 464
Rb	Be	Cl	-	Tetragonal	-	227, 465
Rb	Cd	I	-	-	-	345, 362
Tl	Cr	F	-	-	-	232, 466-467
Tl	Fe	Cl	-	-	-	227, 340
Tl	Sr	Cl	-	-	-	227, 468

Table S11. A-site constituent, B-site constituent, X-site constituent, Pnma unit cell volume (or 20 atom equivalent for different symmetries), structure (Hermann-Mauguin space group, crystal system, and space group number), experimental band gap, and reference(s) for all of the experimentally-observed organic ABX_3 HP (organic cation abbreviations are defined in the text).

A-site	B-site	X-site	V ($Å^3$)	Structure	Band gap (eV)	Ref.
NH4	Mg	F	267.69	Pm-3m, cubic, 221	-	469-470
NH4	Ni	F	270.18	Fm-3m, cubic, 225	-	466, 471
NH4	Zn	F	279.08	Pm-3m, cubic, 221	-	466, 471-472
NH4	Co	F	281.16	Pm-3m, cubic, 221	-	252, 466, 471
NH4	Cu	F	286.32	P4/mbm, tetragonal, 127	-	466, 471, 473
NH4	Fe	F	291.51	Pm-3m, cubic, 221	-	466, 471, 474
NH4	Cr	F	309.84	I4/mcm, tetragonal, 140	-	466, 471, 475
NH4	Mn	F	316.88	Pnma, orthorhombic, 62	-	466, 471, 476
NH4	Cd	F	338.25	Pnma, orthorhombic, 62	-	466, 471, 477
NH4	Sn	F	426.29	R-3, trigonal, 148	-	469, 478
NH4	Fe	Cl	516.30	P63/mmc, hexagonal, 194	-	340
NH4	Mn	Cl	517.28	Pm-3m, cubic, 221	-	479
NH4	Ni	Br	568.40	P63mc, hexagonal, 186	-	363
NH4	Cd	Cl	568.69	Pnma, orthorhombic, 62	-	480-481

NH4	Cd	Br	653.84	Pnma, orthorhombic, 62	-	[480]
HA	Cd	Br	726.60	P21/c, monoclinic, 14	-	[480]
MA	Pb	Cl	734.55	Pm-3m, cubic, 221	3.02	[482]
MA	Sn	Cl	764.41	Pm-3m, cubic, 221	3.65	[482]
FA	Pb	Cl	780.45	Pm-3m, cubic, 221	2.94	[482]
MA	Ge	Br	817.76	Pm-3m, cubic, 221	2.55	[482]
MA	Sn	Br	821.10	Pm-3m, cubic, 221	2.18	[482]
MA	Pb	Br	834.53	Pm-3m, cubic, 221	2.28	[482]
FA	Pb	Br	864.00	Pm-3m, cubic, 221	2.26	[482]
MA	Ge	I	884.90	Pm-3m, cubic, 221	1.95	[482]
FA	Sn	Br	888.42	Pm-3m, cubic, 221	2.47	[482]
AZ	Pb	Br	941.73	P63/mmc, hexagonal, 194	2.81	[483]
FA	Ge	I	970.93	R3m, trigonal, 160	2.20	[484]
MA	Sn	I	971.42	Pm-3m, cubic, 221	1.28	[482]
FA	Sn	I	1007.83	Pm-3m, cubic, 221	1.40	[482]
MA	Pb	I	1014.06	Pm-3m, cubic, 221	1.62	[482]
NH4	Sn	I	1017.33	P1, triclinic, 1	-	[485-486]
FA	Pb	I	1030.01	Pm-3m, cubic, 221	1.50	[482]
ACA	Ge	I	1068.23	P21, monoclinic, 2	2.50	[484]
EA	Sn	I	1071.13	P63mc, hexagonal, 186	2.18	[487]
GA	Sn	I	1083.06	P63/m, hexagonal, 176	1.90	[487]
DMA	Pb	I	1084.60	Cmc21, orthorhombic, 36	-	[363]
IM	Sn	I	1117.20	Pc, monoclinic, 7	2.20	[487]
ACA	Sn	I	1127.22	P63mc, hexagonal, 186	2.15	[487]
TMA	Pb	I	1190.20	P-3, hexagonal, 147	-	[363]
TEMA	Pb	I	1317.40	P63/m, hexagonal, 176	-	[363]

Table S12. A-site constituent, B-site constituent, X-site constituent, Pnma unit cell volume (or 20 atom equivalent for different symmetries; from the Materials Project[11] unless noted), structure (Hermann-Mauguin space group, crystal system, and space group number), and reference(s) for all of the *non*-experimentally-observed inorganic ABX_3 HP.[227, 253, 276, 391]

A-site	B-site	X-site	V (Å^3)	Structure	Ref.
Li	Pb	Cl	103.03	Pm-3m, cubic, 221	[227]
Li	Ca	F	212.84	Pm-3m, cubic, 221	[227]
Li	Ni	F	213.97	R-3, trigonal, 148	[227]
Cs	Ba	F	296.78	Pm-3m, cubic, 221	[227]
Na	Cd	F	302.39	R3c, trigonal, 161	[227]
In	Mn	F	320.48	P1, triclinic, 1	[253]
Cu	Ge	I	337.47	Cm, monoclinic, 8	[227]
Tl	Ag	F	347.32	R3m, monoclinic, 8	[253]
Na	Ca	F	349.81	Pm-3m, cubic, 221	[227]
Rb	Ge	F	362.08	Pm-3m, cubic, 221	[276]
Tl	Ca	F	368.45	R3c, trigonal, 161	[227]
Li	Be	Cl	371.22	Pm-3m, cubic, 221	[227]
Cs	Na	F	395.24	Pnma, orthorhombic, 62	[253]
K	Be	Cl	400.36	Pm-3m, cubic, 221	[227]
Tl	Ge	F	424.58	P21/m, monoclinic, 11	[253]
Cs	In	F	439.34	Fm-3m, cubic, 225	[253]
Na	Pb	F	448.48	Pm-3m, cubic, 221	[227]
Rb	Tl	F	449.18	Fm-3m, cubic, 225	[253]
Tl	Zn	Cl	494.02	Pm-3m, cubic, 221	[227]
Rb	Pd	Cl	501.96	Pm-3m, cubic, 221	[253]
Rb	Zn	Cl	502.40	Pm-3m, cubic, 221	[227]
Li	Sn	Cl	519.49	R3c, trigonal, 161	[253]
Na	Ba	F	531.23	Pm-3m, cubic, 221	[227]
K	Ag	Cl	535.39	R3c, trigonal, 161	[253]
Tl	Ag	Cl	539.24	P4mm, tetragonal, 99	[253]
Na	Mg	Br	540.98	Pm-3m, cubic, 221	[227]
Rb	Ag	Cl	551.88	Pm, monoclinic, 6	[253]
Ag	Ca	Cl	557.58	Pm-3m, cubic, 221	[227]
Cu	Ca	Cl	559.84	Pm-3m, cubic, 221	[227]
Rb	Pd	Br	593.00	Amm2, monoclinic, 6	[253]
Na	Pb	Cl	598.31	R3, trigonal, 146	[227]
K	Ag	Br	627.36	R3c, trigonal, 161	[253]
Tl	Ag	Br	632.23	R3c, trigonal, 161	[253]
In	Pb	Cl	643.42	Cmcm, orthorhombic, 63	[253]

Tl	Ge	Br	644.18	Pnma, orthorhombic, 62	[253]
Rb	Ag	Br	646.44	P1, triclinic, 1	[253]
Tl	Ge	Cl	649.38	P21/m, monoclinic, 11	[253]
Cs	Ag	Br	663.96	Amm2, monoclinic, 6	[253]
Rb	In	Cl	682.26	Fm-3m, cubic, 225	[253]
In	Ge	Cl	686.13	R3c, trigonal, 161	[253]
Rb	Tl	Cl	714.61	Fm-3m, cubic, 225	[227]
K	Mg	I	717.05	P1, triclinic, 1	[227]
K	Ge	Br	740.78	P21/m, monoclinic, 11	[253]
Rb	Mg	I	751.15	P1, triclinic, 1	[227]
Rb	In	Br	782.65	Fm-3m, cubic, 225	[253]
Li	Sr	Br	815.47	Pm-3m, cubic, 221	[227]
Rb	Tl	Br	821.66	Fm-3m, cubic, 225	[253]
Li	Ba	Cl	833.27	Pm-3m, cubic, 221	[227]
K	Ba	Cl	835.59	Pm-3m, cubic, 221	[227]
Cs	Tl	Br	836.08	Fm-3m, cubic, 225	[253]
Li	Ba	Br	951.24	Pm-3m, cubic, 221	[227]
K	Ba	Br	958.63	Pm-3m, cubic, 221	[227]
Rb	Ba	Br	958.86	Pm-3m, cubic, 221	[227]
Cs	In	I	967.41	Fm-3m, cubic, 225	[253, 391]
H	Pb	I	973.84	Pnma, orthorhombic, 62	[227]
Rb	Ba	I	990.78	Pnma, orthorhombic, 62	[227]
K	Hg	I	990.79	Pna21, orthorhombic, 33	[227]
Li	Pb	Br	-	Pm-3m, cubic, 221	[227, 456, 488]
Ag	Cd	Br	-	-	[227]
Ag	Mg	Cl	-	-	[227]
Ag	Pb	F	-	-	[227]
Ag	Sn	Cl	-	-	[227]
Au	Zn	F	-	-	[227]
Cu	Cd	I	-	-	[227]
Cu	Zn	Cl	-	-	[227]
K	Co	I	-	-	[227]
K	Mn	I	-	-	[227]
K	Sm	Cl	-	-	[227]
Li	Cr	Cl	-	-	[227]
Li	Mg	I	-	-	[227]
Li	Mn	I	-	-	[227]
Li	Ni	Cl	-	-	[227]
Li	Pb	F	-	-	[227]
Na	Ba	Br	-	-	[227]
Na	Ba	Cl	-	-	[227]
Na	Be	Cl	-	-	[227]
Na	Ca	I	-	-	[227]
Na	Cd	Br	-	-	[227]
Na	Cd	I	-	-	[227]
Na	Hg	I	-	-	[227]
Na	Mg	I	-	-	[227]
Na	Sn	Cl	-	-	[227]
Na	Sr	Br	-	-	[227]
Na	Sr	Cl	-	-	[227]
Na	Zn	Cl	-	-	[227]
Rb	Ba	F	-	-	[227]
Rb	Mn	I	-	-	[227]
Tl	Be	Cl	-	-	[227]
Tl	Eu	Cl	-	-	[227]
Tl	In	Cl	-	P1, triclinic, 1	[253]

References

(1) Han, G.; Yeu, I. W.; Park, J.; Ye, K. H.; Lee, S.-C.; Hwang, C. S.; Choi, J.-H. Effect of local strain energy to predict accurate phase diagram of III–V pseudobinary systems: case of Ga(As,Sb) and (In,Ga)As. *Journal of Physics D: Applied Physics* **2021,** *54* (4), 045104, DOI: 10.1088/1361-6463/abbf78.

(2) Stringfellow, G. B. Miscibility gaps in quaternary III/V alloys. *Journal of Crystal Growth* **1982,** *58* (1), 194-202, DOI: 10.1016/0022-0248(82)90226-3.
(3) Panish, M. B.; Ilegems, M. Phase equilibria in ternary III–V systems. *Progress in Solid State Chemistry* **1972,** *7*, 39-83, DOI: 10.1016/0079-6786(72)90004-0.
(4) Foster, L. M. A Lattice Parameter Criterion for Miscibility Gaps in the III – V and II – VI Pseudobinary Solid Solutions. *Journal of The Electrochemical Society* **1974,** *121* (12), 1662, DOI: 10.1149/1.2401764.
(5) Asadov, M. M. The HgS + Tl_2Se <-> HgSe + Tl_2S reciprocal system. *(Russian) Journal of Inorganic Chemistry (translated from Zhurnal Neorganicheskoi Khimii)* **1983,** *28*, 1025-1028.
(6) Leute, V.; Köller, H.-J. The Four Quasibinary Phase Diagrams of the Quasiternary System (Hg,Pb) (Se,Te). *Zeitschrift für Physikalische Chemie* **1986,** *149* (2), 213-227, DOI: 10.1524/zpch.1986.149.2.213.
(7) Ohata, K.; Saraie, J.; Tanaka, T. Phase Diagram of the CdS-CdTe Pseudobinary System. *Japanese Journal of Applied Physics* **1973,** *12* (8), 1198, DOI: 10.1143/JJAP.12.1198.
(8) Ohtani, H.; Kojima, K.; Ishida, K.; Nishizawa, T. Miscibility gap in II–VI alloy semiconductor systems. *Journal of Alloys and Compounds* **1992,** *182* (1), 103-114, DOI: 10.1016/0925-8388(92)90579-X.
(9) Tomashik, V.; Oleinik, G.; Mizetskaya, I. The System CdTe--ZnS. *Izv. Akad. Nauk SSSR, Neorg. Mater.* **1978,** *14* (10), 1838-1840.
(10) Tomashyk, V.; Feychuk, P.; Shcherbak, L. *Ternary alloys based on II-VI semiconductor compounds*, CRC Press: 2014; p 526.
(11) Jain, A.; Ong, S. P.; Hautier, G.; Chen, W.; Richards, W. D.; Dacek, S.; Cholia, S.; Gunter, D.; Skinner, D.; Ceder, G.; Persson, K. A. Commentary: The Materials Project: A materials genome approach to accelerating materials innovation. *APL Materials* **2013,** *1* (1), DOI: 10.1063/1.4812323.
(12) Divilov, S.; Eckert, H.; Hicks, D.; Oses, C.; Toher, C.; Friedrich, R.; Esters, M.; Mehl, M. J.; Zettel, A. C.; Lederer, Y.; Zurek, E.; Maria, J.-P.; Brenner, D. W.; Campilongo, X.; Filipović, S.; Fahrenholtz, W. G.; Ryan, C. J.; DeSalle, C. M.; Crealese, R. J.; Wolfe, D. E.; Calzolari, A.; Curtarolo, S. Disordered enthalpy–entropy descriptor for high-entropy ceramics discovery. *Nature* **2024,** *625* (7993), 66-73, DOI: 10.1038/s41586-023-06786-y.
(13) Jung, J.; Yun, Y.; Yang, S. W.; Oh, H. G.; Jeon, A. Y.; Nam, Y.; Heo, Y.-W.; Chae, W.-S.; Lee, S. Ternary diagrams of phase, stability, and optical properties of cesium lead mixed-halide perovskites. *Acta Materialia* **2023,** *246*, 118661, DOI: 10.1016/j.actamat.2022.118661.
(14) Zhang, W.; Liu, H.; Qu, Y.; Cui, J.; Zhang, W.; Shi, T.; Wang, H.-L. B-Site Co-Doping Coupled with Additive Passivation Pushes the Efficiency of Pb–Sn Mixed Inorganic Perovskite Solar Cells to Over 17%. *Advanced Materials* **2023,** *n/a* (n/a), 2309193, DOI: 10.1002/adma.202309193.
(15) Baek, S.; Kim, S.; Noh, J. Y.; Heo, J. H.; Im, S. H.; Hong, K.-H.; Kim, S.-W. Development of Mixed-Cation $Cs_xRb_{1-x}PbX_3$ Perovskite Quantum Dots and Their Full-Color Film with High Stability and Wide Color Gamut. *Advanced Optical Materials* **2018,** *6* (15), 1800295, DOI: 10.1002/adom.201800295.
(16) Zirak, M.; Moyen, E.; Alehdaghi, H.; Kanwat, A.; Choi, W.-C.; Jang, J. Anion- and Cation-Codoped All-Inorganic Blue-Emitting Perovskite Quantum Dots for Light-Emitting Diodes. *ACS Applied Nano Materials* **2019,** *2* (9), 5655-5662, DOI: 10.1021/acsanm.9b01187.
(17) Stand, L.; Zhuravleva, M.; Chakoumakos, B.; Wei, H.; Johnson, J.; Martin, V.; Loyd, M.; Rutstrom, D.; McAlexander, W.; Wu, Y.; Koschan, M.; Melcher, C. L. Characterization of

mixed halide scintillators: $CsSrBrI_2$:Eu, $CsCaBrI_2$:Eu and $CsSrClBr_2$:Eu. *Journal of Luminescence* **2019,** *207*, 70-77, DOI: 10.1016/j.jlumin.2018.10.108.
(18) Wen, T.; Gu, G.; Wang, B.; Zhang, W.; Wang, R. Cyan-rich sunlight-like spectra from Mn^{2+}-doped $CsCd(Cl_{1-y}Br_y)_3$ perovskites with dual tunable emissions and high stability. *Journal of Materials Chemistry C* **2023,** *11* (21), 6989-6998, DOI: 10.1039/D2TC05455H.
(19) Ji, Y.; Wang, M.; Yang, Z.; Wang, H.; Padhiar, M. A.; Shi, J.; Qiu, H.; Bhatti, A. S. In Situ Synthesis of UltraStable TiO_2 Coating Rb^+-Doped Red Emitting $CsPbBrI_2$ Perovskite Quantum Dots. *The Journal of Physical Chemistry C* **2022,** *126* (3), 1542-1551, DOI: 10.1021/acs.jpcc.1c09945.
(20) Lin, Y.-H.; Qiu, Z.-H.; Wang, S.-H.; Zhang, X.-H.; Wu, S.-F. All-inorganic $Rb_xCs_{1-x}PbBrI_2$ perovskite nanocrystals with wavelength-tunable properties for red light-emitting. *Inorganic Chemistry Communications* **2019,** *103*, 47-52, DOI: 10.1016/j.inoche.2019.03.007.
(21) Lee, S.; Moon, J.; Ryu, J.; Parida, B.; Yoon, S.; Lee, D.-G.; Cho, J. S.; Hayase, S.; Kang, D.-W. Inorganic narrow bandgap $CsPb_{0.4}Sn_{0.6}I_{2.4}Br_{0.6}$ perovskite solar cells with exceptional efficiency. *Nano Energy* **2020,** *77*, 105309, DOI: 10.1016/j.nanoen.2020.105309.
(22) Li, N.; Zhu, Z.; Li, J.; Jen, A. K.-Y.; Wang, L. Inorganic $CsPb_{1-x}Sn_xIBr_2$ for Efficient Wide-Bandgap Perovskite Solar Cells. *Advanced Energy Materials* **2018,** *8* (22), 1800525, DOI: 10.1002/aenm.201800525.
(23) Shang, Y.; Li, X.; Lian, W.; Jiang, X.; Wang, X.; Chen, T.; Xiao, Z.; Wang, M.; Lu, Y.; Yang, S. Lead acetate as a superior lead source enables highly efficient and stable all-inorganic lead-tin perovskite solar cells. *Chemical Engineering Journal* **2023,** *457*, 141246, DOI: 10.1016/j.cej.2022.141246.
(24) Wen, Q.; Duan, C.; Zou, F.; Luo, D.; Li, J.; Liu, Z.; Wang, J.; Yan, K. All-inorganic $CsPb_{1-x}Sn_xI_2Br$ perovskites mediated by dicyandiamide additive for efficient 4-terminal tandem solar cell. *Chemical Engineering Journal* **2023,** *452*, 139697, DOI: 10.1016/j.cej.2022.139697.
(25) Zhang, W.; Liu, H.; Qi, X.; Yu, Y.; Zhou, Y.; Xia, Y.; Cui, J.; Shi, Y.; Chen, R.; Wang, H.-L. Oxalate Pushes Efficiency of $CsPb_{0.7}Sn_{0.3}IBr_2$ Based All-Inorganic Perovskite Solar Cells to over 14%. *Advanced Science* **2022,** *9* (11), 2106054, DOI: 10.1002/advs.202106054.
(26) Zhang, Z.; Dai, L.; Zhang, M.; Ban, H.; Liu, Z.; Yu, H.; Gu, A.; Zhang, X.-L.; Chen, S.; Wang, Y.; Shen, Y.; Wang, M. Surface Modification in $CsPb_{0.5}Sn_{0.5}I_2Br$ Inorganic Perovskite Solar Cells: Effects of Bifunctional Dipolar Molecules on Photovoltaic Performance. *ACS Applied Materials & Interfaces* **2023,** *15* (30), 36594-36601, DOI: 10.1021/acsami.3c07018.
(27) Yang, F.; Hirotani, D.; Kapil, G.; Kamarudin, M. A.; Ng, C. H.; Zhang, Y.; Shen, Q.; Hayase, S. All-Inorganic $CsPb_{1-x}Ge_xI_2Br$ Perovskite with Enhanced Phase Stability and Photovoltaic Performance. *Angewandte Chemie International Edition* **2018,** *57* (39), 12745-12749, DOI: 10.1002/anie.201807270.
(28) Hu, Y.; Zhang, Y.; Yang, C.; Li, J.; Wang, L. The cation–anion co-exchange in $CsPb_{1-x}Fe_x(Br_{1-y}Cl_y)_3$ nanocrystals prepared using a hot injection method. *RSC Advances* **2020,** *10* (55), 33080-33085, DOI: 10.1039/D0RA06238C.
(29) Wu, C.; Li, Y.; Xia, Z.; Ji, C.; Tang, Y.; Zhang, J.; Ma, C.; Gao, J. Enhancing Photoluminescence of $CsPb(Cl_xBr_{1-x})_3$ Perovskite Nanocrystals by Fe^{2+} Doping. *Nanomaterials* **2023,** *13* (3), 533, DOI: 10.3390/nano13030533.
(30) Naresh, V.; Lee, N. Zn(II)-Doped Cesium Lead Halide Perovskite Nanocrystals with High Quantum Yield and Wide Color Tunability for Color-Conversion Light-Emitting Displays. *ACS Applied Nano Materials* **2020,** *3* (8), 7621-7632, DOI: 10.1021/acsanm.0c01254.

(31) Sun, H.; Zhang, J.; Gan, X.; Yu, L.; Yuan, H.; Shang, M.; Lu, C.; Hou, D.; Hu, Z.; Zhu, Y.; Han, L. Pb-Reduced $CsPb_{0.9}Zn_{0.1}I_2Br$ Thin Films for Efficient Perovskite Solar Cells. *Advanced Energy Materials* **2019,** *9* (25), 1900896, DOI: 10.1002/aenm.201900896.
(32) Wang, T.; Chen, H.; Yang, Z.; Liang, J.; Dai, S. High-Entropy Perovskite Fluorides: A New Platform for Oxygen Evolution Catalysis. *Journal of the American Chemical Society* **2020,** *142* (10), 4550-4554, DOI: 10.1021/jacs.9b12377.
(33) Belyaev, I. N.; Shurginov, E. A. *Zhurnal Neorganicheskoj Khimii* **1970,** *15*, 1401.
(34) Ghaithan, H. M.; Qaid, S. M. H.; Alahmed, Z. A.; Hezam, M.; Lyras, A.; Amer, M.; Aldwayyan, A. S. Anion Substitution Effects on the Structural, Electronic, and Optical Properties of Inorganic $CsPb(I_{1-x}Br_x)_3$ and $CsPb(Br_{1-x}Cl_x)_3$ Perovskites: Theoretical and Experimental Approaches. *The Journal of Physical Chemistry C* **2021,** *125* (1), 886-897, DOI: 10.1021/acs.jpcc.0c07983.
(35) Ghaithan, H. M.; Qaid, S. M. H.; AlHarbi, K. K.; Bin Ajaj, A. F.; Al-Asbahi, B. A.; Aldwayyan, A. S. Amplified Spontaneous Emission from Thermally Evaporated High-Quality Thin Films of $CsPb(Br_{1-x}Y_x)_3$ (Y = I, Cl) Perovskites. *Langmuir* **2022,** *38* (28), 8607-8613, DOI: 10.1021/acs.langmuir.2c00861.
(36) Jellicoe, T. C.; Richter, J. M.; Glass, H. F. J.; Tabachnyk, M.; Brady, R.; Dutton, S. E.; Rao, A.; Friend, R. H.; Credgington, D.; Greenham, N. C.; Böhm, M. L. Synthesis and Optical Properties of Lead-Free Cesium Tin Halide Perovskite Nanocrystals. *Journal of the American Chemical Society* **2016,** *138* (9), 2941-2944, DOI: 10.1021/jacs.5b13470.
(37) Peedikakkandy, L.; Bhargava, P. Composition dependent optical, structural and photoluminescence characteristics of cesium tin halide perovskites. *RSC Advances* **2016,** *6* (24), 19857-19860, DOI: 10.1039/C5RA22317B.
(38) Scaife, D. E.; Weller, P. F.; Fisher, W. G. Crystal preparation and properties of cesium tin(II) trihalides. *Journal of Solid State Chemistry* **1974,** *9* (3), 308-314, DOI: 10.1016/0022-4596(74)90088-7.
(39) Sharma, S.; Weiden, N.; Weiss, A. Phase Diagrams Of Quasibinary Systems Of The Type: Abx3-A'bx3; Abx3 - Ab'x3 And Abx3 - Abx'3; X = Halogen. *Zeitschrift für physikalische Chemie* **1992,** *175* (1), 63-80.
(40) Lin, Z.-G.; Tang, L.-C.; Chou, C.-P. Infrared properties of $CsGe(Br_xCl_{1-x})_3$, nonlinear optical rhombohedral semiconductor. *Journal of Physics: Condensed Matter* **2007,** *19* (47), 476209, DOI: 10.1088/0953-8984/19/47/476209.
(41) Lin, Z.-G.; Tang, L.-C.; Chou, C.-P. Characterization and properties of infrared NLO crystals: $AGeX_3$ (A=Rb, Cs; X=Cl, Br). *Journal of Crystal Growth* **2008,** *310* (13), 3224-3229, DOI: 10.1016/j.jcrysgro.2008.03.018.
(42) Lüthi, S. R.; Riley, M. J. Ni(II)-Doped $CsCdBrCl_2$: Variation of Spectral and Structural Properties via Mixed-Halide Coordination. *Inorganic Chemistry* **2001,** *40* (2), 196-207, DOI: 10.1021/ic000899l.
(43) Plokker, M. P.; Biner, D. A.; Dusoswa, N.; Dorenbos, P.; Krämer, K. W.; Van Der Kolk, E. Photoluminescence and excited states dynamics of Tm^{2+}-doped $CsCa(Cl/Br)_3$ and $CsCa(Br/I)_3$ perovskites. *Journal of Physics: Materials* **2021,** *4* (4), 045004, DOI: 10.1088/2515-7639/ac24ed.
(44) Li, Y.; Ding, R.; Jia, Z.; Yu, W.; Wang, A.; Liu, M.; Yang, F.; Zhang, Y.; Fang, Q.; Yan, M.; Xie, J.; Sun, X.; Liu, E. Unlocking the intrinsic mechanisms of A-site K/Na doped perovskite fluorides pseudocapacitive cathode materials for enhanced aqueous zinc-based batteries. *Energy Storage Materials* **2023,** *57*, 334-345, DOI: 10.1016/j.ensm.2023.02.020.

(45) Näsström, H.; Becker, P.; Márquez, J. A.; Shargaieva, O.; Mainz, R.; Unger, E.; Unold, T. Dependence of phase transitions on halide ratio in inorganic $CsPb(Br_xI_{1-x})_3$ perovskite thin films obtained from high-throughput experimentation. *Journal of Materials Chemistry A* **2020,** *8* (43), 22626-22631, DOI: 10.1039/D0TA08067E.
(46) Yuan, L.; Yuan, M.; Xu, H.; Hou, C.; Meng, X. Moisture-stimulated reversible thermochromic $CsPbI_{3-x}Br_x$ films: In-situ spectroscopic-resolved structure and optical properties. *Applied Surface Science* **2022,** *573*, 151484, DOI: 10.1016/j.apsusc.2021.151484.
(47) Natta, G.; Passerini, L. Isomorfismo, polimorfismo e morfotropia I.Composti del tipo ABX_3. *Gazzetta Chimica Italiana* **1928,** *58*, 472-484.
(48) Bontemps, N.; Grisolia, C.; Nerozzi, M.; Briat, B. Optical and magneto-optical study of the magnetic properties of $RbFeCl_3$, $RbFeBr_3$, and disordered materials of intermediate composition. *Journal of Applied Physics* **1982,** *53* (3), 2710-2712, DOI: 10.1063/1.330940.
(49) Harrison, A.; Visser, D. Magnetic ordering effects in the random mixed one-dimensional ferromagnet-antiferromagnet system $RbFeCl_{3-x}Br_x$. *Journal of Physics: Condensed Matter* **1989,** *1* (4), 733, DOI: 10.1088/0953-8984/1/4/008.
(50) Beck, H. P.; Schramm, M.; Haberkorn, R. The $InSnCl_3$-Type Arrangement: II. High Pressure Synthesis of $TlPbCl_3$ and of Solid Solutions Containing Rb or Br. *Journal of Solid State Chemistry* **1999,** *146* (2), 351-354, DOI: 10.1006/jssc.1999.8361.
(51) Wang, A.; Ding, R.; Li, Y.; Liu, M.; Yang, F.; Zhang, Y.; Fang, Q.; Yan, M.; Xie, J.; Chen, Z.; Yan, Z.; He, Y.; Guo, J.; Sun, X.; Liu, E. Redox Electrolytes-Assisting Aqueous Zn-Based Batteries by Pseudocapacitive Multiple Perovskite Fluorides Cathode and Charge Storage Mechanisms. *Small* **2023,** *n/a* (n/a), 2302333, DOI: 10.1002/smll.202302333.
(52) Yan, T.; Ding, R.; Huang, Y.; Ying, D.; Tan, C.; Huang, Y.; Yang, F.; Sun, X.; Gao, P.; Liu, E. A novel sodium-ion supercabattery based on vacancy defective Ni–Co–Mn ternary perovskite fluoride electrode materials. *Journal of Materials Chemistry A* **2021,** *9* (25), 14276-14284, DOI: 10.1039/D1TA02894D.
(53) Wang, T.; Fan, J.; Do-Thanh, C.-L.; Suo, X.; Yang, Z.; Chen, H.; Yuan, Y.; Lyu, H.; Yang, S.; Dai, S. Perovskite Oxide–Halide Solid Solutions: A Platform for Electrocatalysts. *Angewandte Chemie International Edition* **2021,** *60* (18), 9953-9958, DOI: 10.1002/anie.202101120.
(54) Wang, X.; Liu, G.; Tang, C.; Tang, H.; Zhang, W.; Ju, Z.; Jiang, J.; Zhuang, Q.; Cui, Y. A novel high entropy perovskite fluoride anode with 3D cubic framework for advanced lithium-ion battery. *Journal of Alloys and Compounds* **2023,** *934*, 167889, DOI: 10.1016/j.jallcom.2022.167889.
(55) Jia, Z.; Ding, R.; Yu, W.; Li, Y.; Wang, A.; Liu, M.; Yang, F.; Sun, X.; Liu, E. Unraveling the Charge Storage and Activity-Enhancing Mechanisms of Zn-Doping Perovskite Fluorides and Engineering the Electrodes and Electrolytes for Wide-Temperature Aqueous Supercabatteries. *Advanced Functional Materials* **2022,** *32* (1), 2107674, DOI: 10.1002/adfm.202107674.
(56) Yang, F.; Ding, R.; Jia, Z.; Yu, W.; Li, Y.; Wang, A.; Liu, M.; Xie, J.; Yan, M.; Fang, Q.; Zhang, Y.; Sun, X.; Liu, E. High specific energy and power sodium-based dual-ion supercabatteries by pseudocapacitive Ni-Zn-Mn ternary perovskite fluorides@reduced graphene oxides anodes with conversion-alloying-intercalation triple mechanisms. *Energy Storage Materials* **2022,** *53*, 222-237, DOI: 10.1016/j.ensm.2022.08.049.
(57) Yu, W.; Ding, R.; Jia, Z.; Li, Y.; Wang, A.; Liu, M.; Yang, F.; Sun, X.; Liu, E. Pseudocapacitive Co-Free Trimetallic Ni-Zn-Mn Perovskite Fluorides Enable Fast-Rechargeable

Zn-Based Aqueous Batteries. *Advanced Functional Materials* **2022,** *32* (19), 2112469, DOI: 10.1002/adfm.202112469.
(58) Huang, Y.; Ding, R.; Ying, D.; Huang, Y.; Tan, C.; Yan, T.; Sun, X.; Liu, E. A F-deficient and high-Mn ternary perovskite fluoride anode with a dominant conversion mechanism for advanced Li-ion batteries. *Chemical Communications* **2021,** *57* (62), 7705-7708, DOI: 10.1039/D1CC00910A.
(59) Huang, Y.-F.; Ding, R.; Ying, D.-F.; Huang, Y.-X.; Yan, T.; Tan, C.-N.; Sun, X.-J.; Liu, E.-H. A novel Li-ion supercapattery by K-ion vacant ternary perovskite fluoride anode with pseudocapacitive conversion/insertion dual mechanisms. *Rare Metals* **2022,** *41* (7), 2491-2504, DOI: 10.1007/s12598-022-01979-2.
(60) Jia, Z.; Shi, W.; Ding, R.; Yu, W.; Li, Y.; Tan, C.; Sun, X.; Liu, E. Conversion-type NiCoMn triple perovskite fluorides for advanced aqueous supercapacitors, batteries and supercapatteries. *Chemical Communications* **2021,** *57* (64), 7962-7965, DOI: 10.1039/D1CC02488D.
(61) Shi, W.; Yu, W.; Ding, R.; Jia, Z.; Li, Y.; Huang, Y.; Tan, C.; Sun, X.; Liu, E. Bipolar redox electrolyte-synergistically mediated NiCoMn-811 high-Ni ternary perovskite fluorides for advanced supercapacitors in both alkaline and neutral media. *Journal of Materials Chemistry A* **2021,** *9* (15), 9624-9633, DOI: 10.1039/D1TA01156A.
(62) Tan, C.; Ding, R.; Huang, Y.; Yan, T.; Huang, Y.; Yang, F.; Sun, X.; Gao, P.; Liu, E. A vacancy-rich perovskite fluoride $K_{0.79}Ni_{0.25}Co_{0.36}Mn_{0.39}F_{2.83}$@rGO anode for advanced Na-based dual-ion batteries. *Chemical Communications* **2021,** *57* (47), 5830-5833, DOI: 10.1039/D1CC01477C.
(63) Yan, T.; Huang, Y.; Ding, R.; Shi, W.; Ying, D.; Jia, Z.; Tan, C.; Huang, Y.; Sun, X.; Liu, E. Pseudocapacitive trimetallic NiCoMn-111 perovskite fluorides for advanced Li-ion supercabatteries. *Nanoscale Advances* **2021,** *3* (19), 5703-5710, DOI: 10.1039/D1NA00329A.
(64) Ying, D.; Li, Y.; Ding, R.; Shi, W.; Xu, Q.; Huang, Y.; Jia, Z.; Yu, W.; Sun, X.; Gao, P.; Liu, E.; Wang, X. Nanosilver-Promoted Trimetallic Ni–Co–Mn Perovskite Fluorides for Advanced Aqueous Supercabatteries with Pseudocapacitive Multielectrons Phase Conversion Mechanisms. *Advanced Functional Materials* **2021,** *31* (24), 2101353, DOI: 10.1002/adfm.202101353.
(65) Mao, H.; Wang, L.; Li, J.; Jiang, X.; Xue, S.; Li, M.; Zhu, J.; Fan, B.; Xu, T.; Shao, G.; Xu, H.; Wang, H.; Zhang, R.; Lu, H. High-Entropy $Cs(Pb_{1/3}Mn_{1/3}Ni_{1/3})Br_3$ Perovskite Nanocrystals Prepared by High Energy Ball Milling and their Luminescence Properties. *Particle & Particle Systems Characterization* **2022,** *39* (9), 2200073, DOI: 10.1002/ppsc.202200073.
(66) Amgar, D.; Binyamin, T.; Uvarov, V.; Etgar, L. Near ultra-violet to mid-visible band gap tuning of mixed cation $Rb_xCs_{1-x}PbX_3$ (X = Cl or Br) perovskite nanoparticles. *Nanoscale* **2018,** *10* (13), 6060-6068, DOI: 10.1039/C7NR09607K.
(67) Linaburg, M. R.; McClure, E. T.; Majher, J. D.; Woodward, P. M. $Cs_{1-x}Rb_xPbCl_3$ and $Cs_{1-x}Rb_xPbBr_3$ Solid Solutions: Understanding Octahedral Tilting in Lead Halide Perovskites. *Chemistry of Materials* **2017,** *29* (8), 3507-3514, DOI: 10.1021/acs.chemmater.6b05372.
(68) Jia, W.; Wei, Q.; Ge, S.; Peng, C.; Huang, T.; Yao, S.; Tian, Y.; Chang, T.; Zeng, R.; Zou, B. Polaronic Magnetic Excitons and Photoluminescence in Mn^{2+}-Doped $CsCdBr_3$ Metal Halides. *The Journal of Physical Chemistry C* **2021,** *125* (32), 18031-18039, DOI: 10.1021/acs.jpcc.1c05127.

(69) Lahoz, F.; Alonso, P. J.; Villacampa, B.; Alcala, R. Spectroscopic properties of Mn^{2+} ions in mixed fluoroperovskites. *Radiation Effects and Defects in Solids* **1995,** *135* (1-4), 163-167, DOI: 10.1080/10420159508229827.
(70) Lahoz, F.; Díaz, M.; Villacampa, B.; Cases, R.; Alcalá, R. Influence of the host lattice on the photoluminescence of Ni^{2+} ions in $Rb_{1-x}Cs_xCaF_3$ and $RbCa_{1-x}Cd_xF_3$ crystals. *Journal of Applied Physics* **1997,** *82* (10), 5121-5125, DOI: 10.1063/1.366314.
(71) Ghigna, P.; Scavini, M.; Mazzoli, C.; Brunelli, M.; Laurenti, C.; Ferrero, C. Experimental disentangling of orbital and lattice energy scales by inducing cooperative Jahn-Teller melting in $KCu_{1-x}Mg_xF_3$ solid solutions. *Physical Review B* **2010,** *81* (7), 073107, DOI: 10.1103/PhysRevB.81.073107.
(72) Oliva, C.; Scavini, M.; Cappelli, S.; Bottalo, C.; Mazzoli, C.; Ghigna, P. Melting of Orbital Ordering in $KMg_xCu_{1-x}F_3$ Solid Solution. *The Journal of Physical Chemistry B* **2007,** *111* (21), 5976-5983, DOI: 10.1021/jp067539p.
(73) Fleury, P. A.; Hayes, W.; Guggenheim, H. J. Magnetic scattering of light in K(NiMg)F3. *Journal of Physics C: Solid State Physics* **1975,** *8* (13), 2183, DOI: 10.1088/0022-3719/8/13/027.
(74) Karmakar, A.; Bhattacharya, A.; Bernard, G. M.; Mar, A.; Michaelis, V. K. Revealing the Local Sn and Pb Arrangements in $CsSn_xPb_{1-x}Br_3$ Perovskites with Solid-State NMR Spectroscopy. *ACS Materials Letters* **2021,** *3* (3), 261-267, DOI: 10.1021/acsmaterialslett.0c00596.
(75) Zhang, X.; Cao, W.; Wang, W.; Xu, B.; Liu, S.; Dai, H.; Chen, S.; Wang, K.; Sun, X. W. Efficient light-emitting diodes based on green perovskite nanocrystals with mixed-metal cations. *Nano Energy* **2016,** *30*, 511-516, DOI: 10.1016/j.nanoen.2016.10.039.
(76) Suzuki, T.; Guo, H.; Kawasaki, I.; Watanabe, I.; Goto, T.; Katayama, K.; Tanaka, H. Disappearance of Gapped Mott Insulating Phase Neighboring Bose Glass Phase in $Tl_{1-x}K_xCuCl_3$ Detected by Longitudinal-Field Muon Spin Relaxation. *Journal of the Physical Society of Japan* **2014,** *83* (8), 084703, DOI: 10.7566/JPSJ.83.084703.
(77) Suzuki, T.; Yamada, F.; Watanabe, I.; Goto, T.; Oosawa, A.; Tanaka, H. Bond-randomness effect on the quantum spin system $Tl_{1-x}K_xCuCl_3$ probed by muon-spin-relaxation method. *Physica B: Condensed Matter* **2009,** *404* (5), 590-593, DOI: 10.1016/j.physb.2008.11.108.
(78) Yamada, F.; Tanaka, H.; Ono, T.; Nojiri, H. Transition from Bose glass to a condensate of triplons in $Tl_{1-x}K_xCuCl_3$. *Physical Review B* **2011,** *83* (2), 020409, DOI: 10.1103/PhysRevB.83.020409.
(79) Chartrand, P.; Pelton, A. D. Thermodynamic Evaluation and Optimization of the LiCl-NaCl-KCl-RbCl-CsCl-$MgCl_2$-$CaCl_2$-$SrCl_2$ System Using The Modified Quasichemical Model. *Canadian Metallurgical Quarterly* **2000,** *39* (4), 405-420, DOI: 10.1179/cmq.2000.39.4.405.
(80) Chornodolskyy, Y.; Stryganyuk, G.; Syrotyuk, S.; Voloshinovskii, A.; Rodnyi, P. Features of the core–valence luminescence and electron energy band structure of $A_{1-x}Cs_xCaCl_3$ (A = K,Rb) crystals. *Journal of Physics: Condensed Matter* **2007,** *19* (47), 476211, DOI: 10.1088/0953-8984/19/47/476211.
(81) Takahashi, K.; Koshimizu, M.; Fujimoto, Y.; Yanagida, T.; Asai, K. Auger-free luminescence characteristics of $Rb_{1-x}Cs_xCaCl_3$. *Journal of the Ceramic Society of Japan* **2018,** *126* (10), 755-760, DOI: 10.2109/jcersj2.18051.
(82) Vaněček, V.; Páterek, J.; Král, R.; Kučerková, R.; Babin, V.; Rohlíček, J.; Cala', R.; Kratochwil, N.; Auffray, E.; Nikl, M. (INVITED) Ultraviolet cross-luminescence in ternary chlorides of alkali and alkaline-earth metals. *Optical Materials: X* **2021,** *12*, 100103, DOI: 10.1016/j.omx.2021.100103.

(83) Dong, Q.; Tian, B.; Zhang, W.; He, L. Facile synthesis of $K_aCs_{1-a}PbBr_3$@ molecular sieve SBA-15 composite with improved luminescence and wet/thermal stability. *Colloids and Surfaces A: Physicochemical and Engineering Aspects* **2022,** *648*, 129258, DOI: 10.1016/j.colsurfa.2022.129258.
(84) Shao, G.; Liu, S.; Ding, L.; Zhang, Z.; Xiang, W.; Liang, X. $K_xCs_{1-x}PbBr_3$ NCs glasses possessing super optical properties and stability for white light emitting diodes. *Chemical Engineering Journal* **2019,** *375*, 122031, DOI: 10.1016/j.cej.2019.122031.
(85) Dintakurti, S. H. S. S. Phase evolution and local structure in [Cs, MA][Pb, Sr][Cl, Br]$_3$ perovskites. Doctoral Nanyang Technological University, 2021.
(86) Dance, J.-M.; Grannec, J.; Tressand, A. *Comptes rendus de l'Académie des Sciences* **1975,** *C281*, 91.
(87) Hu, M.; Chen, M.; Guo, P.; Zhou, H.; Deng, J.; Yao, Y.; Jiang, Y.; Gong, J.; Dai, Z.; Zhou, Y.; Qian, F.; Chong, X.; Feng, J.; Schaller, R. D.; Zhu, K.; Padture, N. P.; Zhou, Y. Sub-1.4eV bandgap inorganic perovskite solar cells with long-term stability. *Nature Communications* **2020,** *11* (1), 151, DOI: 10.1038/s41467-019-13908-6.
(88) Hu, M.; Zhang, Y.; Gong, J.; Zhou, H.; Huang, X.; Liu, M.; Zhou, Y.; Yang, S. Surface Sn(IV) Hydrolysis Improves Inorganic Sn–Pb Perovskite Solar Cells. *ACS Energy Letters* **2023,** *8* (2), 1035-1041, DOI: 10.1021/acsenergylett.2c02435.
(89) Liu, M.; Pasanen, H.; Ali-Löytty, H.; Hiltunen, A.; Lahtonen, K.; Qudsia, S.; Smått, J.-H.; Valden, M.; Tkachenko, N. V.; Vivo, P. B-Site Co-Alloying with Germanium Improves the Efficiency and Stability of All-Inorganic Tin-Based Perovskite Nanocrystal Solar Cells. *Angewandte Chemie International Edition* **2020,** *59* (49), 22117-22125, DOI: 10.1002/anie.202008724.
(90) Borsa, F.; Benard, D. J.; Walker, W. C.; Baviera, A. NMR and birefringence study of structural transitions in disordered crystals: $Rb_xK_{1-x}MnF_3$. *Physical Review B* **1977,** *15* (1), 84-94, DOI: 10.1103/PhysRevB.15.84.
(91) Cousseins, J. C. Etude dans l'etat solide de quelques fluorures ternaires: Synthese; identification; filiation; miscibilite. *Rev. chim. minér* **1964,** *1*, 573-616.
(92) Kapusta, J.; Ph, D.; Ratuszna, A. Vibrational investigation and phase transitions in the $KMnF_3$ doped perovskite crystals (Li^+, Na^+, Rb^+ and Cs^+). *Journal of Physics: Condensed Matter* **2002,** *14* (21), 5433, DOI: 10.1088/0953-8984/14/21/317.
(93) Todorović, P.; Ma, D.; Chen, B.; Quintero-Bermudez, R.; Saidaminov, M. I.; Dong, Y.; Lu, Z.-H.; Sargent, E. H. Spectrally Tunable and Stable Electroluminescence Enabled by Rubidium Doping of $CsPbBr_3$ Nanocrystals. *Advanced Optical Materials* **2019,** *7* (24), 1901440, DOI: 10.1002/adom.201901440.
(94) Wu, H.; Yang, Y.; Zhou, D.; Li, K.; Yu, J.; Han, J.; Li, Z.; Long, Z.; Ma, J.; Qiu, J. Rb^+ cations enable the change of luminescence properties in perovskite ($Rb_xCs_{1-x}PbBr_3$) quantum dots. *Nanoscale* **2018,** *10* (7), 3429-3437, DOI: 10.1039/C7NR07776A.
(95) Lahoz, F.; Villacampa, B.; Alcalá, R.; Marquina, C.; Ibarra, M. R. Cubic-to-tetragonal structural phase transition in $Rb_{1-x}Cs_xCaF_3$ solid solutions: Thermal expansion and EPR studies. *Physical Review B* **1997,** *55* (13), 8148-8154, DOI: 10.1103/PhysRevB.55.8148.
(96) Deng, J.; Xun, J.; Shen, W.; Li, M.; He, R. Phase Regulation of $CsPb_2Br_5$/$CsPbBr_3$ Perovskite Nanocrystals by Doping with Divalent Cations: Implications for Optoelectronic Devices with Enhanced Stability and Reduced Toxicity. *ACS Applied Nano Materials* **2021,** *4* (9), 9213-9222, DOI: 10.1021/acsanm.1c01737.

(97) Straus, D. B.; Cava, R. J. Tuning the Band Gap in the Halide Perovskite $CsPbBr_3$ through Sr Substitution. *ACS Applied Materials & Interfaces* **2022,** *14* (30), 34884-34890, DOI: 10.1021/acsami.2c09275.
(98) Tanaka, H.; Iio, K.; Nagata, K. Magnetic properties of $Rb_{1-x}K_xNiCl_3$, $RbVBr_3$ and $CsNiI_3$. *Journal of Magnetism and Magnetic Materials* **1992,** *104-107*, 829-830, DOI: 10.1016/0304-8853(92)90380-7.
(99) Bernasconi, A.; Rizzo, A.; Listorti, A.; Mahata, A.; Mosconi, E.; De Angelis, F.; Malavasi, L. Synthesis, Properties, and Modeling of $Cs_{1-x}Rb_xSnBr_3$ Solid Solution: A New Mixed-Cation Lead-Free All-Inorganic Perovskite System. *Chemistry of Materials* **2019,** *31* (9), 3527-3533, DOI: 10.1021/acs.chemmater.9b00837.
(100) Daniel, P.; Toulouse, J.; Rousseau, M. Phase transitions in mixed disordered crystals $Rb_{1-x}K_xCaF_3$ ($0 < x < 1$) investigated by Raman spectroscopy. *Eur. Phys. J. AP* **1999,** *5* (1), 33-44, DOI: 10.1051/epjap:1999109.
(101) Jouanneaux, A.; Ph, D.; Bushnell-Wye, G. Structural instabilities in disordered perovskites studied by synchrotron radiation powder diffraction. Proposition for a phase diagram. *Journal of Physics: Condensed Matter* **1998,** *10* (24), 5485, DOI: 10.1088/0953-8984/10/24/024.
(102) Rebrova, N. V.; Grippa, A. Y.; Boiaryntseva, I. A.; Berastegui, P.; Gorbacheva, T. E.; Datsko, Y. N.; Rebrov, A. L.; Dujardin, C.; Calà, R.; Martinazzoli, L.; Auffray, E.; Kononets, V. V. Effects of europium concentration on luminescent and scintillation performance of $Cs_{0.2}Rb_{0.8}Ca_{1-x}Eu_xBr_3$ ($0 \leq x \leq 0.08$) crystals. *Journal of Rare Earths* **2022,** *40* (1), 29-33, DOI: 10.1016/j.jre.2020.08.012.
(103) Rebrova, N. V.; Grippa, A. Y.; Boiaryntseva, I. A.; Berastegui, P.; Gorbacheva, T. E.; Pedash, V. Y.; Galkin, S. N.; Kononets, V. V.; Datsko, Y. N.; Cherginets, V. L. Crystal growth and characterization of Eu^{2+} doped $Cs_{1-x}Rb_xCaBr_3$. *Journal of Alloys and Compounds* **2020,** *816*, 152594, DOI: 10.1016/j.jallcom.2019.152594.
(104) Hidaka, M.; Zhou, Z. Y.; Yamashita, S. Structural phase transitions in $KCdF_3$ and $K_{0.5}Rb_{0.5}CdF_3$. *Phase Transitions* **1990,** *20* (1-2), 83-94, DOI: 10.1080/01411599008206869.
(105) He, S.; Qiang, Q.; Lang, T.; Cai, M.; Han, T.; You, H.; Peng, L.; Cao, S.; Liu, B.; Jing, X.; Jia, B. Highly Stable Orange-Red Long-Persistent Luminescent $CsCdCl_3:Mn^{2+}$ Perovskite Crystal. *Angewandte Chemie International Edition* **2022,** *61* (48), e202208937, DOI: 10.1002/anie.202208937.
(106) Jia, W.; Wei, Q.; Yao, S.; Ge, S.; Peng, C.; Wang, L.; Zhong, X.; peng, H.; Zou, B. Magnetic coupling for highly efficient and tunable emission in $CsCdX_3$:Mn perovskites. *Journal of Luminescence* **2023,** *257*, 119657, DOI: 10.1016/j.jlumin.2022.119657.
(107) Wu, S.; Yuan, L.; Chen, G.; Peng, C.; Jin, Y. All-inorganic Mn^{2+}-doped metal halide perovskite crystals for the late-time detection of X-ray afterglow imaging. *Nanoscale* **2023,** *15* (33), 13628-13634, DOI: 10.1039/D3NR02208K.
(108) Men, L.; Rosales, B. A.; Gentry, N. E.; Cady, S. D.; Vela, J. Lead-Free Semiconductors: Soft Chemistry, Dimensionality Control, and Manganese-Doping of Germanium Halide Perovskites. *ChemNanoMat* **2019,** *5* (3), 334-339, DOI: 10.1002/cnma.201800497.
(109) Ratuszna, A.; Kapusta, J. Structural phase transitions in $KMnF_3$ doped by Li^+, Na^+ and Rb^+. *Phase Transitions* **1997,** *62* (3), 181-198, DOI: 10.1080/01411599708220068.
(110) Shafer, M. W.; McGuire, T. R. Preparation and properties of ferrimagnets in the $RbMgF_3$-$RbCoF_3$ system. *Journal of Physics and Chemistry of Solids* **1969,** *30* (8), 1989-1997, DOI: 10.1016/0022-3697(69)90177-2.

(111) Chen, M.; Ju, M.-G.; Garces, H. F.; Carl, A. D.; Ono, L. K.; Hawash, Z.; Zhang, Y.; Shen, T.; Qi, Y.; Grimm, R. L.; Pacifici, D.; Zeng, X. C.; Zhou, Y.; Padture, N. P. Highly stable and efficient all-inorganic lead-free perovskite solar cells with native-oxide passivation. *Nature Communications* **2019,** *10* (1), 16, DOI: 10.1038/s41467-018-07951-y.
(112) Kama, A.; Tirosh, S.; Itzhak, A.; Ejgenberg, M.; Cahen, D. New Pb-Free Stable Sn–Ge Solid Solution Halide Perovskites Fabricated by Spray Deposition. *ACS Applied Energy Materials* **2022,** *5* (3), 3638-3646, DOI: 10.1021/acsaem.1c04115.
(113) Lv, H.; Tang, X.; Chen, M. Ionic Doping of $CsPbI_3$ Perovskite Nanocrystals Improves Luminescence and Stability in Patterned Large-Area Light-Emitting Diodes. *ACS Applied Nano Materials* **2023,** *6* (20), 18918-18925, DOI: 10.1021/acsanm.3c03358.
(114) Buyers, W. J. L.; Pepper, D. E.; Elliott, R. J. Theory of spin waves in disordered antiferromagnets. I. Application to (Mn, Co)F_2 and K(Mn, Co)F_3. *Journal of Physics C: Solid State Physics* **1972,** *5* (18), 2611, DOI: 10.1088/0022-3719/5/18/011.
(115) Dzyub, I. P. Cluster Theory of Spin Excitations of Mixed Antiferromagnets. Application to $Mn_cCo_{1-c}F_2$ and $KMn_CCo_{1-c}F_3$. *physica status solidi (b)* **1974,** *66* (1), 339-347, DOI: 10.1002/pssb.2220660138.
(116) Komura, H.; Shapiro, M. M.; Stevenson, R. Exciton-magnon cross excitation in the mixed substitutional system $KMn_{1-x}Co_xF_3$. *Physical Review B* **1974,** *9* (8), 3266-3269, DOI: 10.1103/PhysRevB.9.3266.
(117) Chakhmouradian, A. R.; Ross, K.; Mitchell, R. H.; Swainson, I. The crystal chemistry of synthetic potassium-bearing neighborite, $(Na_{1-x}K_x)MgF_3$. *Physics and Chemistry of Minerals* **2001,** *28* (4), 277-284, DOI: 10.1007/s002690100151.
(118) Chartrand, P.; Pelton, A. D. Thermodynamic evaluation and optimization of the LiF-NaF-KF-MgF_2-CaF_2 system using the modified quasi-chemical model. *Metallurgical and Materials Transactions A* **2001,** *32* (6), 1385-1396, DOI: 10.1007/s11661-001-0228-1.
(119) Martin, C. D.; Chaudhur, S.; Grey, C. P.; Parise, J. B. Effect of A-site cation radius on ordering of BX_6 octahedra in (K,Na)MgF_3 perovskite. *American Mineralogist* **2005,** *90* (10), 1522-1533, DOI: 10.2138/am.2005.1693.
(120) Zhao, Y. Crystal Chemistry and Phase Transitions of Perovskite in P–T–X Space: Data for $(K_xNa_{1-x})MgF_3$ Perovskites. *Journal of Solid State Chemistry* **1998,** *141* (1), 121-132, DOI: 10.1006/jssc.1998.7927.
(121) Schmidt, R. E.; Welsch, M.; Kummer-Dörner, S.; Babel, D. Einkristallstrukturuntersuchungen an hexagonalen Fluorperowskiten $AMIIF_3$ (MII=Mg, Mn, Fe, Co, Ni). *Zeitschrift für anorganische und allgemeine Chemie* **1999,** *625* (4), 637-642, DOI: 10.1002/(SICI)1521-3749(199904)625:4<637::AID-ZAAC637>3.0.CO;2-N.
(122) Huang, X.; Hu, J.; Bi, C.; Yuan, J.; Lu, Y.; Sui, M.; Tian, J. B-site doping of $CsPbI_3$ quantum dot to stabilize the cubic structure for high-efficiency solar cells. *Chemical Engineering Journal* **2021,** *421*, 127822, DOI: 10.1016/j.cej.2020.127822.
(123) Skurlov, I. D.; Sokolova, A. V.; Tatarinov, D. A.; Parfenov, P. S.; Kurshanov, D. A.; Ismagilov, A. O.; Koroleva, A. V.; Danilov, D. V.; Zhizhin, E. V.; Mikushev, S. V.; Tcypkin, A. N.; Fedorov, A. V.; Litvin, A. P. Engineering the Optical Properties of $CsPbBr_3$ Nanoplatelets through Cd^{2+} Doping. *Materials* **2022,** *15* (21), 7676, DOI: 10.3390/ma15217676.
(124) Skurlov, I. D.; Yin, W.; Ismagilov, A. O.; Tcypkin, A. N.; Hua, H.; Wang, H.; Zhang, X.; Litvin, A. P.; Zheng, W. Improved One- and Multiple-Photon Excited Photoluminescence from Cd^{2+}-Doped $CsPbBr_3$ Perovskite NCs. *Nanomaterials* **2022,** *12* (1), 151, DOI: 10.3390/nano12010151.

(125) Retuerto, M.; Yin, Z.; Emge, T. J.; Stephens, P. W.; Li, M.-R.; Sarkar, T.; Croft, M. C.; Ignatov, A.; Yuan, Z.; Zhang, S. J.; Jin, C.; Paria Sena, R.; Hadermann, J.; Kotliar, G.; Greenblatt, M. Hole Doping and Structural Transformation in $CsTl_{1-x}Hg_xCl_3$. *Inorganic Chemistry* **2015,** *54* (3), 1066-1075, DOI: 10.1021/ic502400d.
(126) Lin, C.-Q.; Liu, M.-L.; Yang, Z.; Wang, H.; Pan, C.-Y. Mn^{2+} doped $CsPbBr_3$ perovskite quantum dots with high quantum yield and stability for flexible array displays. *Journal of Solid State Chemistry* **2023,** *327*, 124295, DOI: 10.1016/j.jssc.2023.124295.
(127) Yang, Z.; Yuan, X.; Song, Y.; Chen, M.; Xing, K.; Cao, S.; Zheng, J.; Zhao, J. Thickness-Dependent Photoluminescence Properties of Mn-Doped $CsPbBr_3$ Perovskite Nanoplatelets Synthesized at Room Temperature. *The Journal of Physical Chemistry C* **2023,** *127* (43), 21227-21234, DOI: 10.1021/acs.jpcc.3c05639.
(128) Lockwood, D. J.; Coombs, G. J.; Cowley, R. A. Light scattering from the mixed antiferromagnet $KNi_xMn_{1-x}F_3$. *Journal of Physics C: Solid State Physics* **1979,** *12* (21), 4611, DOI: 10.1088/0022-3719/12/21/025.
(129) Skrzypek, D. Critical Behaviour of the Magnetic Resonance in $KNi_xMn_{1-x}F_3$. *physica status solidi (b)* **1990,** *157* (2), 695-700, DOI: 10.1002/pssb.2221570222.
(130) Skrzypek, D. Antiferromagnetic resonance in $KNi_xMn_{1-x}F_3$ crystals. *Physica B: Condensed Matter* **1995,** *205* (3), 279-284, DOI: 10.1016/0921-4526(94)00611-X.
(131) Harrison, A.; Visser, D.; Day, P.; Knop, W.; Steiner, M. Magnetic ordering effects in the random singlet-magnetic ground state system $Rb_{(1-x)}Cs_xFeCl_3$. *Journal of Physics C: Solid State Physics* **1986,** *19* (34), 6811, DOI: 10.1088/0022-3719/19/34/018.
(132) Ratuszna, A. The crystal structures of $(K_xNa_{1-x})MnF_3$ perovskite-type compounds. *Phase Transitions* **1984,** *4* (3), 217-223, DOI: 10.1080/01411598408218596.
(133) Ratuszna, A. Determination of structure distortions in $KMnF_3$ doped with Na^+. *Zeitschrift fur Kristallographie* **1988,** *185*, 521.
(134) Ratuszna, A.; Daniel, P.; Kapusta, J.; Rousseau, M. Experimental evidence for glasslike behavior in a $KMnF_3$: Na^+ crystal from x-ray diffraction and Raman scattering. *Physical Review B* **1998,** *57* (17), 10470-10475, DOI: 10.1103/PhysRevB.57.10470.
(135) Vehse, W. E.; Sherrill, F. A.; Riley, C. R. Lattice Constants for $KMg_{(1-x)}Mn_xF_3$ Crystals. *Journal of Applied Physics* **1972,** *43* (3), 1320-1321, DOI: 10.1063/1.1661275.
(136) Elliott, N.; Pauling, L. The Crystal Structure of Cesium Aurous Auric Chloride, $Cs_2AuAuCl_6$, and Cesium Argentous Auric Chloride, $Cs_2AgAuCl_6$. *Journal of the American Chemical Society* **1938,** *60* (8), 1846-1851, DOI: 10.1021/ja01275a037.
(137) Chartrand, P.; Pelton, A. D. Thermodynamic Evaluation and Optimization of the LiCl-NaCl-KCl-RbCl-CsCl-$MgCl_2$-$CaCl_2$-$SrCl_2$-$BaCl_2$ System Using the Modified Quasichemical Model. *Canadian Metallurgical Quarterly* **2001,** *40* (1), 13-32, DOI: 10.1179/cmq.2001.40.1.13.
(138) Buzare, J. Y.; Foucher, P. Disorder and phase transitions in $Rb_{1-x}K_xCaF_3$: an electron paramagnetic resonance investigation. *Journal of Physics: Condensed Matter* **1991,** *3* (15), 2535, DOI: 10.1088/0953-8984/3/15/009.
(139) Flocken, J. W.; Smith, R. W.; Hardy, J. R.; Stevenson, E. S.; Swearingen, J. Phase transitions in mixed alkali calcium trifluoride solid solutions. *Materials Research Bulletin* **1996,** *31* (9), 1093-1099, DOI: 10.1016/0025-5408(96)00099-2.
(140) Ratuszna, A.; Daniel, P.; Rousseau, M. Optical and X-ray evidence of structural phase transitions in mixed $(Rb_{1-x}K_x)CaF_3$ crystals. *Phase Transitions* **1995,** *54* (1), 43-59, DOI: 10.1080/01411599508200403.

(141) Rousseau, M.; Daniel, P.; Toulouse, J.; Hennion, B. Evidence of disorder in the perovskite crystals $RbCaF_3$ and $Rb_{0.65}K_{0.35}CaF_3$ investigation of phonon acoustic modes by inelastic neutron scattering. *Physica B: Condensed Matter* **1997,** *234-236*, 139-141, DOI: 10.1016/S0921-4526(96)00928-3.
(142) Shen, L.; Zhang, Z.; Zhao, Y.; Yang, H.; Yuan, L.; Chen, Y.; Xiang, W.; Liang, X. Synthesis and optical properties of novel mixed-metal cation $CsPb_{1-x}Ti_xBr_3$-based perovskite glasses for W-LED. *Journal of the American Ceramic Society* **2020,** *103* (1), 382-390, DOI: 10.1111/jace.16760.
(143) Wu, Z.; Zhang, Q.; Li, B.; Shi, Z.; Xu, K.; Chen, Y.; Ning, Z.; Mi, Q. Stabilizing the $CsSnCl_3$ Perovskite Lattice by B-Site Substitution for Enhanced Light Emission. *Chemistry of Materials* **2019,** *31* (14), 4999-5004, DOI: 10.1021/acs.chemmater.9b00433.
(144) Inami, T.; Asano, T.; Ajiro, Y.; Goto, T. Magnetization process of the one-dimensional Ising-like antiferromagnet with nonmagnetic impurity, $CsCo_{1-x}Mg_xCl_3$. *Physica B: Condensed Matter* **1994,** *201*, 204-207, DOI: 10.1016/0921-4526(94)91084-7.
(145) Ohta, H.; Imagawa, S.; Motokawa, M.; Ikeda, H. Electron Paramagnetic Resonance of $CsCo_xMg_{1-x}Cl_3$ and the Determination of Exchange Interactions. *Journal of the Physical Society of Japan* **1993,** *62* (7), 2481-2489, DOI: 10.1143/JPSJ.62.2481.
(146) Mei, E.; Chen, Y.; Chen, Y.; He, Q.; Tong, Y.; Yu, P.; Liang, X.; Xiang, W. Ba-doped $CsPbBr_3$ with high quantum efficiency for wide color gamut on white light-emitting diodes. *Applied Physics Letters* **2021,** *119* (25), DOI: 10.1063/5.0070326.
(147) Liu, H.; Wu, Z.; Shao, J.; Yao, D.; Gao, H.; Liu, Y.; Yu, W.; Zhang, H.; Yang, B. $CsPb_xMn_{1-x}Cl_3$ Perovskite Quantum Dots with High Mn Substitution Ratio. *ACS Nano* **2017,** *11* (2), 2239-2247, DOI: 10.1021/acsnano.6b08747.
(148) Zhang, X.; Wang, F.; Wang, Y.; Wu, X.; Ou, Q.; Zhang, S. Boosting the Photoluminescence Quantum Yield and Stability of Lead-Free $CsEuCl_3$ Nanocrystals via Ni^{2+} Doping. *The Journal of Physical Chemistry Letters* **2023,** *14* (24), 5580-5585, DOI: 10.1021/acs.jpclett.3c01046.
(149) Hu, Y.; Zhang, X.; Yang, C.; Li, J.; Wang, L. Fe^{2+} doped in $CsPbCl_3$ perovskite nanocrystals: impact on the luminescence and magnetic properties. *RSC Advances* **2019,** *9* (57), 33017-33022, DOI: 10.1039/C9RA07069A.
(150) Elbinger, G.; Funke, A.; Kleinert, P.; Rosemann, P.; Keilig, W. Präparation und Eigenschaften von Metallfluoridverbindungen des Typs $Me^{I}Me^{II}F_3$. *Zeitschrift für anorganische und allgemeine Chemie* **1972,** *393* (3), 193-206, DOI: 10.1002/zaac.19723930302.
(151) Shi, W.; Zhang, X.; Chen, H. S.; Matras-Postolek, K.; Yang, P. Transition metal halide derived phase transition from Cs_4PbCl_6 to $CsPb_xM_{1-x}X_3$ for bright white light-emitting diodes. *Journal of Materials Chemistry C* **2021,** *9* (17), 5732-5739, DOI: 10.1039/D1TC01150B.
(152) Rogge, R. B.; Yang, Y. S.; Tun, Z.; Gaulin, B. D.; Fernandez-Baca, J. A.; Nicklow, R. M.; Harrison, A. A neutron scattering study of the quasi-one-dimensional, dilute Ising-like antiferromagnet $CsCo_{0.83}Mg_{0.17}Br_3$. *Journal of Applied Physics* **1993,** *73* (10), 6451-6453, DOI: 10.1063/1.352630.
(153) van Duijn, J.; Gaulin, B. D.; Lumsden, M. A.; Castellan, J. P.; Buyers, W. J. L. Random Fields and the Partially Paramagnetic State of $CsCo_{0.83}Mg_{0.17}Br_3$: Critical Scattering Study. *Physical Review Letters* **2004,** *92* (7), 077202, DOI: 10.1103/PhysRevLett.92.077202.
(154) Yang, Y. S.; Marsiglio, F.; Madsen, M.; Gaulin, B. D.; Rogge, R. B.; Fernandez-Baca, J. A. Spin-wave response in the dilute quasi-one-dimensional Ising-like antiferromagnet

$CsCo_{0.83}Mg_{0.17}Br_3$. *Physical Review B* **2002,** *65* (21), 212408, DOI: 10.1103/PhysRevB.65.212408.
(155) Yao, J.-S.; Ge, J.; Han, B.-N.; Wang, K.-H.; Yao, H.-B.; Yu, H.-L.; Li, J.-H.; Zhu, B.-S.; Song, J.-Z.; Chen, C.; Zhang, Q.; Zeng, H.-B.; Luo, Y.; Yu, S.-H. Ce^{3+}-Doping to Modulate Photoluminescence Kinetics for Efficient $CsPbBr_3$ Nanocrystals Based Light-Emitting Diodes. *Journal of the American Chemical Society* **2018,** *140* (10), 3626-3634, DOI: 10.1021/jacs.7b11955.
(156) Chen, R.; Xu, Y.; Wang, S.; Xia, C.; Liu, Y.; Yu, B.; Xuan, T.; Li, H. Zinc ions doped cesium lead bromide perovskite nanocrystals with enhanced efficiency and stability for white light-emitting diodes. *Journal of Alloys and Compounds* **2021,** *866*, 158969, DOI: 10.1016/j.jallcom.2021.158969.
(157) Cui, K.; Wen, Y.; Han, X.; Hao, Z.; Zhang, J.; Xie, J. Intense blue emission from one-pot synthesized quaternary $CsZn_xPb_{1-x}Br_3$ perovskite quantum dots. *Optical Materials* **2023,** *136*, 113441, DOI: 10.1016/j.optmat.2023.113441.
(158) Tran, P.-N.; Phan, H.-H.; Luu, T.-N.; Tran, Q.-H.; Duong, T.-T. Optimizing the single-source flash thermal evaporation process of Zn-doped $CsPbBr_3$ films for enhanced performance in perovskite LEDs. *Applied Physics A* **2023,** *130* (1), 20, DOI: 10.1007/s00339-023-07179-8.
(159) Shen, X.; Zhang, Y.; Kershaw, S. V.; Li, T.; Wang, C.; Zhang, X.; Wang, W.; Li, D.; Wang, Y.; Lu, M.; Zhang, L.; Sun, C.; Zhao, D.; Qin, G.; Bai, X.; Yu, W. W.; Rogach, A. L. Zn-Alloyed $CsPbI_3$ Nanocrystals for Highly Efficient Perovskite Light-Emitting Devices. *Nano Letters* **2019,** *19* (3), 1552-1559, DOI: 10.1021/acs.nanolett.8b04339.
(160) Wu, Y.; Li, Q.; Chakoumakos, B. C.; Zhuravleva, M.; Lindsey, A. C.; Johnson II, J. A.; Stand, L.; Koschan, M.; Melcher, C. L. Quaternary Iodide $K(Ca,Sr)I_3:Eu^{2+}$ Single-Crystal Scintillators for Radiation Detection: Crystal Structure, Electronic Structure, and Optical and Scintillation Properties. *Advanced Optical Materials* **2016,** *4* (10), 1518-1532, DOI: 10.1002/adom.201600239.
(161) Wu, Y.; Zhuravleva, M.; Lindsey, A. C.; Koschan, M.; Melcher, C. L. Eu^{2+} concentration effects in $KCa_{0.8}Sr_{0.2}I_3:Eu^{2+}$: A novel high-performance scintillator. *Nuclear Instruments and Methods in Physics Research Section A: Accelerators, Spectrometers, Detectors and Associated Equipment* **2016,** *820*, 132-140, DOI: 10.1016/j.nima.2016.03.027.
(162) Kim, S.-Y.; Lee, H.-C.; Nam, Y.; Yun, Y.; Lee, S.-H.; Kim, D. H.; Noh, J. H.; Lee, J.-H.; Kim, D.-H.; Lee, S.; Heo, Y.-W. Ternary diagrams of the phase, optical bandgap energy and photoluminescence of mixed-halide perovskites. *Acta Materialia* **2019,** *181*, 460-469, DOI: 10.1016/j.actamat.2019.10.008.
(163) Meng, F.; Liu, X.; Cai, X.; Gong, Z.; Li, B.; Xie, W.; Li, M.; Chen, D.; Yip, H.-L.; Su, S.-J. Incorporation of rubidium cations into blue perovskite quantum dot light-emitting diodes via FABr-modified multi-cation hot-injection method. *Nanoscale* **2019,** *11* (3), 1295-1303, DOI: 10.1039/C8NR07907B.
(164) Otero-Martínez, C.; Imran, M.; Schrenker, N. J.; Ye, J.; Ji, K.; Rao, A.; Stranks, S. D.; Hoye, R. L. Z.; Bals, S.; Manna, L.; Pérez-Juste, J.; Polavarapu, L. Fast A-Site Cation Cross-Exchange at Room Temperature: Single-to Double- and Triple-Cation Halide Perovskite Nanocrystals. *Angewandte Chemie International Edition* **2022,** *61* (34), e202205617, DOI: 10.1002/anie.202205617.
(165) Gunasekaran, R. K.; Jung, J.; Yang, S. W.; Yun, J.; Yun, Y.; Vidyasagar, D.; Choi, W. C.; Lee, C.-L.; Noh, J. H.; Kim, D. H.; Lee, S. High-throughput compositional mapping of triple-

cation tin–lead perovskites for high-efficiency solar cells. *InfoMat* **2023,** *5* (4), e12393, DOI: 10.1002/inf2.12393.
(166) Saliba, M.; Matsui, T.; Seo, J.-Y.; Domanski, K.; Correa-Baena, J.-P.; Nazeeruddin, M. K.; Zakeeruddin, S. M.; Tress, W.; Abate, A.; Hagfeldt, A.; Grätzel, M. Cesium-containing triple cation perovskite solar cells: improved stability, reproducibility and high efficiency. *Energy & Environmental Science* **2016,** *9* (6), 1989-1997, DOI: 10.1039/C5EE03874J.
(167) Palmstrom, A. F.; Eperon, G. E.; Leijtens, T.; Prasanna, R.; Habisreutinger, S. N.; Nemeth, W.; Gaulding, E. A.; Dunfield, S. P.; Reese, M.; Nanayakkara, S.; Moot, T.; Werner, J.; Liu, J.; To, B.; Christensen, S. T.; McGehee, M. D.; van Hest, M. F. A. M.; Luther, J. M.; Berry, J. J.; Moore, D. T. Enabling Flexible All-Perovskite Tandem Solar Cells. *Joule* **2019,** *3* (9), 2193-2204, DOI: 10.1016/j.joule.2019.05.009.
(168) Gao, L.; Zhang, Y.; Gou, L.; Wang, Q.; Wang, M.; Zheng, W.; Wang, Y.; Yip, H.-L.; Zhang, J. High efficiency pure blue perovskite quantum dot light-emitting diodes based on formamidinium manipulating carrier dynamics and electron state filling. *Light: Science & Applications* **2022,** *11* (1), 346, DOI: 10.1038/s41377-022-00992-5.
(169) Nakamura, T.; Otsuka, K.; Hu, S.; Hashimoto, R.; Morishita, T.; Handa, T.; Yamada, T.; Truong, M. A.; Murdey, R.; Kanemitsu, Y.; Wakamiya, A. Composition–Property Mapping in Bromide-Containing Tin Perovskite Using High-Purity Starting Materials. *ACS Applied Energy Materials* **2022,** *5* (12), 14789-14798, DOI: 10.1021/acsaem.2c02144.
(170) Jesper Jacobsson, T.; Correa-Baena, J.-P.; Pazoki, M.; Saliba, M.; Schenk, K.; Grätzel, M.; Hagfeldt, A. Exploration of the compositional space for mixed lead halogen perovskites for high efficiency solar cells. *Energy & Environmental Science* **2016,** *9* (5), 1706-1724, DOI: 10.1039/C6EE00030D.
(171) Susic, I.; Kama, A.; Gil-Escrig, L.; Dreessen, C.; Palazon, F.; Cahen, D.; Sessolo, M.; Bolink, H. J. Combinatorial Vacuum-Deposition of Wide Bandgap Perovskite Films and Solar Cells. *Advanced Materials Interfaces* **2023,** *10* (4), 2202271, DOI: 10.1002/admi.202202271.
(172) Xiao, H.; Xiong, H.; Li, P.; Jiang, L.; Yang, A.; Lin, L.; Kang, Z.; Yan, Q.; Qiu, Y. Tunable deep-blue luminescence from ball-milled chlorine-rich $Cs_x(NH_4)_{1-x}PbCl_2Br$ nanocrystals by ammonium modulation. *Chemical Communications* **2022,** *58* (23), 3827-3830, DOI: 10.1039/D1CC07125D.
(173) Wang, C.; Liu, Y.; Feng, X.; Zhou, C.; Liu, Y.; Yu, X.; Zhao, G. Phase Regulation Strategy of Perovskite Nanocrystals from 1D Orthomorphic NH_4PbI_3 to 3D Cubic $(NH_4)_{0.5}Cs_{0.5}Pb(I_{0.5}Br_{0.5})_3$ Phase Enhances Photoluminescence. *Angewandte Chemie International Edition* **2019,** *58* (34), 11642-11646, DOI: 10.1002/anie.201903121.
(174) Terada, S.; Oku, T.; Suzuki, A.; Okita, M.; Fukunishi, S.; Tachikawa, T.; Hasegawa, T. Ethylammonium Bromide- and Potassium-Added $CH_3NH_3PbI_3$ Perovskite Solar Cells. *Photonics* **2022,** *9* (11), 791, DOI: 10.3390/photonics9110791.
(175) Sanchez, S. L.; Foadian, E.; Ziatdinov, M.; Yang, J.; Kalinin, S. V.; Liu, Y.; Ahmadi, M. Physics-driven discovery and bandgap engineering of hybrid perovskites. *arXiv* **2023**, 2310.06583, DOI: 10.48550/arXiv.2310.06583.
(176) Gabriel Tomulescu, A.; Nicoleta Leonat, L.; Neațu, F.; Stancu, V.; Toma, V.; Derbali, S.; Neațu, Ș.; Mihai Rostas, A.; Beșleagă, C.; Pătru, R.; Pintilie, I.; Florea, M. Enhancing stability of hybrid perovskite solar cells by imidazolium incorporation. *Solar Energy Materials and Solar Cells* **2021,** *227*, 111096, DOI: 10.1016/j.solmat.2021.111096.
(177) Singh, R. K.; Sharma, P.; Lu, C.-H.; Kumar, R.; Jain, N.; Singh, J. Structural, morphological and thermodynamic parameters investigation of tunable $MAPb_{1-x}Cd_xBr_{3-2x}I_{2x}$

hybrid perovskite. *Journal of Alloys and Compounds* **2021,** *866*, 158936, DOI: 10.1016/j.jallcom.2021.158936.
(178) Singh, R. K.; Sharma, P.; Kumar, R.; Som, S.; Dutta, S.; Jain, N.; Chaurasiya, R.; Meena, M. L.; Ho, J.-S.; Dai, S.-W.; Singh, J.; Lu, C.-H.; Lin, H.-W. $CH_3NH_3Pb_{1-x}Co_xBr_{3-2x}Cl_{2x}$ Perovskite Quantum Dots for Wide-Color Backlighting. *ACS Applied Nano Materials* **2021,** *4* (1), 717-728, DOI: 10.1021/acsanm.0c03019.
(179) Xun, J.; Deng, J.; Shen, W.; Li, M.; He, R. Highly efficient green-emitting nanocrystals of $MAPb_{1-x}Mn_xBr_3$ perovskite with excellent thermal stability. *Optical Materials* **2021,** *122*, 111799, DOI: 10.1016/j.optmat.2021.111799.
(180) Lu, C.; Zhou, J.; Tang, C.; Dai, Q.; Peng, Y.; Lv, W.; Sun, L.; Xu, S.; Hu, W. Ultranarrow-band filterless photodetectors based on $CH_3NH_3PbCl_xBr_{3-x}$ mixed-halide perovskite single crystals. *Nanotechnology* **2023,** *34* (34), 345705, DOI: 10.1088/1361-6528/acd944.
(181) Mazurin, M.; Shelestova, A.; Tsvetkov, D.; Sereda, V.; Ivanov, I.; Malyshkin, D.; Zuev, A. Thermochemical Study of $CH_3NH_3Pb(Cl_{1-x}Br_x)_3$ Solid Solutions. *Materials* **2022,** *15* (21), 7675, DOI: 10.3390/ma15217675.
(182) Pan, Y.; Wang, X.; Xu, Y.; Chai, S.; Wu, J.; Zhao, Z.; Li, Q.; Wu, J.; Chen, J.; Zhu, Z.; Bae, B. S.; Fayemi, O. E.; Zhou, J.; Zhu, Y.; Lei, W. Epitaxy growth of $MAPbBr_xCl_{3-x}$ single-crystalline perovskite films toward spectral selective detection in both broadband and narrowband ranges. *Journal of Materials Chemistry C* **2023,** *11* (40), 13763-13773, DOI: 10.1039/D3TC02300A.
(183) Rajagopal, A.; Stoddard, R. J.; Hillhouse, H. W.; Jen, A. K. Y. On understanding bandgap bowing and optoelectronic quality in Pb–Sn alloy hybrid perovskites. *Journal of Materials Chemistry A* **2019,** *7* (27), 16285-16293, DOI: 10.1039/C9TA05308E.
(184) Liang, F.-X.; Zhou, L.-L.; Hu, Y.; Li, S.-F.; Zhang, Z.-Y.; Li, J.-Y.; Fu, C.; Wu, C.-Y.; Wang, L.; Huang, J.-A.; Luo, L.-B. Self-Driven Narrow-Band Photodetector based on $FAPbBr_{2.5}I_{0.5}$ Single Crystal for Yellow Light Intensity Meter Application. *Advanced Functional Materials* **2023,** *33* (36), 2302175, DOI: 10.1002/adfm.202302175.
(185) Noh, J. H.; Im, S. H.; Heo, J. H.; Mandal, T. N.; Seok, S. I. Chemical Management for Colorful, Efficient, and Stable Inorganic–Organic Hybrid Nanostructured Solar Cells. *Nano Letters* **2013,** *13* (4), 1764-1769, DOI: 10.1021/nl400349b.
(186) Hu, S.; Otsuka, K.; Murdey, R.; Nakamura, T.; Truong, M. A.; Yamada, T.; Handa, T.; Matsuda, K.; Nakano, K.; Sato, A.; Marumoto, K.; Tajima, K.; Kanemitsu, Y.; Wakamiya, A. Optimized carrier extraction at interfaces for 23.6% efficient tin–lead perovskite solar cells. *Energy & Environmental Science* **2022,** *15* (5), 2096-2107, DOI: 10.1039/D2EE00288D.
(187) Turren-Cruz, S.-H.; Pascual, J.; Hu, S.; Sanchez-Diaz, J.; Galve-Lahoz, S.; Liu, W.; Hempel, W.; Chirvony, V. S.; Martinez-Pastor, J. P.; Boix, P. P.; Wakamiya, A.; Mora-Seró, I. Multicomponent Approach for Stable Methylammonium-Free Tin–Lead Perovskite Solar Cells. *ACS Energy Letters* **2024,** *9* (2), 432-441, DOI: 10.1021/acsenergylett.3c02426.
(188) Zhang, H.; Bi, Z.; Zhai, Z.; Gao, H.; Liu, Y.; Jin, M.; Ye, M.; Li, X.; Liu, H.; Zhang, Y.; Li, X.; Tan, H.; Xu, Y.; Yang, L. Revealing Unusual Bandgap Shifts with Temperature and Bandgap Renormalization Effect in Phase-Stabilized Metal Halide Perovskite Thin Films. *Advanced Functional Materials* **2024,** *34* (9), 2302214, DOI: 10.1002/adfm.202302214.
(189) Prasanna, R.; Gold-Parker, A.; Leijtens, T.; Conings, B.; Babayigit, A.; Boyen, H.-G.; Toney, M. F.; McGehee, M. D. Band Gap Tuning via Lattice Contraction and Octahedral Tilting in Perovskite Materials for Photovoltaics. *Journal of the American Chemical Society* **2017,** *139* (32), 11117-11124, DOI: 10.1021/jacs.7b04981.

(190) Wang, J.; Uddin, M. A.; Chen, B.; Ying, X.; Ni, Z.; Zhou, Y.; Li, M.; Wang, M.; Yu, Z.; Huang, J. Enhancing Photostability of Sn-Pb Perovskite Solar Cells by an Alkylammonium Pseudo-Halogen Additive. *Advanced Energy Materials* **2023,** *13* (15), 2204115, DOI: 10.1002/aenm.202204115.
(191) Guo, J.; Fu, Y.; Zheng, W.; Xie, M.; Huang, Y.; Miao, Z.; Han, C.; Yin, W.; Zhang, J.; Yang, X.; Tian, J.; Zhang, X. Entropy-Driven Strongly Confined Low-Toxicity Pure-Red Perovskite Quantum Dots for Spectrally Stable Light-Emitting Diodes. *Nano Letters* **2024,** *24* (1), 417-423, DOI: 10.1021/acs.nanolett.3c04214.
(192) Hsiao, K.-C.; Ho, C.-M.; Lin, T.-H.; Chen, S.-H.; Chang, Y.-H.; Liao, Y.-H.; Chang, J.-M.; Lin, T.-F.; Huang, Y.-C.; Lee, K.-M.; Wu, M.-C. Ceiling of Barium Substitution for B-Site Cation in Organometal Halide Perovskite Solar Cells. *International Journal of Energy Research* **2024,** *2024*, 9990559, DOI: 10.1155/2024/9990559.
(193) Saliba, M.; Matsui, T.; Domanski, K.; Seo, J.-Y.; Ummadisingu, A.; Zakeeruddin, S. M.; Correa-Baena, J.-P.; Tress, W. R.; Abate, A.; Hagfeldt, A.; Grätzel, M. Incorporation of rubidium cations into perovskite solar cells improves photovoltaic performance. *Science* **2016,** *354* (6309), 206-209, DOI: 10.1126/science.aah5557.
(194) Susic, I.; Gil-Escrig, L.; Zanoni, K. P. S.; Roldán-Carmona, C.; Sessolo, M.; Bolink, H. J. Pure Iodide Multication Wide Bandgap Perovskites by Vacuum Deposition. *ACS Materials Letters* **2023,** *5* (12), 3299-3305, DOI: 10.1021/acsmaterialslett.3c01094.
(195) Derbali, S.; Nouneh, K.; Florea, M.; Leonat, L. N.; Stancu, V.; Tomulescu, A. G.; Galca, A. C.; Secu, M.; Pintilie, L.; Touhami, M. E. Potassium-containing triple-cation mixed-halide perovskite materials: Toward efficient and stable solar cells. *Journal of Alloys and Compounds* **2021,** *858*, 158335, DOI: 10.1016/j.jallcom.2020.158335.
(196) Ono, I.; Oku, T.; Suzuki, A.; Fukunishi, S.; Tachikawa, T.; Hasegawa, T. Effects of ethylammonium and rubidium addition to guanidinium-based $CH_3NH_3PbI_3$ perovskite photovoltaic devices prepared at 190 °C in ambient air. *Materials Today Communications* **2024,** *38*, 107623, DOI: 10.1016/j.mtcomm.2023.107623.
(197) Minussi, F. B.; A. Silva, L.; Araújo, E. B. Structure, optoelectronic properties and thermal stability of the triple organic cation $GA_xFA_xMA_{1-2x}PbI_3$ system prepared by mechanochemical synthesis. *Physical Chemistry Chemical Physics* **2022,** *24* (8), 4715-4728, DOI: 10.1039/D1CP04977A.
(198) Minussi, F. B.; Silva Jr., R. M.; Araújo, E. B. Composition-Property Relations for $GA_xFA_yMA_{1-x-y}PbI_3$ Perovskites. *Small* **2024,** *20* (7), 2305054, DOI: 10.1002/smll.202305054.
(199) Wang, S.; Pang, S.; Chen, D.; Zhu, W.; Xi, H.; Zhang, C. Improving perovskite solar cell performance by compositional engineering via triple-mixed cations. *Solar Energy* **2021,** *220*, 412-417, DOI: 10.1016/j.solener.2021.03.036.
(200) Badrooj, M.; Jamali-Sheini, F.; Torabi, N. Zn-doped Pb/Sn hybrid perovskite solar cells: Towards high photovoltaic performance. *Solar Energy* **2022,** *236*, 63-74, DOI: 10.1016/j.solener.2022.02.034.
(201) Soto-Montero, T.; Kralj, S.; Soltanpoor, W.; Solomon, J. S.; Gómez, J. S.; Zanoni, K. P. S.; Paliwal, A.; Bolink, H. J.; Baeumer, C.; Kentgens, A. P. M.; Morales-Masis, M. Single-Source Vapor-Deposition of $MA_{1-x}FA_xPbI_3$ Perovskite Absorbers for Solar Cells. *Advanced Functional Materials* **2023,** *n/a* (n/a), 2300588, DOI: 10.1002/adfm.202300588.
(202) Weber, O. J.; Charles, B.; Weller, M. T. Phase behaviour and composition in the formamidinium–methylammonium hybrid lead iodide perovskite solid solution. *Journal of Materials Chemistry A* **2016,** *4* (40), 15375-15382, DOI: 10.1039/C6TA06607K.

(203) Zhao, C.; Cazorla, C.; Zhang, X.; Huang, H.; Zhao, X.; Li, D.; Shi, J.; Zhao, Q.; Ma, W.; Yuan, J. Fast Organic Cation Exchange in Colloidal Perovskite Quantum Dots toward Functional Optoelectronic Applications. *Journal of the American Chemical Society* **2024,** *146* (7), 4913-4921, DOI: 10.1021/jacs.3c14000.
(204) Ju, D.; Dang, Y.; Zhu, Z.; Liu, H.; Chueh, C.-C.; Li, X.; Wang, L.; Hu, X.; Jen, A. K. Y.; Tao, X. Tunable Band Gap and Long Carrier Recombination Lifetime of Stable Mixed $CH_3NH_3Pb_xSn_{1-x}Br_3$ Single Crystals. *Chemistry of Materials* **2018,** *30* (5), 1556-1565, DOI: 10.1021/acs.chemmater.7b04565.
(205) Kahmann, S.; Chen, Z.; Hordiichuk, O.; Nazarenko, O.; Shao, S.; Kovalenko, M. V.; Blake, G. R.; Tao, S.; Loi, M. A. Compositional Variation in $FAPb_{1-x}Sn_xI_3$ and Its Impact on the Electronic Structure: A Combined Density Functional Theory and Experimental Study. *ACS Applied Materials & Interfaces* **2022,** *14* (30), 34253-34261, DOI: 10.1021/acsami.2c00889.
(206) Lü, X.; Stoumpos, C.; Hu, Q.; Ma, X.; Zhang, D.; Guo, S.; Hoffman, J.; Bu, K.; Guo, X.; Wang, Y.; Ji, C.; Chen, H.; Xu, H.; Jia, Q.; Yang, W.; Kanatzidis, M. G.; Mao, H.-K. Regulating off-centering distortion maximizes photoluminescence in halide perovskites. *National Science Review* **2020,** *8* (9), DOI: 10.1093/nsr/nwaa288.
(207) Dintakurti, S. S. H.; Walker, D.; Bird, T. A.; Fang, Y.; White, T.; Hanna, J. V. A powder XRD, solid state NMR and calorimetric study of the phase evolution in mechanochemically synthesized dual cation $(Cs_x(CH_3NH_3)_{1-x})PbX_3$ lead halide perovskite systems. *Physical Chemistry Chemical Physics* **2022,** *24* (30), 18004-18021, DOI: 10.1039/D2CP02131E.
(208) Chen, M.; Dong, Q.; Xiao, C.; Zheng, X.; Dai, Z.; Shi, Y.; Luther, J. M.; Padture, N. P. Lead-Free Flexible Perovskite Solar Cells with Interfacial Native Oxide Have >10% Efficiency and Simultaneously Enhanced Stability and Reliability. *ACS Energy Letters* **2022,** *7* (7), 2256-2264, DOI: 10.1021/acsenergylett.2c01130.
(209) Hao, F.; Stoumpos, C. C.; Chang, R. P. H.; Kanatzidis, M. G. Anomalous Band Gap Behavior in Mixed Sn and Pb Perovskites Enables Broadening of Absorption Spectrum in Solar Cells. *Journal of the American Chemical Society* **2014,** *136* (22), 8094-8099, DOI: 10.1021/ja5033259.
(210) Im, J.; Stoumpos, C. C.; Jin, H.; Freeman, A. J.; Kanatzidis, M. G. Antagonism between Spin–Orbit Coupling and Steric Effects Causes Anomalous Band Gap Evolution in the Perovskite Photovoltaic Materials $CH_3NH_3Sn_{1-x}Pb_xI_3$. *The Journal of Physical Chemistry Letters* **2015,** *6* (17), 3503-3509, DOI: 10.1021/acs.jpclett.5b01738.
(211) Chu, Y.; Wang, C.; Ma, L.; Feng, X.; Wang, B.; Wu, Y.; Jia, Y.; Zhang, M.; Sun, Y.; Zhang, H.; Zhao, G. Unveiling the photoluminescence regulation of colloidal perovskite quantum dots via defect passivation and lattice distortion by potassium cations doping: Not the more the better. *Journal of Colloid and Interface Science* **2021,** *596*, 199-205, DOI: 10.1016/j.jcis.2021.03.128.
(212) Ali, A.; Park, H.; Mall, R.; Aïssa, B.; Sanvito, S.; Bensmail, H.; Belaidi, A.; El-Mellouhi, F. Machine Learning Accelerated Recovery of the Cubic Structure in Mixed-Cation Perovskite Thin Films. *Chemistry of Materials* **2020,** *32* (7), 2998-3006, DOI: 10.1021/acs.chemmater.9b05342.
(213) Jia, D.; Chen, J.; Zhuang, R.; Hua, Y.; Zhang, X. Antisolvent-Assisted In Situ Cation Exchange of Perovskite Quantum Dots for Efficient Solar Cells. *Advanced Materials* **2023,** *35* (21), 2212160, DOI: 10.1002/adma.202212160.
(214) Liang, F.-C.; Jhuang, F.-C.; Fang, Y.-H.; Benas, J.-S.; Chen, W.-C.; Yan, Z.-L.; Lin, W.-C.; Su, C.-J.; Sato, Y.; Chiba, T.; Kido, J.; Kuo, C.-C. Synergistic Effect of Cation Composition

Engineering of Hybrid $Cs_{1-x}FA_xPbBr_3$ Nanocrystals for Self-Healing Electronics Application. *Advanced Materials* **2023,** *35* (9), 2207617, DOI: 10.1002/adma.202207617.
(215) Pisanu, A. Chemical tuning of hybrid perovskites for solar-driven clean energy technologies. Ph.D. Universita' di Pavia, 2020.
(216) Nagane, S.; Ghosh, D.; Hoye, R. L. Z.; Zhao, B.; Ahmad, S.; Walker, A. B.; Islam, M. S.; Ogale, S.; Sadhanala, A. Lead-Free Perovskite Semiconductors Based on Germanium–Tin Solid Solutions: Structural and Optoelectronic Properties. *The Journal of Physical Chemistry C* **2018,** *122* (11), 5940-5947, DOI: 10.1021/acs.jpcc.8b00480.
(217) Liu, Y.; Gong, Y.-P.; Geng, S.; Feng, M.-L.; Manidaki, D.; Deng, Z.; Stoumpos, C. C.; Canepa, P.; Xiao, Z.; Zhang, W.-X.; Mao, L. Hybrid Germanium Bromide Perovskites with Tunable Second Harmonic Generation. *Angewandte Chemie International Edition* **2022,** *61* (43), e202208875, DOI: 10.1002/anie.202208875.
(218) Liu, J.; Fu, H.; Du, Z.; Ou, D.; Li, S.; Chen, Q.; Yang, W.; Zhao, J.; Zheng, J. Enhanced photothermal stability of in situ grown $FAPbBr_3$ nanocrystals in polyvinylidene fluoride by incorporation of Cd^{2+} ions. *Journal of Materials Chemistry C* **2022,** *10* (46), 17512-17520, DOI: 10.1039/D2TC04100F.
(219) Oku, T.; Uchiya, S.; Okumura, R.; Suzuki, A.; Ono, I.; Fukunishi, S.; Tachikawa, T.; Hasegawa, T. Effects of Co-Addition of Guanidinium and Cesium to $CH_3NH_3PbI_3$ Perovskite Solar Cells. *Inorganics* **2023,** *11* (7), 273, DOI: 10.3390/inorganics11070273.
(220) Deng, J.; Xun, J.; Qin, Y.; Li, M.; He, R. Blue-emitting NH_4^+-doped $MAPbBr_3$ perovskite quantum dots with near unity quantum yield and super stability. *Chemical Communications* **2020,** *56* (79), 11863-11866, DOI: 10.1039/D0CC04912C.
(221) Lu, C.-H.; Singh, R. K.; Chen, T.-Y.; Som, S.; Kumar, R.; Lu, S. A.; Meena, M. L. Rapid synthesis and theoretical analysis of $CH_3NH_3Pb_{1-x}Cd_xBr_3$ perovskite quantum dots for backlight LEDs: A step towards enhanced stability. *Organic Electronics* **2022,** *102*, 106444, DOI: 10.1016/j.orgel.2022.106444.
(222) Klug, M. T.; Osherov, A.; Haghighirad, A. A.; Stranks, S. D.; Brown, P. R.; Bai, S.; Wang, J. T. W.; Dang, X.; Bulović, V.; Snaith, H. J.; Belcher, A. M. Tailoring metal halide perovskites through metal substitution: influence on photovoltaic and material properties. *Energy & Environmental Science* **2017,** *10* (1), 236-246, DOI: 10.1039/C6EE03201J.
(223) Yu, J.; Xu, H.; Wu, L.; Han, Q.; Wu, W. Highly sensitive photodetector of Zn/Bi doped $MAPbBr_3$ single crystals formed homojunction. *Materials Science in Semiconductor Processing* **2022,** *149*, 106824, DOI: 10.1016/j.mssp.2022.106824.
(224) Zhou, Z.; Xu, J.; Liu, Y.; Wei, C.; Zhang, H.; Wang, Q. Zn-alloyed $MAPbBr_3$ crystals with improved thermoelectric and photocatalytic properties. *Materials Chemistry Frontiers* **2021,** *5* (24), 8319-8332, DOI: 10.1039/D1QM00993A.
(225) Abd El-Samad, A. E.; Gad, N.; El-Aasser, M.; Rashad, M. M.; Mourtada Elseman, A. Optoelectronic investigation and simulation study of zinc and cobalt doped lead halide perovskite nanocrystals. *Solar Energy* **2022,** *247*, 553-563, DOI: 10.1016/j.solener.2022.10.061.
(226) Roscoe, S. L.; Haendler, H. M. Synthesis of fluorometallates in methanol. The solid solution $NH_4MnF_3 - NH_4ZnF_3$. *Inorganica Chimica Acta* **1967,** *1*, 73-75, DOI: 10.1016/S0020-1693(00)93142-6.
(227) Xu, Q.; Li, Z.; Liu, M.; Yin, W.-J. Rationalizing Perovskite Data for Machine Learning and Materials Design. *The Journal of Physical Chemistry Letters* **2018,** *9* (24), 6948-6954, DOI: 10.1021/acs.jpclett.8b03232.

(228) Muñoz, I. C.; Cruz-Zaragoza, E.; Favalli, A.; Furetta, C. Thermoluminescence property of $LiMgF_3$ erbium activated phosphor. *Applied Radiation and Isotopes* **2012,** *70* (5), 893-896, DOI: 10.1016/j.apradiso.2012.02.006.
(229) Grebenshchikov, R. G. In *Исследование диаграммы состояния системы $RbF–BeF_2$ и ее отношение к системе $BaO–SiO_2$*, Proceedings of the Academy of Sciences, Institute of Silicate Chemistry of the USSR Academy of Sciences: 1957; pp 316-319.
(230) Sandeep; Rai, D. P.; Shankar, A.; Ghimire, M. P.; Khenata, R.; Bin Omran, S.; Syrotyuk, S. V.; Thapa, R. K. Investigation of the structural, electronic and optical properties of the cubic $RbMF_3$ perovskites (M = Be, Mg, Ca, Sr and Ba) using modified Becke-Johnson exchange potential. *Materials Chemistry and Physics* **2017,** *192*, 282-290, DOI: 10.1016/j.matchemphys.2017.02.005.
(231) Levina, M. E.; Yunakovskaya, E. V. Phase transitions of the metafluoroberyllates $RbBeF_3$ and $CsBeF_3$. *Moscow University Chemistry Bulletin* **1971,** *26* (6), 40-42.
(232) Li, C.; Lu, X.; Ding, W.; Feng, L.; Gao, Y.; Guo, Z. Formability of ABX_3 (X = F, Cl, Br, I) halide perovskites. *Acta Crystallographica Section B* **2008,** *64* (6), 702-707, DOI: 10.1107/S0108768108032734.
(233) Martin, C. D.; Chaudhuri, S.; Grey, C. P.; Parise, J. B. Effect of A-site cation radius on ordering of BX_6 octahedra in (K,Na)MgF_3 perovskite. *American Mineralogist* **2005,** *90* (10), 1522-1533, DOI: 10.2138/am.2005.1693.
(234) Carter, F. L. On the existence of two forms of $NaNiF_3$. *Solid State Communications* **1969,** *7* (14), 993-995, DOI: 10.1016/0038-1098(69)90070-2.
(235) Hoppe, R.; Dähne, W.; Klemm, W. Mangantetrafluorid mit einem Anhang über $LiMnF_5$ und $LiMnF_4$. *Justus Liebigs Annalen der Chemie* **1962,** *658* (1), 1-5, DOI: 10.1002/jlac.19626580102.
(236) Gonzalo, E. C.; Sanjuán, M. L.; Hoelzel, M.; Azcondo, M. T.; Amador, U.; Sobrados, I.; Sanz, J.; García-Alvarado, F.; Kuhn, A. Synthesis and Characterization of $NaNiF_3 \cdot 3H_2O$: An Unusual Ordered Variant of the ReO_3 Type. *Inorganic Chemistry* **2015,** *54* (7), 3172-3182, DOI: 10.1021/ic5026262.
(237) Kaiser, V.; Otto, M.; Binder, F.; Babel, D. Jahn-Teller-Effekt und Kristallstruktur-Verzerrung bei den Kupfer-Fluorperowskiten $NaCuF_3$ und $RbCuF_3$. *Zeitschrift für anorganische und allgemeine Chemie* **1990,** *585* (1), 93-104, DOI: 10.1002/zaac.19905850112.
(238) Yakovlev, S.; Avdeev, M.; Mezouar, M. High-pressure structural behavior and equation of state of $NaZnF_3$. *Journal of Solid State Chemistry* **2009,** *182* (6), 1545-1549, DOI: 10.1016/j.jssc.2009.03.031.
(239) Portier, J.; Tressaud, A.; Dupin, J. Les Pérovskites Fluorées $AgMeF_3$ (Me= Mg, Mn; Co; Ni; Cu; Zn). *Cr. Acad. Sci. C* **1970,** *270*, 216-218.
(240) Tressaud, A.; De Pape, R.; Portier, J.; Hagenmuller, P. Les systemes MF-FeF_2 (M= Li, Na, Rb, Tl). *Comptes Rendus des Seances de l'Academie des Sciences, Serie C: Sciences Chimiques* **1968,** *266*, 984-986.
(241) Bernal, F. L. M.; Sottmann, J.; Wragg, D. S.; Fjellvåg, H.; Fjellvåg, Ø. S.; Drathen, C.; Sławiński, W. A.; Løvvik, O. M. Structural and magnetic characterization of the elusive Jahn-Teller active $NaCrF_3$. *Physical Review Materials* **2020,** *4* (5), 054412, DOI: 10.1103/PhysRevMaterials.4.054412.
(242) Tong, J.; Lee, C.; Whangbo, M. H.; Kremer, R. K.; Simon, A.; Köhler, J. Cooperative Jahn–Teller distortion leading to the spin-1/2 uniform antiferromagnetic chains in triclinic

perovskites $AgCuF_3$ and $NaCuF_3$. *Solid State Sciences* **2010,** *12* (5), 680-684, DOI: 10.1016/j.solidstatesciences.2009.02.028.
(243) Shafer, M. W. The synthesis and characterization of vanadium difluoride, $NaVF_3$, KVF_3, and $RbVF_3$. *Materials Research Bulletin* **1969,** *4* (12), 905-912, DOI: 10.1016/0025-5408(69)90047-6.
(244) Bukhalova, G. A.; Berezhnaya, V. T.; Okol'chishena, N. E. Some properties of compounds of the type $M^{1+}M^{2+}F_3$. *Russian Journal of Inorganic Chemistry* **1969,** *14*, 917-921.
(245) Katrusiak, A.; Ratuszna, A. Phase transitions and the structure of $NaMnF_3$ perovskite crystals as a function of temperature and pressure. *Solid State Communications* **1992,** *84* (4), 435-441, DOI: 10.1016/0038-1098(92)90492-R.
(246) Okazaki, A.; Suemune, Y.; Fuchikami, T. The Crystal Structures of $KMnF_3$, $KFeF_3$, $KCoF_3$, $KNiF_3$ and $KCuF_3$. *Journal of the Physical Society of Japan* **1959,** *14* (12), 1823-1824, DOI: 10.1143/JPSJ.14.1823.
(247) Sintani, K.; Tomono, Y.; Tsuchida, A.; Siratori, K. Influence of Magnetic Ordering on the Lattice Vibration of $KNiF_3$. *Journal of the Physical Society of Japan* **1968,** *25* (1), 99-108, DOI: 10.1143/JPSJ.25.99.
(248) DeVries, R. C.; Roy, R. Fluoride Models for Oxide Systems of Dielectric Interest. The Systems KF—MgF_2 and AgF-ZnF_2. *Journal of the American Chemical Society* **1953,** *75* (10), 2479-2484, DOI: 10.1021/ja01106a059.
(249) Racine, S.; Cipriani, J.; Pontikis, C. Diffusion de la lumiere et excitations magnetiques dans l'antiferromagnetique $KCoF_3$. *Comptes Rendus des Seances de l'Academie des Sciences, Serie B: Sciences Physiques* **1972,** *274*, 16-18.
(250) Szlag, R. G.; Suescun, L.; Dhanapala, B. D.; Rabuffetti, F. A. Rubidium–Alkaline-Earth Trifluoroacetate Hybrids as Self-Fluorinating Single-Source Precursors to Mixed-Metal Fluorides. *Inorganic Chemistry* **2019,** *58* (5), 3041-3049, DOI: 10.1021/acs.inorgchem.8b02988.
(251) Lukina, M. M.; Klientova, G. P. Hydrothermal synthesis of $KZnF_3$ single crystals with a perovskite structure. *Soviet Physics Crystallography (translated from Kristallografiya)* **1969,** *14* (2), 314-315.
(252) Rüdorff, W.; Lincke, G.; Babel, D. Untersuchungen an ternären Fluoriden. (II). Kobalt(II)- und Kupfer(II)-fluoride. *Zeitschrift für anorganische und allgemeine Chemie* **1963,** *320* (1-4), 150-170, DOI: 10.1002/zaac.19633200119.
(253) Lu, S.; Zhou, Q.; Ma, L.; Guo, Y.; Wang, J. Rapid Discovery of Ferroelectric Photovoltaic Perovskites and Material Descriptors via Machine Learning. *Small Methods* **2019,** *3* (11), 1900360, DOI: 10.1002/smtd.201900360.
(254) Syono, Y.; Akimoto, S.-i.; Kohn, K. Structure Relations of Hexagonal Perovskite-Like Compounds ABX_3 at High Pressure. *Journal of the Physical Society of Japan* **1969,** *26* (4), 993-999, DOI: 10.1143/JPSJ.26.993.
(255) Arakawa, M.; Ebisu, H.; Takeuchi, H. EPR study of Cr^{3+} centres in Tl_2MgF_4 and Tl_2ZnF_4 crystals. In *EPR in the 21st Century*; Kawamori, A.; Yamauchi, J.; Ohta, H., Eds.; Elsevier Science B.V.: Amsterdam, 2002; pp 219-224.
(256) van Roekeghem, A.; Carrete, J.; Oses, C.; Curtarolo, S.; Mingo, N. High-Throughput Computation of Thermal Conductivity of High-Temperature Solid Phases: The Case of Oxide and Fluoride Perovskites. *Physical Review X* **2016,** *6* (4), 041061, DOI: 10.1103/PhysRevX.6.041061.

(257) Aleonard, P. S. Fluorometallates obtenus par dissolution d'oxydes metalliques dans bain fondu a base de fluoroborate de potassium. *Comptes Rendus Hebdomadaires des Seances de l'Academie des Sciences* **1965,** *260*, 1977-1980.
(258) Ebisu, H.; Arakawa, M.; Takeuchi, H. An EPR study of trigonally symmetric Cr^{3+} centres in $TlZnF_3$ single crystals. *Journal of Physics: Condensed Matter* **2005,** *17* (29), 4653, DOI: 10.1088/0953-8984/17/29/008.
(259) Wang, F. F. Y.; Kestigian, M. Magnetic Properties of $RbFeF_3$. *Journal of Applied Physics* **1966,** *37* (3), 975-976, DOI: 10.1063/1.1708546.
(260) Williamson, R. F.; Boo, W. O. J. Lower valence fluorides of vanadium. 1. Synthesis and characterization of sodium trifluorovanadate, potassium trifluorovanadate, and rubidium trifluorovanadate. *Inorganic Chemistry* **1977,** *16* (3), 646-648, DOI: 10.1021/ic50169a030.
(261) Petrov, M. P.; Nedlin, G. M. Spin-Density Space Oscillations and Hyperfine Interaction in $RbCoF_3$. *Journal of Applied Physics* **1968,** *39* (2), 1012-1014, DOI: 10.1063/1.1656148.
(262) Daniel, P.; Toulouse, J.; Gesland, J. Y.; Rousseau, M. Raman-scattering investigation of the hexagonal perovskite $RbZnF_3$. *Physical Review B* **1995,** *52* (13), 9129-9132, DOI: 10.1103/PhysRevB.52.9129.
(263) Voloshinovskii, A. V.; Rodnyi, P. A.; Dmitriev, A. G.; Melchakov, E. N.; Pidzyrailo, S. N. Core-valence luminescence of $CsMgCl_3$ and $CsMgF_3$ crystals. *Journal of Applied Spectroscopy* **1993,** *59* (1), 560-562, DOI: 10.1007/BF00663370.
(264) Scatturin, V.; Corliss, L.; Elliott, N.; Hastings, J. Magnetic structures of 3d transition metal double fluorides, $KMeF_3$. *Acta Crystallographica* **1961,** *14* (1), 19-26, DOI: 10.1107/S0365110X61000036.
(265) Knox, K. Perovskite-like fluorides. I. Structures of $KMnF_3$, $KFeF_3$, $KNiF_3$ and $KZnF_3$. Crystal field effects in the series and in $KCrF_3$ and $KCuF_3$. *Acta Crystallographica* **1961,** *14* (6), 583-585, DOI: 10.1107/S0365110X61001868.
(266) Cousseins, J. C.; De Kozak, A. Sur les fluorures doubles de chrome bivalent de potassium ou de rubidium. *Comptes Rendus des Seances de l'Academie des Sciences, Serie C: Sciences Chimiques* **1966,** *263* (25), 1533-1535.
(267) Bachmann, B.; Müller, B. G. Einkristalluntersuchungen an Fluoroperowskiten $MPdF_3$ (M = Rb, K) und PdF_2. *Zeitschrift für anorganische und allgemeine Chemie* **1993,** *619* (2), 387-391, DOI: 10.1002/zaac.19936190225.
(268) Teaney, D. T.; Freiser, M. J.; Stevenson, R. W. H. Discovery of a Simple Cubic Antiferromagnet: Antiferromagnetic Resonance in $RbMnF_3$. *Physical Review Letters* **1962,** *9* (5), 212-214, DOI: 10.1103/PhysRevLett.9.212.
(269) Eastman, D. E.; Shafer, M. W. Antiferromagnetic Resonance in Cubic $TlMnF_3$. *Journal of Applied Physics* **2004,** *38* (3), 1274-1276, DOI: 10.1063/1.1709576.
(270) Alter, E.; Hoppe, R. Uber Fluoropalladate(II): $KPdF_3$, $RbPdF_3$, $TlPdF_3$ und K_2PdF_4. *Zeitschrift für anorganische und allgemeine Chemie* **1974,** *408* (2), 115-120, DOI: 10.1002/zaac.19744080205.
(271) Popov, A. I.; Kiselev, Y. M. ChemInform Abstract: Synthesis and Characterization of the Higher Fluorides of Silver and Alkali Metals. *ChemInform* **1988,** *19* (27), DOI: 10.1002/chin.198827039.
(272) Hidaka, M.; Hosogi, S. The crystal structure of $KCdF_3$. *J. Phys. France* **1982,** *43* (8), 1227-1232, DOI: 10.1051/jphys:019820043080122700.

(273) Longo, J. M.; Kafalas, J. A.; O'Connor, J. R.; Goodenough, J. B. Magnetic and Optical Properties of the High- and Low-Pressure Forms of $CsCoF_3$. *Journal of Applied Physics* **1970,** *41* (3), 935-936, DOI: 10.1063/1.1659031.
(274) Bulou, A.; Nouet, J.; Hewat, A. W.; Schäfer, F. J. Structural phase transitions in $KCaF_3$ - DSC, birefringence and neutron powder diffraction results. *Ferroelectrics* **1980,** *25* (1), 375-378, DOI: 10.1080/00150198008207024.
(275) Wu, G.-Q.; Hoppe, R. Neue Fluoro-Perowskite zweiwertiger Lanthaniden. Zur Kenntnis von $CsEuF_3$, $CsYbF_3$ und $RbYbF_3$. *Zeitschrift für anorganische und allgemeine Chemie* **1983,** *504* (9), 55-59, DOI: 10.1002/zaac.19835040907.
(276) Alam, M. S.; Saiduzzaman, M.; Biswas, A.; Ahmed, T.; Sultana, A.; Hossain, K. M. Tuning band gap and enhancing optical functions of $AGeF_3$ (A = K, Rb) under pressure for improved optoelectronic applications. *Scientific Reports* **2022,** *12* (1), 8663, DOI: 10.1038/s41598-022-12713-4.
(277) Muetterties, E. L. Chemistry of the Difluorides of Germanium and Tin. *Inorganic Chemistry* **1962,** *1* (2), 342-345, DOI: 10.1021/ic50002a029.
(278) Rousseau, M.; Gesland, J. Y.; Julliard, J.; Nouet, J.; Zarembowitch, J.; Zarembowitch, A. Changement de phase structural dans $RbCdF_3$ et $TlCdF_3$. *J. Physique Lett.* **1975,** *36* (5), 121-124, DOI: 10.1051/jphyslet:01975003605012100.
(279) Steiner, M.; Krüger, W.; Babel, D. Proof of ferromagnetic chains in $CsNiF_3$ by neutron diffraction. *Solid State Communications* **1971,** *9* (3), 227-229, DOI: 10.1016/0038-1098(71)90123-2.
(280) Jex, H.; Maetz, J.; Müllner, M. Cubic-to-tetragonal phase transition in $RbCaF_3$ investigated by diffraction experiments with neutrons, x rays, and γ rays from a Mössbauer source. *Physical Review B* **1980,** *21* (3), 1209-1218, DOI: 10.1103/PhysRevB.21.1209.
(281) Odenthal, R. H.; Hoppe, R. Fluorargentate(II) der Alkalimetalle. *Monatshefte für Chemie / Chemical Monthly* **1971,** *102* (5), 1340-1350, DOI: 10.1007/BF00917190.
(282) Hebecker, C. Neue ternäre Fluoride mit einwertigem Thallium und Silber als Kationen. *Naturwissenschaften* **1973,** *60* (3), 154-154, DOI: 10.1007/BF00594787.
(283) Pilania, G.; Balachandran, P. V.; Kim, C.; Lookman, T. Finding New Perovskite Halides via Machine Learning. *Frontiers in Materials* **2016,** *3*, DOI: 10.3389/fmats.2016.00019.
(284) Dance, J.-M.; Kerkouri, N.; Soubeyroux, J.-L.; Darriet, J.; Tressaud, A. Cationic substitutions in fluorides of hexagonal perovskite type. III. The $CsNi_{1-x}Cd_xF_3$ system: Crystal chemistry and trimeric magnetic interactions in $CsNi_{34}Cd_{14}F_3$. *Materials Letters* **1982,** *1* (2), 49-52, DOI: 10.1016/0167-577X(82)90004-0.
(285) Steinfink, H.; Brunton, G. D. The crystal structure of $CsBeF_3$. *Acta Crystallographica Section B* **1968,** *24* (6), 807-810, DOI: 10.1107/S0567740868003225.
(286) Hoppe, R.; Homann, R. Über $CsHgF_3$, $RbHgF_3$ und $KHgF_3$. *Zeitschrift für anorganische und allgemeine Chemie* **1969,** *369* (3-6), 212-216, DOI: 10.1002/zaac.19693690312.
(287) Gómez-Peralta, J. I.; Bokhimi, X. Ternary halide perovskites for possible optoelectronic applications revealed by Artificial Intelligence and DFT calculations. *Materials Chemistry and Physics* **2021,** *267*, 124710, DOI: 10.1016/j.matchemphys.2021.124710.
(288) Spector, J.; Villeneuve, G.; Hanebali, L.; Cros, C. NMR Investigations of the Li^+ ion mobility in the double chlorides Li_2MgCl_4 and $LiMgCl_3$. *Materials Letters* **1982,** *1* (2), 43-48, DOI: 10.1016/0167-577X(82)90003-9.

(289) Cros, C.; Hanebali, L.; Latie´, L.; Villeneuve, G. r.; Gang, W. Structure, ionic motion and conductivity in some solid-solutions of the $LiClMCl_2$ systems (M=Mg,V,Mn). *Solid State Ionics* **1983,** *9-10*, 139-147, DOI: 10.1016/0167-2738(83)90223-0.
(290) Foulon, J.; Durand, J.; Larbot, A.; Cot, L.; Soufiane, A. Crystal structures of $MSnF_3$ for M= K, Rb, Tl; ionic mobility. *European Journal of Solid State and Inorganic Chemistry* **1993,** *30*, 87-99, DOI: 10.1002/chin.199321003.
(291) Zhang, J.; Hong, G. Luminescence properties of Ce^{3+} in KMF_3 (M=Mg,Ca,Sr,Ba) hosts with perovskite structure. *Journal of Rare Earth Society: English Edition* **1997,** (2), 75-78.
(292) Weidenborner, J. E.; Bednowitz, A. L. Structures of ferrimagnetic fluorides of ABF_3 type. I. $RbNiF_3$. *Acta Crystallographica Section B* **1970,** *26* (10), 1464-1468, DOI: 10.1107/S0567740870004338.
(293) Wu, G.; Hoppe, R. Zur Kenntnis der Fluoride zweiwertiger Lanthanoide. II. Über die Synthese von $MLnF_3$ aus $MLnF_4$. *Zeitschrift für anorganische und allgemeine Chemie* **1984,** *514* (7), 92-98, DOI: 10.1002/zaac.19845140712.
(294) Yamane, Y.; Yamada, K.; Inoue, K. Mechanochemical synthesis and order–disorder phase transition in fluoride ion conductor $RbPbF_3$. *Solid State Ionics* **2008,** *179* (17), 605-610, DOI: 10.1016/j.ssi.2008.04.022.
(295) Retuerto, M.; Emge, T.; Hadermann, J.; Stephens, P. W.; Li, M. R.; Yin, Z. P.; Croft, M.; Ignatov, A.; Zhang, S. J.; Yuan, Z.; Jin, C.; Simonson, J. W.; Aronson, M. C.; Pan, A.; Basov, D. N.; Kotliar, G.; Greenblatt, M. Synthesis and Properties of Charge-Ordered Thallium Halide Perovskites, $CsTl^{+}_{0.5}Tl^{3+}_{0.5}X_3$ (X = F or Cl): Theoretical Precursors for Superconductivity? *Chemistry of Materials* **2013,** *25* (20), 4071-4079, DOI: 10.1021/cm402423x.
(296) Ashby, E. C.; Smith, R. S.; Goel, A. B. Comparative studies on the addition reactions of the Normant reagent ("CH3MgBr" + CuBr) and the new tetrahydrofuran-soluble magnesium methylcuprates MgmCun(CH3)2m+n with phenylacetylene. *The Journal of Organic Chemistry* **1981,** *46* (25), 5133-5139, DOI: 10.1021/jo00338a013.
(297) Hönle, W.; Miller, G.; Simon, A. Preparation, crystal structures, and electronic properties of $LiGaCl_3$ and $LiGaI_3$. *Journal of Solid State Chemistry* **1988,** *75* (1), 147-155, DOI: 10.1016/0022-4596(88)90312-X.
(298) Schmitz-Dumont, O.; Bergerhoff, G.; Hartert, E. Über den Einfluß des Kationenradius auf die Bildungsenergie von Anlagerungsverbindungen. VII. Die Systeme Alkalifluorid/Bleifluorid. *Zeitschrift für anorganische und allgemeine Chemie* **1956,** *283* (1-6), 314-329, DOI: 10.1002/zaac.19562830131.
(299) Arif, H.; Tahir, M. B.; Sagir, M.; Znaidia, S.; Alrobei, H.; Alzaid, M. First-principles calculations to investigate “H” and “K” doped $RbSrF_3$ for photovoltaic applications. *Optik* **2022,** *271*, 169864, DOI: 10.1016/j.ijleo.2022.169864.
(300) Klasens, H.; Zalm, P.; Huysman, F. The manganese emission in ABF_3-compounds. *Philips Research Reports* **1953,** *8*, 441-451.
(301) Sommerdijk, J. L.; Bril, A. Divalent europium luminescence in perovskite-like alkaline-earth alkaline fluorides. *Journal of Luminescence* **1976,** *11* (5), 363-367, DOI: 10.1016/0022-2313(76)90021-1.
(302) Fedoseeva, N.; Spevakova, I.; Petrakovskii, G.; Chuev, V.; Petrov, S. Magnetic structure and magnetic field behaviour of $NaMnCl_3$. *Journal of Magnetism and Magnetic Materials* **1980,** *15-18*, 539-541, DOI: 10.1016/0304-8853(80)91166-X.

(303) Thao Tran, T.; Shiv Halasyamani, P. Synthesis and characterization of $ASnF_3$ ($A=Na^+$, K^+, Rb^+, Cs^+). *Journal of Solid State Chemistry* **2014,** *210* (1), 213-218, DOI: 10.1016/j.jssc.2013.11.025.
(304) Visser, D.; Prodan, A. Disorder in $KNiCl_3$ as observed by electron diffraction. *physica status solidi (a)* **1980,** *58* (2), 481-488, DOI: 10.1002/pssa.2210580218.
(305) Hayatullah; Murtaza, G.; Khenata, R.; Mohammad, S.; Naeem, S.; Khalid, M. N.; Manzar, A. Structural, elastic, electronic and optical properties of $CsMCl_3$ (M=Zn, Cd). *Physica B: Condensed Matter* **2013,** *420*, 15-23, DOI: 10.1016/j.physb.2013.03.011.
(306) Lim, A. R.; Jeong, S.-Y. ^{133}Cs nuclear magnetic resonance study in $CsZnCl_3$ single crystals of perovskite ABX_3 type. *Physica B: Condensed Matter* **2008,** *403* (18), 3217-3220, DOI: 10.1016/j.physb.2008.04.007.
(307) Seifert, H.-J.; Klatyk, K. Über die Systeme Alkalimetallchlorid/Chrom(II)-chlorid. *Zeitschrift für anorganische und allgemeine Chemie* **1964,** *334* (3-4), 113-124, DOI: 10.1002/zaac.19643340302.
(308) Gurewitz, E.; Makovsky, J.; Shaked, H. Neutron-diffraction study of the magnetic structure of $KFeCl_3$. *Physical Review B* **1974,** *9* (3), 1071-1076, DOI: 10.1103/PhysRevB.9.1071.
(309) Haseda, T.; Wada, N.; Hata, M.; Amaya, K. Spin ordering in a triangular X-Y antiferromagnet : $CsFeCl_3$ and $RbFeCl_3$. *Physica B+C* **1981,** *108* (1), 841-842, DOI: 10.1016/0378-4363(81)90725-7.
(310) Seifert, H.-J.; Klatyk, K. Über die Systeme $RbCl/FeCl_2$ und $CsCl/FeCl_2$. *Zeitschrift für anorganische und allgemeine Chemie* **1966,** *342* (1-2), 1-9, DOI: 10.1002/zaac.19663420102.
(311) Zodkevitz, A.; Makovsky, J.; Kalman, Z. H. The Preparation and Crystal Structure of $TlMnCl_3$, $TlFeCl_3$, $TlCoCl_3$ and $TlNiCl_3$. *Israel Journal of Chemistry* **1970,** *8* (5), 755-762, DOI: 10.1002/ijch.197000095.
(312) Brynestad, J.; Yakel, H. L.; Smith, G. P. Temperature Dependence of the Absorption Spectrum of Nickel(II)-Doped $KMgCl_3$ and the Crystal Structure of $KMgCl_3$. *The Journal of Chemical Physics* **2004,** *45* (12), 4652-4664, DOI: 10.1063/1.1727550.
(313) Gurewitz, E.; Horowitz, A.; Shaked, H. Magnetic spiral structure of $KMnCl_3$—a neutron-diffraction study. *Physical Review B* **1979,** *20* (11), 4544-4549, DOI: 10.1103/PhysRevB.20.4544.
(314) Onken, D. R.; Perrodin, D.; Vogel, S. C.; Bourret, E. D.; Moretti, F. The crystal structure of $TlMgCl_3$ from 290 K to 725 K. *Acta Crystallographica Section E* **2020,** *76* (11), 1716-1719, DOI: 10.1107/S2056989020013201.
(315) Asmussen, R. W.; Larsen, T. K.; Soling, H. The crystal structure of $RbNiCl_3$ and $RbNiBr_3$. The Weiss constant in relation to the crystal structure of some double halides of the type $ANiX_3$. *Acta Chemica Scandinavica* **1969,** *23*, 2055-2060, DOI: 10.3891/acta.chem.scand.23-2055.
(316) Jongen, L.; Gloger, T.; Beekhuizen, J.; Meyer, G. Divalent Titanium: The Halides $ATiX_3$ (A = K, Rb, Cs; X = Cl, Br, I). *Zeitschrift für anorganische und allgemeine Chemie* **2005,** *631* (2-3), 582-586, DOI: 10.1002/zaac.200400464.
(317) Engberg, Å.; Soling, H. On the crystal structures of $RbCoCl_3$ and Rb_3CoCl_5. *Acta Chemica Scandinavica* **1967,** *21*, 168-174, DOI: 10.3891/acta.chem.scand.21-0168.
(318) Scholten, M.; Dronskowski, R.; Jacobs, H. $InCrBr_3$: A Ternary Indium Bromide Containing Jahn−Teller Unstable Cr^{2+} and the Magnetic Structures of $InCrBr_3$ and $InFeBr_3$. *Inorganic Chemistry* **1999,** *38* (11), 2614-2620, DOI: 10.1021/ic981383t.

(319) Narsimlu, N.; Srinivasu, D.; Sastry, G. S. Study of optical and transport properties of $K_2CuCl_4 \cdot 2H_2O$ single crystal. *Crystal Research and Technology* **1994,** *29* (4), 577-582, DOI: 10.1002/crat.2170290423.
(320) Willett, R. D.; Dwiggins, C., Jr.; Kruh, R. F.; Rundle, R. E. Crystal Structures of $KCuCl_3$ and NH_4CuCl_3. *The Journal of Chemical Physics* **2004,** *38* (10), 2429-2436, DOI: 10.1063/1.1733520.
(321) Horowitz, A.; Amit, M.; Makovsky, J.; Dor, L. B.; Kalman, Z. H. Structure types and phase transformations in $KMnCl_3$ and $TlMnCl_3$. *Journal of Solid State Chemistry* **1982,** *43* (2), 107-125, DOI: 10.1016/0022-4596(82)90220-1.
(322) Seifert, H.-J.; Ehrlich, P. Über die Systeme $NaCl/VCl_2$, KCl/VCl_2 und $CsCl/VCl_2$. *Zeitschrift für anorganische und allgemeine Chemie* **1960,** *302* (5-6), 284-288, DOI: 10.1002/zaac.19603020506.
(323) Meyer, G.; Packruhn, U. Chlorotitanate(II): $RbTiCl_3$ und $CsTiCl_3$. *Zeitschrift für anorganische und allgemeine Chemie* **1985,** *524* (5), 90-94, DOI: 10.1002/zaac.19855240512.
(324) Rüegg, C.; Cavadini, N.; Furrer, A.; Güdel, H. U.; Krämer, K.; Mutka, H.; Wildes, A.; Habicht, K.; Vorderwisch, P. Bose–Einstein condensation of the triplet states in the magnetic insulator $TlCuCl_3$. *Nature* **2003,** *423* (6935), 62-65, DOI: 10.1038/nature01617.
(325) Niel, M.; Cros, C.; Le Flem, G.; Pouchard, M. Sur les chlorures doubles de vanadium+II: les phases $TlVCl_3$ et NH_4VCl_3. *Comptes rendus de l'Académie des Sciences* **1975,** *280* (17), 1093-1095.
(326) Devaney, K. O.; Freedman, M. R.; McPherson, G. L.; Atwood, J. L. Electron paramagnetic resonance studies of manganese(II) and nickel(II) in three structural phases of rubidium magnesium chloride and the crystal structure of 6H-rubidium magnesium chloride. *Inorganic Chemistry* **1981,** *20* (1), 140-145, DOI: 10.1021/ic50215a030.
(327) Fedoseeva, N. V.; Velikanova, T. A.; Zvegintsev, A. G. High-pressure cubic phase of $RbMnCl_3$ - magnetic properties. *physica status solidi (a)* **1979,** *51* (1), K93-K96, DOI: 10.1002/pssa.2210510157.
(328) Seifert, H.-J.; Fink, H.; Thiel, G.; Uebach, J. Thermodynamische und strukturelle Untersuchungen an den Verbindungen der Systeme KCl/MCl_2 (M = Ca, Cd, Co, Ni). *Zeitschrift für anorganische und allgemeine Chemie* **1985,** *520* (1), 151-159, DOI: 10.1002/zaac.19855200118.
(329) Harada, M. Jahn-Teller Phase Transitions in $RbCuCl_3$. *Journal of the Physical Society of Japan* **1983,** *52* (5), 1646-1657, DOI: 10.1143/JPSJ.52.1646.
(330) Spitsyn, V. I.; Kryuchkov, S. V.; Grigoriev, M. S.; Kuzina, A. F. Polynuclear Clusters of Technetium. Part 1. Synthesis, Crystal and Molecular Structure of Bromide Octanuclear Prismatic and Hexanuclear Octahedral Clusters of Technetium. *Doklady Akademii Nauk SSSR* **1988,** *288*, 389-393, DOI: 10.1002/chin.198849036.
(331) Hauser, A.; Falk, U.; Fischer, P.; Furrer, A.; Güdel, H. U. Neutron scattering investigation of 1D and 3D magnetic ordering and excitations in AVX_3 (A = Rb, Cs; X = Cl, Br, I). *Journal of Magnetism and Magnetic Materials* **1983,** *31-34*, 1139-1140, DOI: 10.1016/0304-8853(83)90832-6.
(332) Filip, M. R.; Giustino, F. Computational Screening of Homovalent Lead Substitution in Organic–Inorganic Halide Perovskites. *The Journal of Physical Chemistry C* **2016,** *120* (1), 166-173, DOI: 10.1021/acs.jpcc.5b11845.

(333) Minkiewicz, V. J.; Cox, D. E.; Shirane, G. The magnetic structures of $RbNiCl_3$ and $CsNiCl_3$. *Solid State Communications* **1970,** *8* (12), 1001-1005, DOI: 10.1016/0038-1098(70)90505-3.
(334) Achiwa, N. Linear Antiferromagnetic Chains in Hexagonal $ABCl_3$-Type Compounds (A; Cs, or Rb, B; Cu, Ni, Co, or Fe). *Journal of the Physical Society of Japan* **1969,** *27* (3), 561-574, DOI: 10.1143/JPSJ.27.561.
(335) Crama, W. J. On the cooperative Jahn-Teller effect in ternary chromium(II) and copper(II) halides. Ph.D. Rijksuniversiteit Leiden (Netherlands), 1980.
(336) Ewald, B.; Kudla, C.; Heines, P.; Keller, H.-L.; Lathe, C. Investigation of the group subgroup transition in $AgPbBr_3$. **2002**, 2.
(337) Kovalenko, E. N.; Yunakova, O. N.; Yunakov, N. N. The exciton absorption spectrum of thin films of ternary compounds in the AgBr–$PbBr_2$ system. *Low Temperature Physics* **2018,** *44* (8), 856-859, DOI: 10.1063/1.5049171.
(338) Jouini, N.; Guen, L.; Tournoux, M. Structure de $TlFeBr_3$: Distorsion du type perovskite hexagonale 2L. *Materials Research Bulletin* **1982,** *17* (11), 1421-1427, DOI: 10.1016/0025-5408(82)90228-8.
(339) Bogdanova, A. V.; Zaslavskaya, N. P.; Sinichka, E. V.; Fedyna, M. F.; Mokra, I. R.; Gasinets, S. M. Synthesis and Crystal Structure of Compounds $TlCdCl_3$ and $TlCdBr_3$. *Inorganic Materials (translated from Neorganicheskie Materialy)* **1993,** *29*, 664-666, DOI: 10.1002/chin.199346021.
(340) Witteveen, H. T.; Veen, J. A. R. v. Magnetic susceptibilities of the compounds $AFeCl_3$ (A=Tl,Rb,NH_4,Cs) with antiferromagnetic linear chains. *The Journal of Chemical Physics* **1973,** *58* (1), 186-191, DOI: 10.1063/1.1678903.
(341) Weiss, A.; Damm, K. Notizen: Zur Kenntnis des Natrium-trichloromercurats (II) $Na(HgCI_3)$. Über Quecksilberhalogenide IV. *Zeitschrift für Naturforschung B* **1954,** *9* (1), 82-82, DOI: 10.1515/znb-1954-0116.
(342) Zhang, J.; Corbett, J. D. Synthesis and structure of The Novel Layered Phase $CsTi_2Cl_7$. *Zeitschrift für anorganische und allgemeine Chemie* **1990,** *580* (1), 36-44, DOI: 10.1002/zaac.19905800105.
(343) Seifert, H. J.; Krimmel, T.; Heinemann, W. Über die Systeme TlX/MnX_2 und AgX/MnX_2 (X=Cl, Br, I). *Journal of thermal analysis* **1974,** *6* (1), 175-182, DOI: 10.1007/BF01911498.
(344) Hönle, W.; Simon, A. Darstellung und Kristallstrukturen von $LiGaBr_4$ und $LiGaBr_3$. *Zeitschrift für Naturforschung B* **1986,** *41* (11), 1391-1398, DOI: 10.1515/znb-1986-1113.
(345) Natarajan, M.; Secco, E. A. Electrical conductivity and phase transformation studies on the mixed metal halides $RbCdX_3$ (X = Cl, Br, I) and Cs_2CuBr_4. *physica status solidi (a)* **1976,** *33* (1), 427-433, DOI: 10.1002/pssa.2210330146.
(346) Wells, A. F. 332. The crystal structure of $CsCuCl_3$ and the crystal chemistry of complex halides ABX_3. *Journal of the Chemical Society (Resumed)* **1947,** (0), 1662-1670, DOI: 10.1039/JR9470001662.
(347) Gurewitz, E.; Shaked, H. Neutron diffraction study of the crystallographic and magnetic structures of potassium tribromoferrate(II). *Acta Crystallographica Section B* **1982,** *38* (11), 2771-2775, DOI: 10.1107/S0567740882009923.
(348) Seifert, H. J.; Klatyk, K. Das System $CsCl/CrCl_2$. *Naturwissenschaften* **1962,** *49* (23), 539-539, DOI: 10.1007/BF00626806.
(349) Goodyear, J.; Kennedy, D. J. The crystal structure of $CsMnCl_3$. *Acta Crystallographica Section B* **1973,** *29* (4), 744-748, DOI: 10.1107/S0567740873003286.

(350) Hirakawa, K.; Yoshizawa, H.; Ubukoshi, K. Magnetic and Neutron Scattering Study of One-Dimensional Heisenberg Antiferromagnet $CsVCl_3$. *Journal of the Physical Society of Japan* **1982,** *51* (4), 1119-1122, DOI: 10.1143/JPSJ.51.1119.
(351) Loef, E. v.; Pandian, L. S.; Kaneshige, N.; Ciampi, G.; Stand, L.; Rutstrom, D.; Tratsiak, Y.; Zhuravleva, M.; Melcher, C.; Shah, K. S. Crystal Growth, Density Functional Theory, and Scintillation Properties of $TlCaX_3$ (X = Cl, Br, I). *IEEE Transactions on Nuclear Science* **2023,** *70* (7), 1378-1383, DOI: 10.1109/TNS.2023.3258065.
(352) Kuok, M. H.; Tang, S. H. A Raman Study of $KCdBr_3$ Single Crystals. *physica status solidi (b)* **1988,** *147* (2), K195-K199, DOI: 10.1002/pssb.2221470261.
(353) Dronskowski, R. $InFeBr_3$ and $InMnBr_3$: Synthesis, Crystal Structure, Magnetic Properties, and Electronic Structure. *Inorganic Chemistry* **1994,** *33* (25), 5927-5933, DOI: 10.1021/ic00103a047.
(354) Seifert, H.-J.; Dau, E. Über die Systeme Alkalimetallbromid/Mangan(II)-bromid. *Zeitschrift für anorganische und allgemeine Chemie* **1972,** *391* (3), 302-312, DOI: 10.1002/zaac.19723910311.
(355) Meyer, G. Neue Chlor-Perowskite mit zweiwertigen Lanthaniden: $CsLn^{II}Cl_3$ (Ln^{II} = Sm, Eu, Tm, Yb). *Naturwissenschaften* **1978,** *65* (5), 258-258, DOI: 10.1007/BF00368570.
(356) Bill, J.; Lerch, K.; Laqua, W. $Cs_2Ag^{I}Ag^{III}Cl_6$. Eine gemischtvalente Verbindung mit dreiwertigem Silber. *Zeitschrift für anorganische und allgemeine Chemie* **1990,** *589* (1), 7-11, DOI: 10.1002/zaac.19905890102.
(357) Reshak, A. H.; Kityk, I. V.; Alahmed, Z. A.; Levkovets, S.; Fedorchuk, A. O.; Myronchuk, G.; Plucinski, K. J.; Kamarudin, H.; Auluck, S. Experimental and theoretical investigation of the electronic structure and optical properties of $TlHgCl_3$ single crystal. *Optical Materials* **2015,** *47*, 445-452, DOI: 10.1016/j.optmat.2015.06.018.
(358) Schölten, M.; Dronskowski, R. Crystal structure of indium magnesium tribromide, $InMgBr_3$. *Zeitschrift für Kristallographie - New Crystal Structures* **1997,** *212* (1), 5-5, DOI: 10.1524/ncrs.1997.212.1.5.
(359) Meyer, G.; Corbett, J. D. Reduced ternary halides of scandium: $RbScX_3$ (X = chlorine, bromine) and $CsScX_3$ (X = chlorine, bromine, iodine). *Inorganic Chemistry* **1981,** *20* (8), 2627-2631, DOI: 10.1021/ic50222a047.
(360) Huang, S.; Shan, H.; Xuan, W.; Xu, W.; Hu, D.; Zhu, L.; Huang, C.; Sui, W.; Xiao, C.; Zhao, Y.; Qiang, Y.; Gu, X.; Song, J.; Zhou, C. High-Performance Humidity Sensor Based on $CsPdBr_3$ Nanocrystals for Noncontact Sensing of Hydromechanical Characteristics of Unsaturated Soil. *physica status solidi (RRL) – Rapid Research Letters* **2022,** *16* (6), 2200017, DOI: 10.1002/pssr.202200017.
(361) Schüpp, B. Präparation und Charakterisierung neuer Halogenopalladate mit besonderem Schwergewicht bezüglich mehrkerniger Halogenopalladatgruppen. Ph.D. Universität Dortmund, 1999.
(362) Kar, M.; Körzdörfer, T. Computational high throughput screening of inorganic cation based halide perovskites for perovskite only tandem solar cells. *Materials Research Express* **2020,** *7* (5), 055502, DOI: 10.1088/2053-1591/ab8c0d.
(363) Wittenburg, G. Untersuchungen von Struktur-Eigenschafts-Beziehungen bei Trihalogenometallaten AMX_3 von Germanium(II), Zinn(II) und Blei(II). Ph.D. Universität Freiburg (Breisgau), 2000.

(364) Takeda, Y.; Shimada, M.; Kanamaru, F.; Koizumi, M. Structure and Properties of $CsFeBr_3$. *Journal of the Physical Society of Japan* **1974,** *37* (1), 276-276, DOI: 10.1143/JPSJ.37.276.
(365) Meyer, G. Reduced ternary rare earth halides: State of the art. *Journal of the Less Common Metals* **1983,** *93* (2), 371-380, DOI: 10.1016/0022-5088(83)90190-X.
(366) Seifert, H.-J.; Haberhauer, D. Über die Systeme Alkalimetallbromid/Calciumbromid. *Zeitschrift für anorganische und allgemeine Chemie* **1982,** *491* (1), 301-307, DOI: 10.1002/zaac.19824910139.
(367) Peresh, E. Y.; Lazarev, V. B.; Tsigika, V. V.; Orinchaj, A. V.; Balog, I. S.; Tkachenko, V. I.; Pogojda, I. I. Homogeneity regions, preparation and analysis of single crystals of certain compounds of Cs(Tl)X-Ge(Sn,Pb,Cd)X_2 systems, where X=Cl, Br, I. *Izv Akad Nauk SSSR, Neorg Mater* **1985,** *21* (5), 774-778.
(368) Pakhomov, V. I.; Goryunov, A. V. On the nature of complex formation in some inorganic halides. *Russian Journal of Inorganic Chemistry* **1993,** *38* (9), 1402-1408.
(369) Dronskowski, R. Synthesis, Crystal Structure, and Electronic Structure of $InCdBr_3$. *Journal of Solid State Chemistry* **1995,** *116* (1), 45-52, DOI: 10.1006/jssc.1995.1180.
(370) Mahendran, K. H.; Nagaraj, S.; Sridharan, R.; Gnanasekaran, T. Differential scanning calorimetric studies on the phase diagram of the binary LiCl–$CaCl_2$ system. *Journal of Alloys and Compounds* **2001,** *325* (1), 78-83, DOI: 10.1016/S0925-8388(01)01387-1.
(371) Demchenko, P.; Khyzhun, O. Y.; Fochuk, P. M.; Levkovets, S. I.; Myronchuk, G. L.; Parasyuk, O. V. Single crystal growth, structure and properties of $TlHgBr_3$. *Optical Materials* **2015,** *49*, 94-99, DOI: 10.1016/j.optmat.2015.08.026.
(372) Huart, J. Étude de trois halogénomercurates de thallium. *Bulletin de Minéralogie* **1965,** *88* (1), 65-68, DOI: 10.3406/bulmi.1965.5806.
(373) Zandbergen, H. W. Neutron powder diffraction and magnetic measurements on $TlMnI_3$ and $TlFeI_3$. *Journal of Solid State Chemistry* **1981,** *37* (2), 189-203, DOI: 10.1016/0022-4596(81)90085-2.
(374) Seifert, H. J.; Langenbach, U. Thermoanalytische und röntgenographische Untersuchungen an Systemen Alkalichlorid/Calciumchlorid. *Zeitschrift für anorganische und allgemeine Chemie* **1969,** *368* (1-2), 36-43, DOI: 10.1002/zaac.19693680107.
(375) Hauser, A.; Falk, U.; Fischer, P.; Güdel, H. U. Magnetic order in AVX_3 (A = Rb, Cs, $(CD_3)_4$ N; X = Cl, Br, I): A neutron diffraction study. *Journal of Solid State Chemistry* **1985,** *56* (3), 343-354, DOI: 10.1016/0022-4596(85)90184-7.
(376) Witteveen, H. T.; Van Veen, J. A. R. Magnetic susceptibilities of polycrystalline samples of the compounds $ANiCl_3$ (A = Rb, NH_4, Tl, Cs) and $ANiBr_3$ (A = Rb, Cs). *Journal of Physics and Chemistry of Solids* **1974,** *35* (3), 337-346, DOI: 10.1016/S0022-3697(74)80027-2.
(377) Lachgar, A.; Dudis, D. S.; Dorhout, P. K.; Corbett, J. D. Synthesis and properties of two novel line phases that contain linear scandium chains, lithium scandium iodide ($LiScI_3$) and sodium scandium iodide ($Na_{0.5}ScI_3$). *Inorganic Chemistry* **1991,** *30* (17), 3321-3326, DOI: 10.1021/ic00017a019.
(378) Vaills, Y.; Buzaré, J. Y.; Gibaud, A.; Launay, C. X-ray investigations of the cubic to tetragonal phase transition in $CsCaCl_3$ at T_c = 95 K. *Solid State Communications* **1986,** *60* (2), 139-141, DOI: 10.1016/0038-1098(86)90546-6.
(379) Macdonald, M. A.; Mel'chakov, E. N.; Munro, I. H.; Rodnyi, P. A.; Voloshinovsky, A. S. Radiative core-valence transitions in $CsMgCl_3$ and $CsSrCl_3$. *Journal of Luminescence* **1995,** *65* (1), 19-23, DOI: 10.1016/0022-2313(95)00051-Q.

(380) Matsushita, N.; Ahsbahs, H.; Hafner, S. S.; Kojima, N. Crystal Structure of Mixed-Valence Gold Compound, $Cs_2Au^{I}Au^{III}Cl_6$ up to 18 GPa. *The Review of High Pressure Science and Technology* **1998,** *7*, 329-331, DOI: 10.4131/jshpreview.7.329.
(381) Goodyear, J.; Ali, E. M.; Sutherland, H. H. Rubidium tribromomanganate. *Acta Crystallographica Section B* **1980,** *36* (3), 671-672, DOI: 10.1107/S0567740880004074.
(382) Li, T.-I.; Stucky, G. D. Exchange interactions in polynuclear transition metal complexes. Structural properties of cesium tribromocuprate(II), $CsCuBr_3$, a strongly coupled copper(II) system. *Inorganic Chemistry* **1973,** *12* (2), 441-445, DOI: 10.1021/ic50120a040.
(383) Lin, Z.-G.; Tang, L.-C.; Chou, C.-P. Study on mid-IR NLO crystals $CsGe(Br_xCl_{1-x})_3$. *Optical Materials* **2008,** *31* (1), 28-34, DOI: 10.1016/j.optmat.2008.01.004.
(384) Li, T.-I.; Stucky, G. D. The effect of exchange coupling on the spectra of transition metal ions. The crystal structure and optical spectrum of $CsCrBr_3$. *Acta Crystallographica Section B* **1973,** *29* (7), 1529-1532, DOI: 10.1107/S0567740873004863.
(385) Messer, D. Die Kristallstruktur von $RbGeCl_3$. *Zeitschrift für Naturforschung B* **1978,** *33* (4), 366-369, DOI: 10.1515/znb-1978-0403.
(386) Schilling, G.; Meyer, G. Ternäre Bromide und Iodide zweiwertiger Lanthanide und ihre Erdalkali-Analoga vom Typ AMX_3 und AM_2X_5. *Zeitschrift für anorganische und allgemeine Chemie* **1996,** *622* (5), 759-765, DOI: 10.1002/zaac.19966220502.
(387) Meyer, G.; Hinz, D. J.; Flörke, U. Crystal structure of caesium titanium tribromide, $CsTiBr_3$. *Zeitschrift für Kristallographie - Crystalline Materials* **1993,** *208* (1-2), 370-371, DOI: 10.1524/zkri.1993.208.12.370.
(388) Hohnstedt, C.; Meyer, G. Metallothermische Reduktion des Tribromids und -iodids von Dysprosium mit Alkalimetallen. *Zeitschrift für anorganische und allgemeine Chemie* **1993,** *619* (8), 1374-1378, DOI: 10.1002/zaac.19936190809.
(389) Tumram, P. V.; Kautkar, P. R.; Acharya, S. A.; Moharil, S. V. NIR Emission and $Eu^{2+}Nd^{3+}$ Energy Transfer in $KSrCl_3:Eu^{2+}$, Nd^{3+} phosphor. *Materials Today: Proceedings* **2017,** *4* (14), 12582-12585, DOI: 10.1016/j.matpr.2017.10.065.
(390) Schüpp, B.; Keller, H.-L. $CsPdCl_3$ – eine Verbindung mit $[Pd_2Cl_6]$-Baugruppen und anorganischem Kation. *Zeitschrift für anorganische und allgemeine Chemie* **1999,** *625* (11), 1944-1950, DOI: 10.1002/(SICI)1521-3749(199911)625:11<1944::AID-ZAAC1944>3.0.CO;2-V.
(391) McCall, K. M.; Friedrich, D.; Chica, D. G.; Cai, W.; Stoumpos, C. C.; Alexander, G. C. B.; Deemyad, S.; Wessels, B. W.; Kanatzidis, M. G. Perovskites with a Twist: Strong In^{1+} Off-Centering in the Mixed-Valent $CsInX_3$ (X = Cl, Br). *Chemistry of Materials* **2019,** *31* (22), 9554-9566, DOI: 10.1021/acs.chemmater.9b04095.
(392) Fink, H.; Seifert, H.-J. Über die Systeme des Europium(II)- und Strontiumchlorids mit Alkalimetallchloriden und Thalliumchlorid [1]. *Zeitschrift für anorganische und allgemeine Chemie* **1980,** *466* (1), 87-96, DOI: 10.1002/zaac.19804660111.
(393) Khan, K.; Sahariya, J.; Soni, A. Structural, electronic and optical modeling of perovskite solar materials $ASnX_3$ (A = Rb, K; X = Cl, Br): First principle investigations. *Materials Chemistry and Physics* **2021,** *262*, 124284, DOI: 10.1016/j.matchemphys.2021.124284.
(394) Sumio, I.; Yoshihiro, I. The congruent melting compounds in the system KCl–$SnCl_2$. *Chemistry Letters* **1983,** *12* (12), 1803-1806, DOI: 10.1246/cl.1983.1803.
(395) McPherson, G. L.; McPherson, A. M.; Atwood, J. L. Structures of $CsMgBr_3$, $CsCdBr_3$ and $CsMgI_3$— diamagnetic linear chain lattices. *Journal of Physics and Chemistry of Solids* **1980,** *41* (5), 495-499, DOI: 10.1016/0022-3697(80)90180-8.

(396) Ch'ih-fa, L.; Morozov, L. S. Thermal and tensimetric investigation of systems formed by tin(II) chloride with alkali metal and ammonium chloride. *Zhurnal Neorganicheskoy Khimii* **1963,** *8* (3), 708-711.
(397) Schilling, G.; Kunert, C.; Schleid, T.; Meyer, G. Metallothermische Reduktion der Tribromide und -iodide von Thulium und Ytterbium mit Alkalimetallen. *Zeitschrift für anorganische und allgemeine Chemie* **1992,** *618* (12), 7-12, DOI: 10.1002/zaac.19926180102.
(398) Cox, D. E.; Merkert, F. C. The preparation, crystal growth and perfection of double halides of $CsNiCl_3$ type. *Journal of Crystal Growth* **1972,** *13-14*, 282-284, DOI: 10.1016/0022-0248(72)90170-4.
(399) Bird, S. R. A.; Donaldson, J. D.; Silver, J. The Mössbauer effect in tin(II) compounds. Part XII. The spectra of the chloro- and bromo-stannates(II). *Journal of the Chemical Society, Dalton Transactions* **1972,** (18), 1950-1953, DOI: 10.1039/DT9720001950.
(400) Kuznetsova, I. Y.; Kovaleva, I. S.; Fedorov, V. A. Cs_2CdBr_4-$CsPbBr_3$ and $CsCdBr_3$-$CsPbBr_3$ joins of the $CdBr_2$-$PbBr_2$-CsBr ternary system. *Zhurnal Neorganicheskoj Khimii* **2002,** *47* (6), 1010-1012.
(401) Huang, J.; Lei, T.; Siron, M.; Zhang, Y.; Yu, S.; Seeler, F.; Dehestani, A.; Quan, L. N.; Schierle-Arndt, K.; Yang, P. Lead-free Cesium Europium Halide Perovskite Nanocrystals. *Nano Letters* **2020,** *20* (5), 3734-3739, DOI: 10.1021/acs.nanolett.0c00692.
(402) Zandbergen, H. W.; Verschoor, G. C.; IJdo, D. J. W. The structures of thallium cadmium triiodide and dirubidium iron tetraiodide. *Acta Crystallographica Section B* **1979,** *35* (6), 1425-1427, DOI: 10.1107/S0567740879006580.
(403) Strähle, J.; Gelinek, J.; Kölmel, M. Über den thermischen Abbau einiger Alkalimetall- und Ammoniumhalogenoaurate(III) und die Kristallstruktur der Zersetzungsprodukte $Rb_2Au_2Br_6$, $Rb_3Au_3Cl_8$ und $Au(NH_3)Cl_3$. *Zeitschrift für anorganische und allgemeine Chemie* **1979,** *456* (1), 241-260, DOI: 10.1002/zaac.19794560125.
(404) Alexandrov, K. S.; Besnosikov, B. V.; Posdnjakova, L. A. Successive phase transitions in perovskites. II. Structures of distorted phases. *Ferroelectrics* **1976,** *12* (1), 197-198, DOI: 10.1080/00150197608241424.
(405) Nagaraj, S.; Vishnuvardhan, C. V.; Ghosh, S.; Sridharan, R. Phase diagram study of $CaBr_2$–LiBr system using DTA. *Journal of Thermal Analysis and Calorimetry* **2014,** *115* (2), 1835-1839, DOI: 10.1007/s10973-013-3507-3.
(406) Matsushita, N.; Fukuhara, F.; Kojima, N. A three-dimensional bromo-bridged mixed-valence gold(I,III) compound, $Cs_2Au^{I}Au^{III}Br_6$. *Acta Crystallographica Section E* **2005,** *61* (6), i123-i125, DOI: 10.1107/S1600536805016594.
(407) Beck, H. P.; Tratzky, H.; Kallmayer, V.; Stöwe, K. The $InSnCl_3$-Type Arrangement: I. A New ABX_3 Structure Type with Close Cation–Cation Contacts. *Journal of Solid State Chemistry* **1999,** *146* (2), 344-350, DOI: 10.1006/jssc.1999.8360.
(408) Lv, S.; Wu, Q.; Meng, X.; Kang, L.; Zhong, C.; Lin, Z.; Hu, Z.; Chen, X.; Qin, J. A promising new nonlinear optical crystal with high laser damage threshold for application in the IR region: synthesis, crystal structure and properties of noncentrosymmetric $CsHgBr_3$. *Journal of Materials Chemistry C* **2014,** *2* (33), 6796-6801, DOI: 10.1039/C4TC00565A.
(409) Scholten, M.; Dronskowski, R.; Staffel, T.; Meyer, G. Synthesis and Crystal Structure of Potassium Indium Tribromide, $KInBr_3$. *Zeitschrift für anorganische und allgemeine Chemie* **1998,** *624* (11), 1741-1745, DOI: 10.1002/(SICI)1521-3749(1998110)624:11<1741::AID-ZAAC1741>3.0.CO;2-W.

(410) Kuok, M. H.; Tan, L. S.; Shen, Z. X.; Huan, C. H.; Mok, K. F. A Raman study of $RbSnBr_3$. *Solid State Communications* **1996,** *97* (6), 497-501, DOI: 10.1016/0038-1098(95)00625-7.
(411) Tang, L. C.; Huang, J. Y.; Chang, C. S.; Lee, M. H.; Liu, L. Q. New infrared nonlinear optical crystal $CsGeBr_3$: synthesis, structure and powder second-harmonic generation properties. *Journal of Physics: Condensed Matter* **2005,** *17* (46), 7275, DOI: 10.1088/0953-8984/17/46/011.
(412) Thiele, G.; Rotter, H. W.; Schmidt, K. D. Die Kristallstrukturen und Phasentransformationen von $RbGeBr_3$. *Zeitschrift für anorganische und allgemeine Chemie* **1988,** *559* (1), 7-16, DOI: 10.1002/zaac.19885590101.
(413) Li, T.-I.; Stucky, G. D.; McPherson, G. L. The crystal structure of $CsMnCl_3$ and a summary of the structures of RMX_3 compounds. *Acta Crystallographica Section B* **1973,** *29* (6), 1330-1335, DOI: 10.1107/S0567740873004450.
(414) Monzel, H.; Schramm, M.; Stöwe, K.; Beck, H. P. Zur Neuuntersuchung des Phasendiagramms $RbCl/PbCl_2$. *Zeitschrift für anorganische und allgemeine Chemie* **2000,** *626* (2), 408-411, DOI: 10.1002/(SICI)1521-3749(200002)626:2<408::AID-ZAAC408>3.0.CO;2-A.
(415) Natarajan, M.; Prakash, B. Phase transitions in ABX_3 type halides. *physica status solidi (a)* **1971,** *4* (3), K167-K172, DOI: 10.1002/pssa.2210040331.
(416) Sebastian, M.; Peters, J. A.; Stoumpos, C. C.; Im, J.; Kostina, S. S.; Liu, Z.; Kanatzidis, M. G.; Freeman, A. J.; Wessels, B. W. Excitonic emissions and above-band-gap luminescence in the single-crystal perovskite semiconductors $CsPbBr_3$ and $CsPbCl_3$. *Physical Review B* **2015,** *92* (23), 235210, DOI: 10.1103/PhysRevB.92.235210.
(417) Jouini, N.; Guen, L.; Tournoux, M. Le systeme $TlI-GeI_2$ - Structure cristalline de $TlGeI_3$. *Annales de Chimie (- Science des Materiaux) (Paris)* **1982,** *7* (1), 45-51.
(418) Linaburg, M. R. Studies of Halide Perovskites $CsPbX_3$, $RbPbX_3$ ($X=Cl^-$, Br^-, I^-), and Their Solid Solutions. The Ohio State University, 2015.
(419) Baopeng, C.; Shihua, W.; Xinhua, Z. Synthesis and structure of $AEuI_3$ (A=Rb, Cs) and AEu_2I_5 (A=K, Rb, Cs). *Journal of Alloys and Compounds* **1992,** *181* (1), 511-514, DOI: 10.1016/0925-8388(92)90348-D.
(420) Idrissi, S.; Mounkachi, O.; Bahmad, L.; Benyoussef, A. Study of the electronic and opto-electronic properties of the perovskite $KPbBr_3$ by DFT and TDDFT methods. *Computational Condensed Matter* **2022,** *33*, e00617, DOI: 10.1016/j.cocom.2021.e00617.
(421) Kaladevi, C. Studies on some ternary alkali lead bromide crystals. Ph.D. Manonmaniam Sundaranar University, 2011.
(422) Zandbergen, H. W. Neutron powder diffraction and magnetic measurements on $RbTiI_3$, $RbVI_3$, and $CsVI_3$. *Journal of Solid State Chemistry* **1981,** *37* (3), 308-317, DOI: 10.1016/0022-4596(81)90492-8.
(423) Travis, W.; Glover, E. N. K.; Bronstein, H.; Scanlon, D. O.; Palgrave, R. G. On the application of the tolerance factor to inorganic and hybrid halide perovskites: a revised system. *Chemical Science* **2016,** *7* (7), 4548-4556, DOI: 10.1039/C5SC04845A.
(424) Hoffman, J. B.; Schleper, A. L.; Kamat, P. V. Transformation of Sintered $CsPbBr_3$ Nanocrystals to Cubic $CsPbI_3$ and Gradient $CsPbBr_xI_{3-x}$ through Halide Exchange. *Journal of the American Chemical Society* **2016,** *138* (27), 8603-8611, DOI: 10.1021/jacs.6b04661.
(425) Maity, G.; Pradhan, S. K. Composition related structural transition between mechanosynthesized $CsPbBr_3$ and $CsPb_2Br_5$ perovskites and their optical properties. *Journal of Alloys and Compounds* **2020,** *816*, 152612, DOI: 10.1016/j.jallcom.2019.152612.

(426) Paul, M.; Seifert, H. J. EMF-measurements with galvanic bromine cells in the systems RBr/MBr_2 (M=Sr, Ba). *Journal of thermal analysis* **1989,** *35* (2), 585-593, DOI: 10.1007/BF01904460.
(427) Thiele, G.; Rotter, H. W.; Schmidt, K. D. Die Kristallstrukturen und Phasentransformationen des tetramorphen $RbGeI_3$. *Zeitschrift für anorganische und allgemeine Chemie* **1989,** *571* (1), 60-68, DOI: 10.1002/zaac.19895710106.
(428) Ehrenberg, H.; Fuess, H.; Hesse, S.; Zimmermann, J.; von Seggern, H.; Knapp, M. Structures of $CsEuBr_3$ and its degradation product $Cs_2EuBr_5 \cdot 10H_2O$. *Acta Crystallographica Section B* **2007,** *63* (2), 201-204, DOI: 10.1107/S0108768106049032.
(429) Bourret-Courchesne, E. D.; Bizarri, G. A.; Borade, R.; Gundiah, G.; Samulon, E. C.; Yan, Z.; Derenzo, S. E. Crystal growth and characterization of alkali-earth halide scintillators. *Journal of Crystal Growth* **2012,** *352* (1), 78-83, DOI: 10.1016/j.jcrysgro.2012.01.014.
(430) Zhang, J.; Qi, R. Y.; Corbett, J. D. Two novel titanium halide phases: KTi_4Cl_{11} and $CsTi_{4.3}I_{11}$. *Inorganic Chemistry* **1991,** *30* (25), 4794-4798, DOI: 10.1021/ic00025a022.
(431) Seifert, H. J.; Kischka, K. H. Investigations on systems AX/MnX_2 (A = Li-Cs, TI; X = Cl, Br, I) by DTA and X-ray analysis. *Thermochimica Acta* **1978,** *27* (1), 85-93, DOI: 10.1016/0040-6031(78)85023-0.
(432) Hamideddine, I.; Tahiri, N.; Bounagui, O. E.; Ez-Zahraouy, H. Ab initio study of structural and optical properties of the halide perovskite KBX_3 compound. *Journal of the Korean Ceramic Society* **2022,** *59* (3), 350-358, DOI: 10.1007/s43207-021-00178-6.
(433) Howie, R. A.; Moser, W.; Starks, R. G.; Woodhams, F. W. D.; Parker, W. Potassium tin(II) sulphate and related tin apatites: Mössbauer and X-ray studies. *Journal of the Chemical Society, Dalton Transactions* **1973,** (14), 1478-1484, DOI: 10.1039/DT9730001478.
(434) Wang Shi, H.; Zhoa, M. Phase diagram of YbI_2-RbI binary system and structural investigation of $RbYbI_3$. *Journal of the Less Common Metals* **1987,** *127*, 219-224, DOI: 10.1016/0022-5088(87)90381-X.
(435) Khyzhun, O. Y.; Fochuk, P. M.; Kityk, I. V.; Piasecki, M.; Levkovets, S. I.; Fedorchuk, A. O.; Parasyuk, O. V. Single crystal growth and electronic structure of $TlPbI_3$. *Materials Chemistry and Physics* **2016,** *172*, 165-172, DOI: 10.1016/j.matchemphys.2016.01.058.
(436) Lin, W.; He, J.; McCall, K. M.; Stoumpos, C. C.; Liu, Z.; Hadar, I.; Das, S.; Wang, H.-H.; Wang, B.-X.; Chung, D. Y.; Wessels, B. W.; Kanatzidis, M. G. Inorganic Halide Perovskitoid $TlPbI_3$ for Ionizing Radiation Detection. *Advanced Functional Materials* **2021,** *31* (13), 2006635, DOI: 10.1002/adfm.202006635.
(437) Hohnstedt, C.; Meyer, G. The first ternary iodides with divalent dysprosium. *Naturwissenschaften* **1991,** *78* (10), 462-463, DOI: 10.1007/BF01134384.
(438) Marshall, K. P.; Tao, S.; Walker, M.; Cook, D. S.; Lloyd-Hughes, J.; Varagnolo, S.; Wijesekara, A.; Walker, D.; Walton, R. I.; Hatton, R. A. $Cs_{1-x}Rb_xSnI_3$ light harvesting semiconductors for perovskite photovoltaics. *Materials Chemistry Frontiers* **2018,** *2* (8), 1515-1522, DOI: 10.1039/C8QM00159F.
(439) Thiele, G.; Serr, B. R. Crystal structure of rubidium triiodostannate(II), $RbSnI_3$. *Zeitschrift für Kristallographie - Crystalline Materials* **1995,** *210* (1), 64-64, DOI: 10.1524/zkri.1995.210.1.64.
(440) Debbichi, L.; Lee, S.; Cho, H.; Rappe, A. M.; Hong, K.-H.; Jang, M. S.; Kim, H. Mixed Valence Perovskite $Cs_2Au_2I_6$: A Potential Material for Thin-Film Pb-Free Photovoltaic Cells with Ultrahigh Efficiency. *Advanced Materials* **2018,** *30* (12), 1707001, DOI: 10.1002/adma.201707001.

(441) Kitagawa, H.; Sato, H.; Kojima, N.; Kikegawa, T.; Shimomura, O. Metallization and phase transitions of the three-dimensional halogen-bridge mixed-valence complex $Cs_2Au_2I_6$ under high pressure. *Solid State Communications* **1991,** *78* (11), 989-995, DOI: 10.1016/0038-1098(91)90220-P.
(442) Krishnamoorthy, T.; Ding, H.; Yan, C.; Leong, W. L.; Baikie, T.; Zhang, Z.; Sherburne, M.; Li, S.; Asta, M.; Mathews, N.; Mhaisalkar, S. G. Lead-free germanium iodide perovskite materials for photovoltaic applications. *Journal of Materials Chemistry A* **2015,** *3* (47), 23829-23832, DOI: 10.1039/C5TA05741H.
(443) Haupt, H. J.; Huber, F.; Preut, H. Darstellung und Kristallstruktur von Rubidiumtrijodoplumbat(II). *Zeitschrift für anorganische und allgemeine Chemie* **1974,** *408* (2), 209-213, DOI: 10.1002/zaac.19744080215.
(444) Jung, M.-H.; Rhim, S. H.; Moon, D. TiO_2/$RbPbI_3$ halide perovskite solar cells. *Solar Energy Materials and Solar Cells* **2017,** *172*, 44-54, DOI: 10.1016/j.solmat.2017.07.011.
(445) Xie, Y.; Wang, S.; Zhao, X. Phase diagram and structure of $CsSm_{(1-x)}Yb_xI_3$ systems. *Journal of Alloys and Compounds* **1996,** *241* (1), 40-43, DOI: 10.1016/0925-8388(96)02196-2.
(446) Li, Y.; Ding, Y.; Li, Y.; Liu, H.; Meng, X.; Cong, Y.; Zhang, J.; Li, X.; Chen, X.; Qin, J. Synthesis, Crystal Structure and Nonlinear Optical Property of $RbHgI_3$. *Crystals* **2017,** *7* (5), 148-11, DOI: 10.3390/cryst7050148.
(447) Eperon, G. E.; Stranks, S. D.; Menelaou, C.; Johnston, M. B.; Herz, L. M.; Snaith, H. J. Formamidinium lead trihalide: a broadly tunable perovskite for efficient planar heterojunction solar cells. *Energy & Environmental Science* **2014,** *7* (3), 982-988, DOI: 10.1039/C3EE43822H.
(448) Møller, C. K. *The structure of cæsium plumbo iodide $CsPbI_3$*, Munksgaard: 1959; Vol. 32, p 18.
(449) Naskar, A.; Khanal, R.; Choudhury, S. Role of Chemistry and Crystal Structure on the Electronic Defect States in Cs-Based Halide Perovskites. *Materials* **2021,** *14* (4), 1032-13, DOI: 10.3390/ma14041032.
(450) Riccardi, R.; Sinistri, C.; Campari, G. Y.; Magistris, A. Binary Systems Formed by Alkali Bromides with Barium or Strontium Bromide. *Zeitschrift für Naturforschung A* **1970,** *25* (5), 781-785, DOI: 10.1515/zna-1970-0536.
(451) Pidzyrajlo, N. S.; Triska, T. V.; Khapko, Z. A. In *Recombination luminescence of $CsCdI_3$ monocrystals*, Theses of the 23 all-union conference on luminescence, USSR, USSR, 1976; p 89.
(452) Kuku, T. A. Structure and ionic conductivity of $CuCdCl_3$. *Solid State Ionics* **1987,** *25* (2), 105-108, DOI: 10.1016/0167-2738(87)90109-3.
(453) Gallo, N.; Bianco, V. D.; Doronzo, S. Mercury thiocyanate and cadmium iodide complexes with KCNS and KI in methylmethacrylate. *Journal of Inorganic and Nuclear Chemistry* **1972,** *34* (7), 2374-2375, DOI: 10.1016/0022-1902(72)80178-7.
(454) Nishiwaki, Y.; Iio, K. In *9aSH-2 Dielectricity and magnetism of hexagonal $RbCoBr_3$ related substance $ACoX_3$ (A=K,Tl B=Cl,Br) (dielectric, region 10)*, The Physical Society of Japan Lecture Summary Collection, 2002; p 830.
(455) Boltalin, A. I.; Korenev, Y. M. Reaction between KF and PbF_2 in Solid and Gas Phases. *(Russian) Journal of Inorganic Chemistry (translated from Zhurnal Neorganicheskoi Khimii)* **1996,** *41* (6), 924-927.
(456) Deschene, C. In-Situ Monitoring of Cation and Anion Exchange in Perovskite Nanoparticles for Applications in Catalysis, Sensing, and Batteries. Syracuse University, 2019.

(457) Sawada, K.; Tanaka, M. Formation of bromo complexes of cobalt(II) in acetic acid. *Journal of Inorganic and Nuclear Chemistry* **1977,** *39* (2), 339-344, DOI: 10.1016/0022-1902(77)80026-2.
(458) Soubeyroux, J. L.; Cros, C.; Gang, W.; Kanno, R.; Pouchard, M. Neutron diffraction investigation of the cationic distribution in the structure of the spinel-type solid solutions $Li_{2-2x}M_{1+x}Cl_4$ (M = Mg, V): Correlation with the ionic conductivity and NMR data. *Solid State Ionics* **1985,** *15* (4), 293-300, DOI: 10.1016/0167-2738(85)90132-8.
(459) Pulcinelli, S. H.; Senegas, J.; Tanguy, B.; Menil, F.; Portier, J. Préparation et étude structurale par ratons X et RMN d'un fluorure de composition $LiZnF_3$. *Rev. chim. minér* **1986,** *23* (2), 238-249.
(460) Gordo, E.; Chen, G. Z.; Fray, D. J. Toward optimisation of electrolytic reduction of solid chromium oxide to chromium powder in molten chloride salts. *Electrochimica Acta* **2004,** *49* (13), 2195-2208, DOI: 10.1016/j.electacta.2003.12.045.
(461) Loon, C. J. J.; Ijdo, D. J. W. The crystal structure of Na_6MnCl_8 and $Na_2Mn_3Cl_8$ and some isostructural compounds. *Acta Crystallographica Section B* **1975,** *31* (3), 770-773, DOI: 10.1107/S0567740875003779.
(462) Li, Q.-J.; Sprouster, D.; Zheng, G.; Neuefeind, J. C.; Braatz, A. D.; McFarlane, J.; Olds, D.; Lam, S.; Li, J.; Khaykovich, B. Complex Structure of Molten NaCl–$CrCl_3$ Salt: Cr–Cl Octahedral Network and Intermediate-Range Order. *ACS Applied Energy Materials* **2021,** *4* (4), 3044-3056, DOI: 10.1021/acsaem.0c02678.
(463) Földvári, I.; Voszka, R.; Morlin, Z. The Properties of Ni Ions in NaCl Single Crystals. I. Vacuum Ultraviolet, Ionic Conductivity, and X-Ray Diffraction Studies. *physica status solidi (b)* **1978,** *89* (1), 235-240, DOI: 10.1002/pssb.2220890130.
(464) Komarek, K.; Herasymenko, P. Equilibria between Titanium Metal and Solutions of Titanium Dichloride in Fused Sodium Chloride. *Journal of The Electrochemical Society* **1958,** *105* (4), 216, DOI: 10.1149/1.2428803.
(465) Dubovoj, P. G. Formation of compounds in the RbCl-$BeCl_2$ system. *Ukrainskij Khimicheskij Zhurnal* **1979,** *45* (12), 1234-1235.
(466) Babel, D. In *Structural chemistry of octahedral fluorocomplexes of the transition elements*, Structure and Bonding, Berlin, Heidelberg, 1967//; Jørgensen, C. K.; Neilands, J. B.; Nyholm, R. S.; Reinen, D.; Williams, R. J. P., Eds. Springer Berlin Heidelberg: Berlin, Heidelberg, 1967; pp 1-87.
(467) Liang, L.; Wencong, L.; Nianyi, C. On the criteria of formation and lattice distortion of perovskite-type complex halides. *Journal of Physics and Chemistry of Solids* **2004,** *65* (5), 855-860, DOI: 10.1016/j.jpcs.2003.08.021.
(468) Yanagida, T.; Fujimoto, Y.; Arai, M.; Koshimizu, M.; Kato, T.; Nakauchi, D.; Kawaguchi, N. Comparative studies of scintillation properties of Tl-based crystals. *Sensors and Materials* **2020,** *32* (4), 1351-1356.
(469) Smith, D. Hindered Rotation of the Ammonium Ion in the Solid State. *Chemical Reviews* **1994,** *94* (6), 1567-1584, DOI: 10.1021/cr00030a005.
(470) Charpin, P.; Roux, N.; Ehnetsmann, J. *Compt. Rend.* **1968,** *267 C*, 484-486.
(471) Rüdorbf, W.; Kandler, J.; Babel, D. Untersuchungen an ternären Fluoriden. I. Struktur, Magnetismus und Reflexionsspektren von Alkali-, Ammonium- und Thallium-Nickel(II)-fluoriden. *Zeitschrift für anorganische und allgemeine Chemie* **1962,** *317* (5-6), 261-287, DOI: 10.1002/zaac.19623170502.

(472) Meyer, G.; Böhmer, N. Korrosion von Messing und Bronze durch Ammoniumhalogenide. *Zeitschrift für anorganische und allgemeine Chemie* **2000,** *626* (6), 1332-1334, DOI: 10.1002/(SICI)1521-3749(200006)626:6<1332::AID-ZAAC1332>3.0.CO;2-X.
(473) Troyanov, S. I.; Morozov, I. V.; Korenev, Y. M. The synthesis and crystal structure of ammonium fluorocuprates NH_4CuF_3 and $(NH_4)_2CuF_4$. *Russian journal of inorganic chemistry* **1993,** *38* (6), 909-913, DOI: 10.1002/chin.199352035.
(474) Portier, M. J.; Tressaud, A.; Dupin, J. L.; de Pape, R. Structures et proprietes magnetiques de quelques composes de formule M Fe F_3 (M = Na, K, Rb, Cs, NH_4, T1). *Materials Research Bulletin* **1969,** *4* (1), 45-50, DOI: 10.1016/0025-5408(69)90015-4.
(475) Kozak, A. d. *Rev. chim. minér* **1971,** *8*, 301-335.
(476) Hoppe, R.; Liebe, W.; Dähne, W. Über Fluoromanganate der Alkalimetalle. *Zeitschrift für anorganische und allgemeine Chemie* **1961,** *307* (5-6), 276-289, DOI: 10.1002/zaac.19613070507.
(477) Le Bail, A.; Fourquet, J. L.; Rubín, J.; Palacios, E.; Bartolomé, J. NH_4CdF_3: Structure of the low temperature phase. *Physica B: Condensed Matter* **1990,** *162* (3), 231-236, DOI: 10.1016/0921-4526(90)90017-O.
(478) Bergerhoff, G.; Goost, L. Ammoniumtrifluorostannat(II). *Acta Crystallographica Section B* **1973,** *29* (3), 632-633, DOI: 10.1107/S0567740873003031.
(479) Shachar, G.; Makovsky, J.; Shaked, H. Neutron diffraction and magnetic measurements of polycrystalline NH_4MnCl_3. *Solid State Communications* **1971,** *9* (9), 493-495, DOI: 10.1016/0038-1098(71)90131-1.
(480) Krishnan, V. G.; Dou, S.-q.; Weiss, A. Structure and Bonding of Tribromocadmates, $ACdBr_3$, A = NH_4, Rb, Cs, CH_3NH_3, $(CH_3)_2NH_2$, $(CH_3)_4N$], [H_2NNH_3, and $(H_2N)_3C$. An X-ray Diffraction and $^{79\text{-}81}$Br NQR Study. *Zeitschrift für Naturforschung A* **1991,** *46* (12), 1063-1082, DOI: 10.1515/zna-1991-1212.
(481) Rolies, M. M.; De Ranter, C. J. A new investigation of ammonium cadmium chloride. *Acta Crystallographica Section B* **1978,** *34* (10), 3057-3059, DOI: 10.1107/S0567740878010018.
(482) Das, T.; Di Liberto, G.; Pacchioni, G. Density Functional Theory Estimate of Halide Perovskite Band Gap: When Spin Orbit Coupling Helps. *The Journal of Physical Chemistry C* **2022,** *126* (4), 2184-2198, DOI: 10.1021/acs.jpcc.1c09594.
(483) Tian, J.; Cordes, D. B.; Quarti, C.; Beljonne, D.; Slawin, A. M. Z.; Zysman-Colman, E.; Morrison, F. D. Stable 6H Organic–Inorganic Hybrid Lead Perovskite and Competitive Formation of 6H and 3C Perovskite Structure with Mixed A Cations. *ACS Applied Energy Materials* **2019,** *2* (8), 5427-5437, DOI: 10.1021/acsaem.9b00419.
(484) Stoumpos, C. C.; Frazer, L.; Clark, D. J.; Kim, Y. S.; Rhim, S. H.; Freeman, A. J.; Ketterson, J. B.; Jang, J. I.; Kanatzidis, M. G. Hybrid Germanium Iodide Perovskite Semiconductors: Active Lone Pairs, Structural Distortions, Direct and Indirect Energy Gaps, and Strong Nonlinear Optical Properties. *Journal of the American Chemical Society* **2015,** *137* (21), 6804-6819, DOI: 10.1021/jacs.5b01025.
(485) Huan, T. D.; Tuoc, V. N.; Minh, N. V. Layered structures of organic/inorganic hybrid halide perovskites. *Physical Review B* **2016,** *93* (9), 094105, DOI: 10.1103/PhysRevB.93.094105.
(486) Yamada, K.; Matsui, T.; Tsuritani, T.; Okuda, T.; Ichiba, S. ^{127}I-NQR, ^{119}Sn Mössbauer Effect, and Electrical Conductivity of $MSnI_3$ (M = K, NH_4, Rb, Cs, and CH_3NH_3). *Zeitschrift für Naturforschung A* **1990,** *45* (3-4), 307-312, DOI: 10.1515/zna-1990-3-416.

(487) Stoumpos, C. C.; Mao, L.; Malliakas, C. D.; Kanatzidis, M. G. Structure–Band Gap Relationships in Hexagonal Polytypes and Low-Dimensional Structures of Hybrid Tin Iodide Perovskites. *Inorganic Chemistry* **2017,** *56* (1), 56-73, DOI: 10.1021/acs.inorgchem.6b02764.
(488) Belabbas, M.; Marbouh, N.; Arbouche, O.; Hussain, A. Optoelectronic properties of the novel perovskite materials $LiPb(Cl:Br:I)_3$ for enhanced hydrogen production by visible photo-catalytic activity: Theoretical prediction based on empirical formulae and DFT. *International Journal of Hydrogen Energy* **2020,** *45* (58), 33466-33477, DOI: 10.1016/j.ijhydene.2020.09.066.